



universität
wien

DISSERTATION

Titel der Dissertation

„Kinesin motor function at the microtubule plus-end“

Verfasserin

Christine Mieck, M. Sc.

angestrebter akademischer Grad

Doctor of Philosophy (PhD)

Wien, 2012

Studienkennzahl lt. Studienblatt: A 094 490

Dissertationsgebiet lt. Studienblatt: Molekulare Biologie

Betreuerin / Betreuer: Dr. Stefan Westermann

Contents

<u>SUMMARY</u>	<u>5</u>
<u>ZUSAMMENFASSUNG</u>	<u>7</u>
<u>1 INTRODUCTION</u>	<u>9</u>
1.1 THE EUKARYOTIC CELL CYCLE AND CELL DIVISION	9
1.1.1 THE MAIN REGULATORY ELEMENTS OF THE CELL CYCLE.....	10
1.1.2 THE CELL CYCLE OF <i>SACCHAROMYCES CEREVISIAE</i>	11
1.2 THE SPINDLE APPARATUS.....	13
1.2.1 MICROTUBULES AND NUCLEATION	13
1.2.2 ANATOMY OF THE MITOTIC SPINDLE.....	16
1.2.3 ASSEMBLY OF THE MITOTIC SPINDLE	17
1.3 MICROTUBULE ASSOCIATED PROTEINS	18
1.4 KINESINS – BIOPHYSICAL AND REGULATORY ASPECTS.....	21
1.4.1 CHARACTERISTICS OF THE KINESIN-8 FAMILY	24
1.4.2 CHARACTERISTICS OF THE KINESIN-14 FAMILY.....	27
1.4.3 MITOTIC CONTRIBUTIONS OF KINESIN-8 AND KINESIN-14 MOTORS IN BUDDING YEAST	28
<u>2 AIM OF THE WORK.....</u>	<u>32</u>
<u>3 RESULTS.....</u>	<u>34</u>
3.1 RESULTS 1: MOLECULAR MECHANISMS OF KINESIN-8 REGULATION IN BUDDING YEAST	34
3.1.1 EXPRESSION AND DYNAMIC LOCALIZATION OF KIP3P DURING CELL CYCLE PROGRESSION.....	34
3.1.2 ANALYSIS OF AFFINITY TAG PURIFIED NATIVE KIP3P	35
3.1.3 KIP3P IS PHOSPHORYLATED BY CDC28P-CLB2P	37
3.1.4 <i>IN VIVO</i> LOCALIZATION STUDIES OF KIP3P TAIL-TRUNCATIONS AND PHOSPHOMUTANTS.....	40
3.1.5 EXPRESSION OF THE TAIL-TRUNCATION KIP3P ¹⁻⁷⁰⁵ CONFERS BENOMYL SENSITIVITY	43
3.1.6 THE TAIL-TRUNCATED KIP3P ¹⁻⁷⁰⁵ HAS OPPOSITE EFFECTS ON SPINDLE AND ASTRAL MTs	45

Table of Contents

3.1.7	BIOCHEMICAL CHARACTERIZATION OF KIP3P AND ITS TAIL-TRUNCATION MUTANT.....	47
3.2	RESULTS 2: MOLECULAR ANALYSIS OF KINESIN-14 AT THE MICROTUBULE PLUS-END	53
3.2.1	THE KAR3 ACCESSORY PROTEIN CIK1P CO-PURIFIES SEVERAL +TIPS	53
3.2.2	LOCALIZATION OF KAR3P DURING MITOSIS	56
3.2.3	THE SPINDLE LOCALIZATION OF KAR3P-CIK1P DEPENDS ON BIM1P IN ANAPHASE.....	57
3.2.4	EXPRESSION AND PURIFICATION OF FULL-LENGTH KAR3P-CIK1P.....	58
3.2.5	KAR3P-CIK1P DIRECTLY INTERACTS WITH BIM1P.....	60
3.2.6	DISSECTING THE INTERACTION INTERFACE OF KAR3P-CIK1P AND BIM1P	61
3.2.7	BIM1P ASSISTS KAR3P-CIK1P IN MT-BINDING	64
3.2.8	REGULATION OF KAR3P DURING THE CELL CYCLE	66
4	DISCUSSION	69
4.1	INSIGHTS INTO THE ROLE OF THE KINESIN-8 KIP3 DURING MITOSIS.....	69
4.1.1	THE SUBCELLULAR LOCALIZATION OF KIP3 UNRAVELS THE NEED FOR REGULATION OF ITS DEPOLYMERASE ACTIVITY	69
4.1.2	REGULATION OF KIP3 BY CDC28	72
4.1.3	CONTRIBUTION OF KIP3'S TAIL DOMAIN IN REGULATING MT LENGTH HOMEOSTASIS	73
4.2	UNDERSTANDING KINESIN-14 MOTOR FUNCTION AT THE MT PLUS-END	77
4.2.1	THE EB1 HOMOLOGUE BIM1 TARGETS KAR3-CIK1 TO THE MT PLUS-END.....	77
4.2.2	DEFINING THE BINDING INTERFACE BETWEEN KAR3-CIK1 AND BIM1.....	80
4.2.3	KAR3 IS HIGHLY PHOSPHORYLATED DURING MITOSIS	82
5	MATERIAL & METHODS.....	83
5.1	STRAINS & PLASMIDS	83
5.1.1	STRAINS	83
5.1.2	PLASMIDS	86
5.2	YEAST GENETICS.....	86
5.2.1	YEAST STRAIN CONSTRUCTION	86
5.2.2	SPOT ASSAY.....	87

5.3	LIVE-CELL IMAGING	87
5.4	TANDEM AFFINITY PURIFICATION OF KIP3 FROM YEAST EXTRACTS AND MASS SPECTROMETRY ANALYSIS	88
5.5	EXPRESSION AND PURIFICATIONS OF KINESIN COMPLEXES	89
5.5.1	OVEREXPRESSION OF KAR3-CIK1-FLAG COMPLEXES IN YEAST.....	89
5.5.2	PURIFICATION OF FLAG-TAGGED KAR3-CIK1 FROM YEAST USING M2 AFFINITY AGAROSE	90
5.5.3	EXPRESSION AND PURIFICATION OF KIP3 CONSTRUCTS USING BACULO-VIRUS INFECTED Sf9 INSECT CELLS.....	91
5.6	KINASE ASSAYS	92
5.7	MICROTUBULE CO-SEDIMENTATION ASSAY / DEPOLYMERASE ASSAY	92
5.8	SIZE EXCLUSION CHROMATOGRAPHY OF MOTOR COMPLEXES	93
5.9	<i>IN VITRO</i> BINDING ASSAYS	93
5.10	TIRF MICROSCOPY SETUP	94
6	<u>ABBREVIATIONS</u>	95
7	<u>REFERENCES</u>	97
8	<u>CURRICULUM VITAE</u>	109
9	<u>ACKNOWLEDGEMENT</u>	111

Summary

Accurate segregation of the duplicated genetic material during mitosis not only requires the essential load-bearing connection between kinetochores and microtubules, but also elements that control microtubule dynamics and spindle behavior. Although none of the four nuclear kinesins in budding yeast is individually required for viability, a variety of microtubule-based processes are ensured and regulated by these motor molecules. This study analyzes the motor function of budding yeast kinesin-8 and kinesin-14 at the microtubule plus-end. Besides their biochemical similarity in behaving as motile plus-end destabilizing enzymes, these two kinesins control divergent functions during mitosis and differ in their underlying regulation of motor activity.

The family of kinesin-8 motors combines plus-end directed motility with depolymerization activity to provide length-dependent regulation of microtubules (Varga et al., 2006). Recent studies have focused on describing the biochemical activity of kinesin-8 molecules (Mayr et al., 2011; Stumpff et al., 2011; Su et al., 2011; Weaver et al., 2011), but how the cell spatially and temporally coordinates the activities of microtubule polymerases and depolymerases to allow spindle morphogenesis remains an important open question. This study showed that truncations of the carboxyterminus of budding yeasts kinesin-8 Kip3 have differential effects on motor function in cells. While large truncations abolished dimerization and phenocopied a kip3 deletion, short truncations led to increased benomyl sensitivity and thus behaved like hyperactive mutants. Detailed analysis of the Kip3¹⁻⁷⁰⁵ mutant revealed that it had opposite effects on different microtubule populations within the cell: while anaphase spindles were shorter than in wild-type cells, astral microtubules were hyperelongated and failed to productively interact with the cell cortex. The carboxyterminus of Kip3 was identified as the major site of phosphorylation by the Cdc28 kinase and a Kip3 mutant defective in

phosphorylation was compromised in localization and motor function. The study shows that the intrinsic biochemical activity of kinesin-8 molecules can only partially explain their cellular activity and it identifies the extreme carboxyterminus as the crucial determinant for context-dependent control of Kip3 function.

The minus-end directed kinesin-14 family members have a dual role in ensuring spindle elongation and integrity: they crosslink parallel microtubules in the proximity of the spindle poles and slide antiparallel microtubules that overlap in the spindle midzone. The budding yeast homologue Kar3 has been reported to discriminate these two functions by heterodimerization with two different adapter proteins. Kar3 in complex with Vik1 accumulates at spindle poles, while heterodimer formation with Cik1 targets the motor to the spindle midzone (Manning et al., 1999). Despite these observations especially the mechanism of plus-end targeting of the minus-end directed Kar3-Cik1 complex has remained elusive. Here, biochemical assays combined with live-cell microscopy has uncovered a novel interaction partner of Kar3-Cik1. I could show that the kinesin heterodimer relies on the EB1 homologue Bim1 for its midzone localization *in vivo* and forms a robust complex with Bim1 *in vitro*. I identified the C-terminus of Bim1 and the N-terminal interface of Kar3-Cik1 as critical elements for this interaction. Consistent with the *in vivo* observations Bim1 increases the MT binding activity of the motor *in vitro*. In addition this study discovered that Kar3 changes in expression level and phosphorylation state according to the cell cycle. The discovered mechanism provides an interesting deviation from canonical EB1-cargo interactions because the SxIP motif of Cik1 is only part of a composite binding interface and it might be controlled in trans by phosphorylation of the N-terminus of Kar3.

Zusammenfassung

Für die korrekte Weitergabe des Erbmaterials bedarf es abgesehen von der belastbaren, tragfähigen Verbindung zwischen Kinetochor und Mikrotubulus (MT) einer genauen Koordination der MT-Dynamik. Kinesine regulieren Mikrotubuli (MTs)-basierte Prozesse, sind jedoch für das Überleben der Hefe entbehrlich. In dieser Arbeit setze ich mich mit der Funktion des Hefe Kinesin-8 und Kinesin-14 auseinander. Obwohl diese Proteine Gemeinsamkeiten aufzeigen, beispielsweise sind sie beweglich und destabilisieren das Plus-Ende der Mikrotubuli, beteiligen sie sich an verschiedenen mitotischen Prozessen und unterscheiden sich hinsichtlich ihrer Regulation.

Vertreter der Kinesin-8 Familie können sich selbstständig zum Plus-Ende der Mikrotubuli bewegen, wo sie dann abhängig von der Mikrotubulus-Länge einen destabilisierenden Effekt ausüben (Varga et al., 2006). Kürzlich wurde gezeigt, dass die carboxyterminale Domäne des Kinesin-8 der Hefe, Kip3, entscheidenden Einfluss auf die Aktivität dieses Motorproteins hat (Mayr et al., 2011; Stumpff et al., 2011; Su et al., 2011; Weaver et al., 2011). Dennoch bleibt es größtenteils ungeklärt wie die Zelle die Funktionen von Kip3 zeitlich und räumlich reguliert. Im Rahmen der vorliegenden Arbeit charakterisierten wir eine carboxyterminal verkürzte Version von Kip3 die einen unterschiedlichen Effekt auf verschiedene MT-Populationen hat und eine Sensitivität gegenüber Benomyl vermittelt. Vermutlich sind daher zusätzliche Faktoren an der Regulation des Motorproteins beteiligt. Die eingehende Untersuchung bezüglich der Phosphorylierung von Kip3 zeigte, dass dieses Kinesin von der Zellzykluskinase Cdc28 posttranslational modifiziert wird. Die Mutation der phosphorylierten Aminosäuren verändert die subzelluläre Lokalisation des Motorproteins und dessen Aktivität.

Kinesin-14 Moleküle haben eine duale Rolle während der Etablierung der mitotischen Spindel: sie vernetzen parallele MTs an den Spindelpolen und verschieben antiparallele MTs gegeneinander, die sich in der Spindelmitte überlappen. Das Kinesin-14 der Bäckerhefe (Kar3) nimmt diese unterschiedlichen Funktionen wahr indem es mit einem von zwei Adapterproteinen interagiert. Kar3-Vik1 akkumuliert an den Spindelpolen, Kar3-Cik1 hingegen ist in der Spindelmitte zu finden (Manning et al., 1999). Kar3 und das jeweilige Adapterprotein zeigen eine gegenseitige Abhängigkeit in Bezug auf ihre Lokalisation. Daher ist anzunehmen, dass die Komplexbildung aus Kar3 und Cik1 ein spezielles Interface bildet, welches zu der korrekten Lokalisierung führt. Der exakte Mechanismus wie der Motorkomplex Kar3-Cik1 zum Plus-Ende rekrutiert wird bleibt unklar. Unsere biochemischen und mikroskopischen Analysen identifizierten Bim1 als neuen Interaktionspartner des Motorkomplex Kar3-Cik1. Die *in vivo* Lokalisation von Kar3 in der Mitte der Spindel ist abhängig von Bim1. Die carboxyterminale Domäne von Bim1 und die aminoternale Domäne von Cik1 sind entscheidende Elemente für deren Interaktion. In Übereinstimmung mit den *in vivo* Beobachtungen steigert die Interaktion mit Bim1 die Mikrotubuli-Bindungsaktivität des Motorkomplexes *in vitro*. Zusätzlich konnten wir zeigen, dass Kar3's Phosphorylierungsstatus und Expressionslevel alternieren in Anlehnung an den Zellzyklus.

1 Introduction

1.1 The eukaryotic cell cycle and cell division

Every living organism consists of cells that undergo division to multiply. This principle is a fundament of cell biology for over 150 years and was perfectly phrased by Rudolf Virchow in 1858: “*Omnis cellula e cellula*”. Between an adult human being and its origin, a single fertilized egg, lies an uncountable number of cell divisions. Before cell division occurs the cell has to grow in size, duplicate its genetic material and provide equal segregation of its chromosomes. These processes are strictly ordered in the cell cycle and give rise to two nascent cells that have identical chromosome sets, a centrosome and the appropriate organelles. The first (G1) of the four distinct cell cycle phases is characterized by a high biosynthesis rate and enormous cell growth. The chromosomes are duplicated once per cell cycle in S phase by the replication machinery. Before cell division the cell undergoes growth in gap 2 phase (G2) where biosynthesis occurs. Chromosome segregation in mitosis (M) is immediately followed by cytokinesis where cell cleavage is coordinated. The mitotic phase can be further subdivided according to chromosome morphology and functional rearrangements into prophase, metaphase, anaphase and telophase. Cell cycle duration varies between organisms and cell types, ranging from 8 min per cell cycle progression in drosophila embryos up to a year in some liver cells. Budding yeast has a generation time of about 90 min when cultured at permissive temperature and with adequate nutrient supply. Under suboptimal conditions or because of their differentiation status cells can exit the cell cycle and rest in a quiescent state (G0).

1.1.1 The main regulatory elements of the cell cycle

It is of substantial priority for the cell to precisely coordinate the timing of cell cycle phases and transitions both regarding order and completion. Errors during cell cycle progression due to misregulation often provoke fatal consequences such as chromosomal loss or unequal distribution of the genetic material. A challenging requirement for a cell cycle surveillance system is the integration of external signals to respond to environmental changes while controlling the accuracy of the processes of each cell cycle stage. The order of cell cycle events is ensured by the interdependence of events and feedback signals towards the cell cycle control system. In case of monitored problems in a particular phase, the safeguarding control system delays cell cycle progression.

This complex regulation is guaranteed by the interplay of cyclin-dependent kinases (Cdk) and their activating subunits, cyclins. The naming of cyclins arose from the observation of their oscillating appearance through the cell cycle (Pines, 1987). This fluctuation is a consequence of protein synthesis and destruction by the ubiquitin mediated proteasome machinery. Cyclins are classified according to the time window of expression and function as G1, G1/S, S and M cyclins. In contrast, Cdk abundance is constant over the cell cycle. Hence the presence of different cyclins determines the activity of the Cdk by forming distinct cyclin-Cdk complexes. Upon cyclin-Cdk interaction the catalytic kinase subunit is phosphorylating target proteins that execute processes to drive cell cycle progression. Different cyclin-Cdk complex compositions dictate the set of downstream targets. Every cyclin-Cdk complex has a particular time window to operate and modify downstream targets during the cell cycle. Activation and inhibition of different cyclin-Cdk activity are often interdependent and irreversible, thus the cell cycle progression is only possible in one direction.

The regulatory network is interspersed with phase transition checkpoints (Hartwell and Weinert, 1989). The first checkpoint between G1 and S phase is also called Start and monitors the commitment of a cell to duplicate and segregate chromosomes. Progression through the second major checkpoint (G2/M checkpoint) is initiated by the interaction of M phase cyclins with Cdk. The transition from meta- to anaphase simultaneously marks the third major checkpoint progression, which is followed by sister-chromatid segregation and cytokinesis.

1.1.2 The cell cycle of *Saccharomyces cerevisiae*

Cyclins and Cdks are conserved among eukaryotes as well as their concerted cell cycle regulation principle. Thus, the single-celled fungi can be counted to the simplest eukaryotes and serve as excellent examples to illustrate the molecular mechanism of cell cycle regulation in more detail. In *Saccharomyces cerevisiae* a single Cdk, Cdc28 (homologue to Cdk1 in other organisms), interacts during one cell cycle with the 9 budding yeast cyclins and orchestrates the cell cycle.

In early G1 phase cyclin Cln3 can accumulate in a growth dependent manner since Cln3 is not ubiquitinated by the APC^{cdh1}. Concomitantly, Cln3-Cdc28 activity gradually increases until beyond a certain threshold level the active heterodimer of G1 cyclin and Cdc28 stimulates regulatory factors that induce expression of the G1/S cyclins (Cln1 and Cln2) and S cyclins (Clb5 and Clb6). The primary function of G1/S-Cdc28 complexes is to coordinate progression through the first checkpoint (Start). Among the targets of the active G1/S-Cdc28 complexes are the APC^{cdh1}, which is inactivated by phosphorylation and transcription factors to stimulate S cyclin expression. Although S cyclins immediately bind Cdc28 after their biosynthesis this cyclin-Cdk complex are inactive at this point because of the additionally bound specific Clb-Cdc28 inhibitor Sic1. In late G1 the activity of G1/S-Cdc28 peaks and the complex targets Sic1 for

phosphorylation thereby provoking its SCF-mediated ubiquitination and destruction. Thus, the inhibition of the Clb-Cdc28 complexes is relieved and their activity initiates events required for chromosome duplication in S phase. Since Sic1 is one of the targets of Clb-Cdc28, Clb5 and Clb6 promote their own activation via this positive feedback loop and generate a switch-like phase transition into S phase. S phase cyclins bound to Cdc28 play a crucial role for efficient initiation of DNA replication by activating origins of replication in a timely regulated manner. In late S phase the gene expression of M phase cyclins is switched on and M cyclin (Clb1-4)-Cdc28 complexes accumulate during the proceeding S phase. Budding yeast is devoid of a defined G2 phase, because preparations for mitosis simultaneously occur during S phase. The M phase cyclin-Cdc28 combinations promote spindle formation and mitotic entry, while in parallel suppressing mitotic exit and cytokinesis. As the cell reaches metaphase, the M-Cdks activate the APC^{Cdc20} complex by phosphorylation and initiate Clb5, securin and their own degradation. Securin destruction relieves separase from its inhibited state and facilitates cleavage of cohesin molecules that hold sister chromatids together. Activation of the APC thereby causes sister chromatid separation and segregation. The proteolytic inactivation of M-Cdk1 consequently triggers Cdc20 dissociation from the APC and facilitates complex formation of APC^{Cdh1} that targets S- and M-type cyclins for destruction throughout G1 phase. This enables dephosphorylation of Cdk1 substrates by the Cdc14 phosphatase to allow spindle disassembly and cytokinesis.

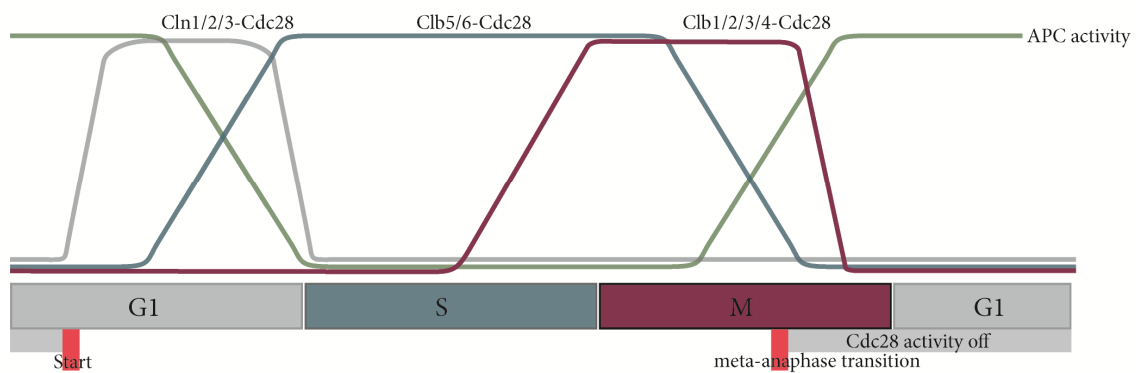


Figure 1. Schematic illustration budding yeasts cell cycle cascade. Accumulation of the indicated cyclin fraction triggers cell cycle progression in complex with the major cell cycle kinase Cdc28 (adapted from Morgan, 2006)

1.2 The spindle apparatus

All eukaryotic cells achieve equal chromosome segregation by building a mitotic spindle that is attached to sister chromatids and pulls them into the area of the two nascent cells. This spindle is a complex entity of bipolar microtubule arrays, associated proteins and centrosomes.

1.2.1 Microtubules and nucleation

As part of the cellular cytoskeleton microtubules (MTs) contribute to a variety of cellular processes. Apart from serving as the primary structural element of the mitotic spindle, MTs organize the cytoplasm, mediate intracellular trafficking and contribute to cell morphology. Although a MT is physically characterized by an intrinsic rigidity, MT based processes are often very dynamic and flexible.

The basic building blocks of MTs are heterodimers of α - and β -Tubulin that polymerize in a head-to-tail fashion to form linear protofilaments and 13 laterally aligned protofilaments form a 25nm wide hollow cylinder – the microtubulus (Desai and

Mitchison, 1997). Within this MT architecture the individual Tubulin subunits are tightly bound in the lattice - removal and addition of building blocks is only possible at the accessible MT ends. These two ends can be distinguished by the identity of the terminating Tubulin subunit that confers MT polarity. Addition of new Tubulin heterodimers occurs at the β -Tubulin exposed MT plus-end, whereas α -Tubulin decorates the slowly growing minus-end. Tubulin belongs to the class of GTPases and the free Tubulin dimer in solution is bound to two GTP molecules. While the nucleotide state of the α -Tubulin is stable, GTP hydrolysis of the β -Tubulin bound GTP takes place upon binding to the MT end. Importantly GDP-bound Tubulin has a lower microtubule-binding affinity and adopts a more curved conformation when exposed at the MT tip (Wang and Nogales, 2005). In case the rate of GTP-Tubulin addition exceeds the rate of GTP hydrolysis, a GTP cap forms at the MT end and facilitates ongoing MT growth. In contrast, a high GTP hydrolysis rate combined with a low Tubulin association rate results in the exposure of low-affinity GDP-Tubulin at the MT end. This situation decreases the likelihood for the addition of new Tubulin dimers and simultaneously provokes GDP-Tubulin dissociation from the tip. An inherent feature of MTs is their tendency to switch rapidly between periods of growth and shrinkage at the MT plus-end due to changes in their Tubulin association rate and GTP hydrolysis (Mitchison and Kirschner, 1984). This dynamic instability of MTs enables the cell to rapidly reorganize the cytoskeleton in order to adapt to spatial rearrangements or according to cell cycle required needs. Even a single microtubulus can interconvert repeatedly between rapid growth (rescue) and shrinkage events (catastrophe) *in vivo* and *in vitro* (Walker et al., 1988; Wordeman and Mitchison, 1994). MT dynamics are affected by the amount of free Tubulin and microtubule associated proteins that modulate Tubulin turnover rates, microtubule stability or induce particular protofilament conformations (see section 1.3).

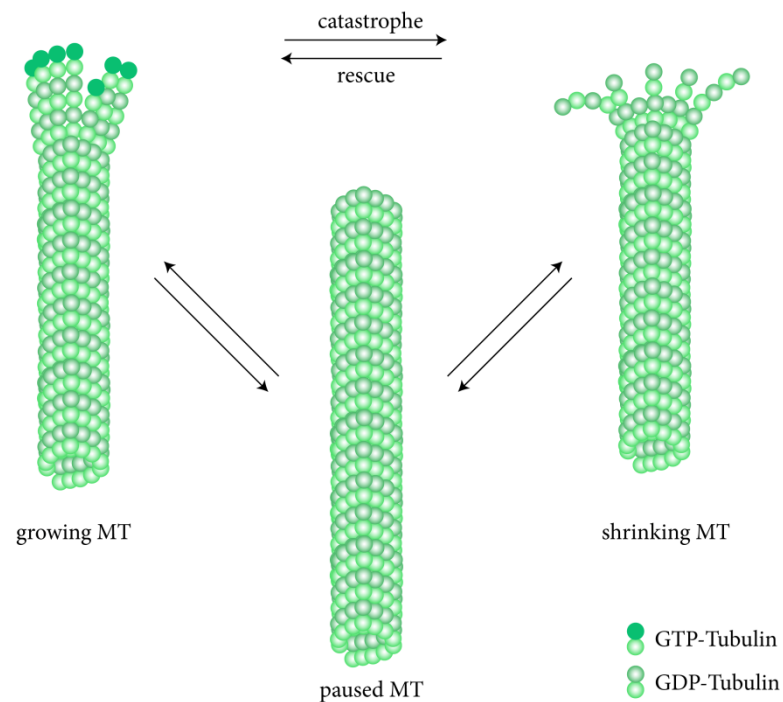


Figure 2. Schematic illustration of microtubule dynamics. MTs rapidly cycle between phases of growth and shrinkage primarily at the MT plus-end. Growth is characterized by the addition of GTP-Tubulin dimers and lattice incorporation that facilitates nucleotide hydrolysis of the β -Tubulin bound GTP. In response to low Tubulin concentrations or MAP induced destabilization MTs rapidly depolymerize (catastrophe) by protofilament peeling.

Another regulating event for MT based structures is the nucleation process. Spontaneous *de novo* nucleation of MTs is a slow process even under condition of excessive Tubulin concentration because short MT intermediates are energetically unfavored and tend to disassemble (Rice et al., 2008). To overcome this problem, cells have evolved preexisting nucleation sites, the γ -Tubulin ring complex (γ -TuRC) and the γ -Tubulin small complex (γ TuSC). The specialized Tubulin version, γ -Tubulin facilitates MT growth *in vitro* (Stearns and Kirschner, 1994) and is essential for proper MT organization in the majority of eukaryotes. These nucleation centers are embedded in the microtubule organizing centers (MTOC), the centrosome or its fungal analogue the spindle pole body (SPB). However nucleation sites are not always part of subcellular

organelles. Plants and frog oocytes are devoid of centrosomes, although they can assemble a bipolar spindle and MT nucleation processes are mediated by γ -TuRC.

1.2.2 Anatomy of the mitotic spindle

The fusiform shape of the spindle arises because the minus-ends of MTs are embedded in spindle poles while the plus-ends point outwards from the poles with a subset of antiparallel MTs overlapping in the spindle midzone. Electron microscopic studies of the spindle led to the discrimination of three MT categories according to their subcellular localization and function: the plus-ends of kinetochore MTs are attached to kinetochores (Nicklas and Kubai, 1985; McDonald et al., 1992), astral MTs extend towards the cell cortex and position the spindle in the cellular context (Aist et al., 1991) and interpolar MTs interdigitate in the spindle midzone (McDonald et al., 1979; Ding et al., 1993; Mastronarde et al., 1993).

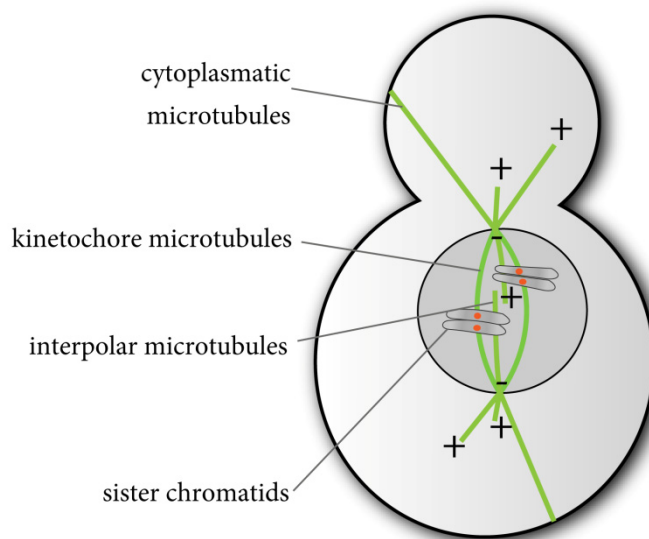


Figure 3. Spindle anatomy of budding yeast. The three MT categories are indicated in a schematic metaphase spindle configuration.

As described above MT nucleating centrosomes are central components of the mitotic spindle. The fungal functional analogue of the centrosome, the spindle pole body, is embedded in the nuclear envelope and nucleates both cytoplasmatic and nuclear microtubules. The life cycle of centrosomes must be coordinated with the cell cycle. A G1 cell possesses one centrosome or SPB, whereas the construction of the bipolar mitotic spindle in M phase requires SPB duplication. This process occurs once per cell cycle in S phase and both centrosomes stay physically linked in juxtaposition until early mitosis. Upon separation, they move to opposing sides of the nucleus thereby facilitating the formation of a bipolar spindle. The equal distribution of centrosomes/SPBs into daughter cells is accomplished in cytokinesis.

The plus-ends of kinetochore MTs connect the inheritable material of the cell to the spindle apparatus via physical association with kinetochores. This multiprotein structure assembles on centromeric DNA and functions not only in relaying forces generated by microtubules but also accomplishes the recognition and correction of erroneous kinetochore-microtubule attachments (Lampert and Westermann, 2011).

1.2.3 Assembly of the mitotic spindle

The initial step for the establishment of a bipolar spindle in most animal cells is the separation of centrosomes in prophase. The underlying molecular mechanism that drives centrosomes to move apart from each other is still under debate, but it seems to rely on forces created by motor proteins. The juxtaposed centrosomes nucleate MTs and those are thought to exhibit pushing forces when encountering the neighboring centrosome (Cytrynbaum et al., 2003). The tetrameric plus-end directed kinesin-5 motor proteins assist centrosomal repulsion by crosslinking and sliding of antiparallel microtubules thereby producing an outward force that pushes the centrosomes apart (Blangy et al., 1995). Interestingly, while inhibition of kinesin-5 motors causes the

formation of monopolar spindles (Mayer et al., 1999), simultaneous depletion of minus-end directed kinesin-14 motors restores bipolar spindle formation suggesting the existence of a redundant mechanism involved in centrosome separation and the formation of a bipolar spindle (Saunders and Hoyt, 1992). The second important player for this process is the minus-end directed motor dynein. Its localization to the cortex and attachment to astral MTs generates an outward directed force that aids centrosome separation (Sharp et al., 1999; Ferenz et al., 2009). After successful centrosome separation the spindle is increasing in size in a self-organizing manner that depends on the balancing forces of motor proteins, the process of microtubule nucleation and additional factors that stabilize and crosslink microtubules. Kinesin-5 family members play a crucial role in sorting and crosslinking MTs near their plus-ends within the emerging bipolar spindle meshwork (Kapitein et al., 2005). Minus-ends are focused at spindle poles by the minus-end directed dynein and kinesin-14 molecules. The fine-tuning of spindle assembly is achieved by the action and interplay of a broad variety of microtubule associated proteins that regulate each other or influence microtubule dynamics.

1.3 Microtubule associated proteins

In living cells, a plethora of microtubule associated proteins (MAPs) regulate MT dynamics spatiotemporally. Originally identified as co-purifying proteins in Tubulin preparations, MAPs may bind to soluble, unpolymerized Tubulin, but also to the MT lattice or preferentially to MT ends. According to the consequences on MTs MAPs are classified into stabilizing factors, plus-end tracking proteins (+TIPs), polymerases, depolymerases and cross-linking proteins.

The most prominent example of a MT stabilizer is the protein tau, which is primarily expressed in the central nervous system. Interestingly, while unmodified tau binds along the length of MTs, the phosphorylated and acetylated versions of tau exhibit decreased MT binding affinity and are prone to aggregate (Drechsel et al., 1992; Biernat et al., 1993; Cohen et al., 2011). Aberrant accumulation of insoluble tau is implicated in the pathogenesis of neurodegenerative tauopathies, such as Alzheimer's disease.

The diverse set of plus-end tracking proteins share a common localization pattern, namely by preferentially decorating the growing MT plus-ends. This particular localization enables them to constitute a complex network that allow MAPs to interact, crosstalk and compete with each other in order to regulate MT dynamics and coordinate connections to other cellular components. Although the majority of +TIPs possesses an intrinsic MT binding affinity, their ability to enrich at the plus-end depends on different strategies. +TIPs can either autonomously recognize the structure of a MT plus-end, diffuse along the MT lattice or reach the MT tip as a cargo of a molecular motor (Galjart, 2010; Maurer et al., 2012). However, a large subpopulation of +TIPs depends on the interaction with one of the end-binding (EB) proteins for their localization at the MT plus-end. The evolutionary conserved group of EB family members exerts autonomous plus-end tracking by the help of its N-terminal calponin homology domain, thereby governing the association of hitchhiking +TIPs to the MT end (Bieling et al., 2007). The fission yeast EB protein Mal3 binds in proximity to the exchangeable GTP-binding site of β -Tubulin at the MT end and is therefore in a position to sense the nucleotide state (Maurer et al., 2012). This observation supports the idea of a mechanistic coupling of EB's plus-end tracking behavior to the dynamic instability of MTs. Recruitment of numerous +TIPs to EB proteins is mediated by the C-terminal EB homology domain and occurs in two binding modes: first, EB's C-terminal EEY motif is bound by CAP-Gly domains of CLIPs or dynactin's large subunit p150^{Glued}. Second, the conserved Ser-x-Ile-Pro (SxIP) motif targets a variety of structurally

unrelated +TIPs to EBs (Hayashi et al., 2005; Honnappa et al., 2009). Among those are CLIP associated proteins (CLASPs), the kinesin MCAK or the yeast Aurora B homologue Ipl1 (Gouveia and Akhmanova, 2010; Zimniak et al., 2012).

Comparing MT assembly kinetics *in vivo* and *in vitro* reveals that MT growth rates of purified Tubulin *in vitro* are tremendously lower when performed at cellular Tubulin concentrations (Gard and Kirschner, 1987b; Kinoshita et al., 2001). This difference is attributed to the presence of members of the Dis1/XMAP215 family *in vivo* (Kinoshita et al., 2002). Accordingly, purified XMAP215 from egg extracts accelerates MT growth rates about 10-fold *in vitro* (Gard and Kirschner, 1987a). Homologues of XMAP215 are present in all eukaryotes and share a conserved domain, the TOG domain (Gard et al., 2004). Different family members contain two to five TOG domains and each individual domain is capable to bind a Tubulin dimer. Single-molecule experiments demonstrated that XMAP215 acts as a polymerizing enzyme that processively catalyzes the addition of Tubulin dimers to the MT protofilament (Brouhard et al., 2008). This reaction can be reversed: in the absence of Tubulin XMAP215 promotes MT destabilization (Brouhard et al., 2008).

MT depolymerizing enzymes can be found among the class of molecular motor proteins. While myosins interact with actin filaments, dyneins and kinesins use MT tracks to move within the cell (Vale, 2003). This ATP dependent motility of MT motor proteins accounts for the versatile functions that are covered by kinesins: MT based transport of cargos, coordination of the MT network and in some cases the regulation of MT dynamics (Hirokawa, 1998; Hirokawa et al., 2009; Gouveia and Akhmanova, 2010). For instance kinesin-13, kinesin-14 and kinesin-8 family members have been shown to destabilize MT ends *in vivo* and *in vitro* (Desai et al., 1999; Howard and Hyman, 2007; Su et al., 2012). The overall domain architecture, biophysical properties and the

contribution of the budding yeast kinesin families to mitotic processes will be discussed in the following section.

1.4 Kinesins – biophysical and regulatory aspects

The identification of kinesins as force-generating MT motors dates back more than 25 years (Brady, 1985; Scholey et al., 1985; Vale et al., 1985). Since then genetic and biochemical studies have identified a multitude of kinesins that can be phylogenetically clustered into 15 families (Hirokawa et al., 2009). The most conserved feature among kinesins is the motor domain composed of nucleotide and MT-binding sites. Kinesins have evolved by combining the core motor domain with a variety of nonmotor regions that dictate specificity in cargo binding, regulation and localization (Verhey and Hammond, 2009). According to the location of the motor domain within the polypeptide chain, kinesin families can be further classified: kinesins composed of an aminoterminal motor domain undergo plus-end directed motility, whereas a carboxyterminal motor domain arrangement corresponds to minus-end directed motility. The central motor domain architecture within the kinesin-13 family is accompanied with a MT destabilizing activity instead of endowing the motor with directed movement (Lawrence et al., 2004). However, this generalization is not true for all kinesin families. Some kinesin-8 and kinesin-14 motors show motility and MT depolymerization activity simultaneously (Endow et al., 1994b; Sproul et al., 2005; Gupta et al., 2006; Varga et al., 2006; Mayr et al., 2007). Independent of the motor domain location, the majority of kinesins is composed of head (motor domain), neck, stalk and tail domain. The head undergoes conformational changes that depend on the nucleotide state. Whether ATP, ADP-Pi, ADP or no nucleotide is bound dictates different conformations that concomitantly translate into different affinities for MTs (Hackney, 1994). Vice versa, the binding event to the MT influences the kinetics of the nucleotide state transitions thereby provoking conformational changes within the head.

Movement is generated by transducing the conformational changes of the head into the neck region whose orientation determines the direction of the motor. The stalk region promotes dimerization of kinesins that is a requirement for processive movement (Gilbert et al., 1995). Processivity is defined as the distance covered before the motor dissociates from the MT track. A precise coordination between the ATP cycles of the two heads is essential to prevent premature MT detachment. The mechanochemical cycle of processive kinesin movement is described in the hand-over-hand model with the front head attached to the MT and ADP bound while the rear head detaches upon ATP binding and taking a 16 nm step to become the new leading head (Yildiz et al., 2004). In average the kinesin dimer consumes one ATP molecule to take an 8 nm step along the MT, exactly the distance between adjacent Tubulin heterodimers (Svoboda et al., 1993; Schnitzer and Block, 1997).

In contrast to processive kinesins, the minus-end directed kinesin-14 family members are nonprocessive motor molecules that achieve MT based motility by a different mechanism. Instead of stepping towards the minus-end they perform a powerstroke induced by ATP binding involving a lever-arm rotation and bending (Endres et al., 2006; Rank et al., 2012).

Though the biophysical properties of kinesins are well established, it is of biological importance to unravel the regulation of motor proteins regarding their activity at the correct subcellular destination. Considering the parameters of a kinesin that can be modulated the complexity of such a regulation becomes obvious: ATP hydrolysis, cargo binding and release, affinity to MTs or the motor localization can be influenced and fine-tuned by several mechanisms (Verhey and Hammond, 2009). Since regulation often depends on the divergent nonmotor elements, regulation mechanisms cannot be generalized or applied to several kinesin classes. For instance, the ability to prevent futile ATP consumption in the absence of a cargo by adopting an autoinhibitory state is so far

only observed for kinesin-1, kinesin-2, kinesin-3 and kinesin-7 family members. This mechanism has been best studied for kinesin-1 and revealed backfolding of the tail domain in a way that the nonmotor region contacts the Switch I helix of the motor domain and prevents ADP release (Hackney and Jiang, 2000). A second mechanism of autoinhibition was proposed for kinesin-1, kinesin-2 and kinesin-3 motors in which processivity and coordinated stepping behavior is influenced by nonmotor regions binding to the kinesin neck and separating the motor domains (Hammond et al., 2010; Verhey et al., 2011). Upon cargo binding or phosphorylation the folded kinesins become released from the autoinhibited state. For example, a single phosphorylation event within the C-terminal domain of autoinhibited kinesin-5, Eg5, by Cdk1 is sufficient to increase the MT binding efficiency (Cahu et al., 2008). Similarly, the CENP-E (kinesin-7 family) unfolds upon phosphorylation by the kinases Mps1 and Cdk1 which results in an increase of processivity (Espeut et al., 2008). Posttranslational modifications of kinesins especially by phosphorylation are potent tools to influence the activity of kinesins since several parameters can be modulated. Phosphorylation and dephosphorylation by diverse kinases and phosphatases govern events such as the described release of autoinhibition or cargo loading. They can also regulate the affinity to MTs and control the motor activity in a spatiotemporal manner in the cellular context (Verhey and Hammond, 2009).

Further ways to influence kinesin motor function are the regulation of the protein level and their nuclear or cytoplasmic sequestration (Verhey and Hammond, 2009). Motor and nonmotor MAPs also influence each other on the MT track either via direct interactions but also by sterical hindrance, since the physical occupancy of the microtubule generates molecular crowding of obstacles thereby constricting movement (Leduc et al., 2012). More recently, different Tubulin isoforms and posttranslational modifications of MTs are discussed as biochemical cues to navigate kinesins (Janke and Bulinski, 2011). Another interesting mechanism to control motor localization within the

mitotic spindle is used by the kinesin-14 Kar3 of *S. cerevisiae*. This motor is heterodimerizing with either one of two noncatalytic adaptor proteins, Cik1 and Vik1. Dependent on the heterodimer composition Kar3 localizes to spindle pole bodies in case of Kar3-Vik1 or to plus-ends of MTs when associated with Cik1 (Manning et al., 1999). A detailed description of Kar3's role during mitosis is continued in subsection 1.4.2.

1.4.1 Characteristics of the kinesin-8 family

The well-conserved kinesin-8 family participates in mitosis by combining its plus-end directed motility with the capacity to regulate MT dynamics. So far the coexistence of both activities is mechanistically not completely understood, although kinesin-8s have structural elements in common both with motile kinesins and with robust depolymerases such as kinesin-13s. Typical for a plus-end directed motor, kinesin-8's motor domain is N-terminally located rather than central as in kinesin-13 members. However, kinesin-8s share an unique finger-like Loop2 with nonmotile kinesin-13s, which has been shown to be essential for the depolymerization activity of the latter family (Ogawa et al., 2004; Peters et al., 2010). Loss of kinesin-8 activity causes long cellular microtubules in eukaryotes, even though the MT destabilizing activity of the particular homologues is highly heterogeneous and still subject of some controversy (Cottingham and Hoyt, 1997; West et al., 2001; Gandhi et al., 2004; Rischitor et al., 2004; Mayr et al., 2007). Biochemical and single-molecule microscopy assays performed with the budding yeast kinesin-8 motor, Kip3, conveyed a length-dependent depolymerase activity of Kip3 (Varga et al., 2006). Prerequisite for this behavior is the extraordinary processivity of kinesin-8 molecules and a velocity that exceeds the MT growth rate of $1 - 1.4 \mu\text{m min}^{-1}$. After randomly landing on the MT lattice, the highly processive plus-end directed motility ensures that almost all motors reach the plus-end. Kip3 has a plus-end-residence time that is inversely correlated to its concentration and dissociation of a single motor is coupled with the removal of one Tubulin dimer (Varga et al., 2009).

Longer MTs have more potential Kip3 landing sites and accordingly a higher concentration of MT destabilizing motors at the plus-end. Indeed Kip3's depolymerization rate changes in direct proportion to the MT length (Varga et al., 2006; 2009). The length-dependent depolymerization model serves as one tool for cells to control the overall length of their MTs, for example during the processes of spindle positioning in yeast (Gupta et al., 2006) or chromosome congression in human cells (Mayr et al., 2007). In conflict to the notion of kinesin-8 motors as MT depolymerizing enzymes that was derived from *in vitro* experiments are *in vivo* observations from several studies in budding yeast and HeLa cells. Unexpectedly, microtubule-shortening during meta- and anaphase was nearly twice as fast in the absence of the respective kinesin-8 compared to control cells (Gupta et al., 2006; Stumpff et al., 2008). Besides the elevated frequency of catastrophes also rescue events increased upon loss of kinesin-8s. Consistent with this observation, depletion of the human Kif18A slowed chromosome oscillation velocities (Mayr et al., 2007). Taken together the human kinesin-8 motor seem to dampen the processes of MT dynamics *in vivo* (Du et al., 2010).

One possible explanation for the discrepancy between *in vitro* and *in vivo* observations of kinesin-8's impact on MT dynamics could be the different nature of microtubules: single-molecule studies employed GMPCPP-stabilized microtubules that resemble the straight GTP-Tubulin conformation which is found *in vivo* exclusively at the tip of growing MTs in form of the GTP cap. Once a microtubule plus-end is uncapped *in vivo* depolymerization of GDP-Tubulin microtubules proceed through the protofilament peeling of microtubules. In the cellular context the accumulation of kinesin-8 motors at the plus-end could stabilize neighboring Tubulin subunits thereby slowing the depolymerization rate (Gardner et al., 2008b). In contrast, the *in vitro* setup facilitates ongoing MT destabilization due to the GMPCPP-induced Tubulin conformation. Therefore, it is still under debate whether kinesin-8 motors can be counted as actively

depolymerizing enzymes, catastrophe-promoting factors or as a decelerator of MT dynamics. Recently several studies contributed to unravel the functions of the kinesin-8 tail domain. A nonmotor MT binding site within the tail increases the processivity and prolongs end-residence time of human and budding yeasts kinesin-8 as determined by single-molecule experiments (Stumpff et al., 2011; Su et al., 2011). Since these two parameters are required for depolymerase activity, the tail contributes to the efficiency of kinesin-8 motors to destabilize MTs. Interestingly the tail domain also promoted microtubule stabilization (Su et al., 2011). The current working model implicates a MT stabilizing effect of kinesin-8s at low motor concentrations, whereas a high motor concentration at the plus-end favors MT destabilization (Su et al., 2011).

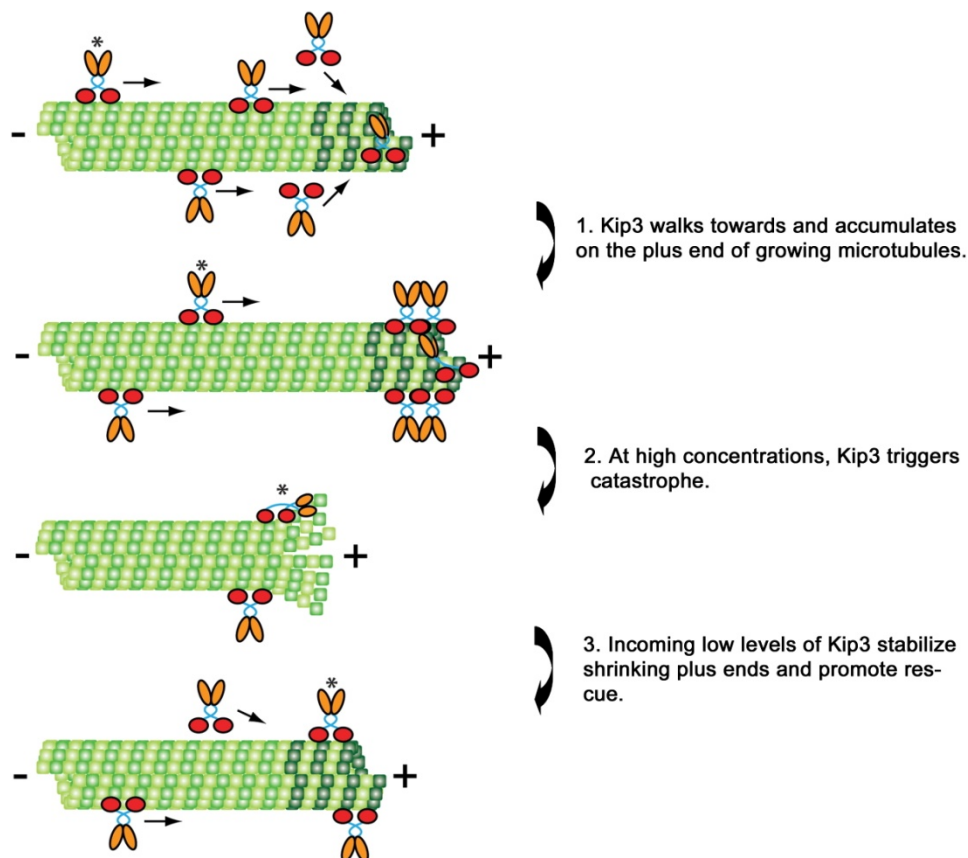


Figure 4. Current working model of Kip3's dual-mode regulation of MT length. The motor induces MT destabilization at high concentration, whereas exerts a stabilizing effect on MTs with lower motor decoration (Su et al., 2011).

As described for kinesins in general the nonmotor domains are predominantly a mediator of cargo binding. Several interactions between kinesin-8 molecules and other MAPs have been described, although the conservation of those among eukaryotes is yet to be determined. For budding yeasts kinesin-8 an association with Stu2 was reported that was surprisingly mediated by the N-terminal half of the motor protein (Gandhi et al., 2011). The nonmotor domains of fission yeast kinesin-8 motors contribute to spindle checkpoint silencing via association with type 1 phosphatase, PP1 (Meadows et al., 2011). In human cells Kif18A targets the astrin-CLASP complex to kinetochores (Manning et al., 2010) and Kif18B interacts with EB1 and MCAK to promote MT depolymerization (Tanenbaum et al., 2011).

1.4.2 Characteristics of the kinesin-14 family

The duality of behaving as depolymerase while harboring a motor domain that enables motility is characteristic for only two kinesin families: the plus-end directed kinesin-8s described above and the minus-end directed kinesin-14 family. Kinesin-14 members are slow, nonprocessive motors whose carboxyterminal motor domain links via coiled-coils to an ATP independent microtubule binding tail. The presence of multiple MT-binding sites in kinesin-14 dimers endows them with the capacity to crosslink and slide adjacent microtubules. Kinesin-14's function is highly conserved and critical for spindle organization during meiosis and mitosis (Hatsumi and Endow, 1992; Saunders and Hoyt, 1992). Defects in kinesin-14 activity compromise spindle organization in cells: splayed multipolar spindles, disorganized spindle poles, unusually long cytoplasmic microtubules and a slight increase in spindle length are caused by the loss of kinesin-14 function (Saunders et al., 1997; Troxell et al., 2001; Goshima et al., 2005). These phenotypic defects can be traced back to kinesin-14's ability to bundle parallel microtubules close to the spindle poles and to slide anti-parallel microtubules in the spindle midzone (Endow et al., 1994a; Fink et al., 2009). The force generated by kinesin-

14 motors within the spindle antagonizes the effects of the plus-end directed kinesin-5 family (Tao et al., 2006). By crosslinking and sliding anti-parallel interpolar MTs of the midzone, kinesin-5 proteins mediate a poleward flux coupled to an increase in pole-pole distance. In contrast, kinesin-14 motors exert inward directed forces and thus counterbalance the kinesin-5 induced spindle elongation (Brust-Mascher et al., 2009). Consistently the absence of motors of both families can restore defects caused by inhibition of either kinesin-5 or kinesin-14 motors (Saunders and Hoyt, 1992).

1.4.3 Mitotic contributions of kinesin-8 and kinesin-14 motors in budding yeast

From the four nuclear kinesins of budding yeast, the presence of only two motor species, Cin8 (kinesin-5) in combination with either Kar3 (kinesin-14) or Kip3 (kinesin-8), is sufficient to guarantee viability (Cottingham et al., 1999). Genetic studies revealed partly overlapping and redundant functions for Kip3 and Kar3 during spindle positioning and in supporting the structural spindle integrity. An obvious explanation would be the need for at least one MT plus-end destabilizing kinesin (Cottingham et al., 1999). However, Kip3 and Kar3 participate in different mitotic processes and their underlying regulatory modes are divergent.

The plus-end directed Kip3 regulates microtubule dynamics that account for the proper function of spindle-based processes during cell division. In cooperation with several +TIPs it plays a crucial role in correctly positioning the mitotic spindle with respect to the bud (Gupta et al., 2006). For efficient kinetochore microtubule attachment in early mitosis Kip3 transports Stu2 to the MT plus-end and thereby facilitates the collection of scattered kinetochores (Gandhi et al., 2011). During metaphase Kip3 regulates kinetochore MT length and promotes kinetochore clustering (Wargacki et al., 2010b). In late mitosis spindle disassembly is orchestrated by multiple pathways and is essential for cell cycle progression. Besides APC^{cdh1} and the Aurora B homolog Ipl1 it has been

demonstrated that Kip3 drives sustained interpolar MT depolymerization (Woodruff et al., 2010). Though the biophysical properties of Kip3 are well studied it remains an open question how the cell spatially and temporally coordinates the activity of this depolymerase throughout the cell cycle.

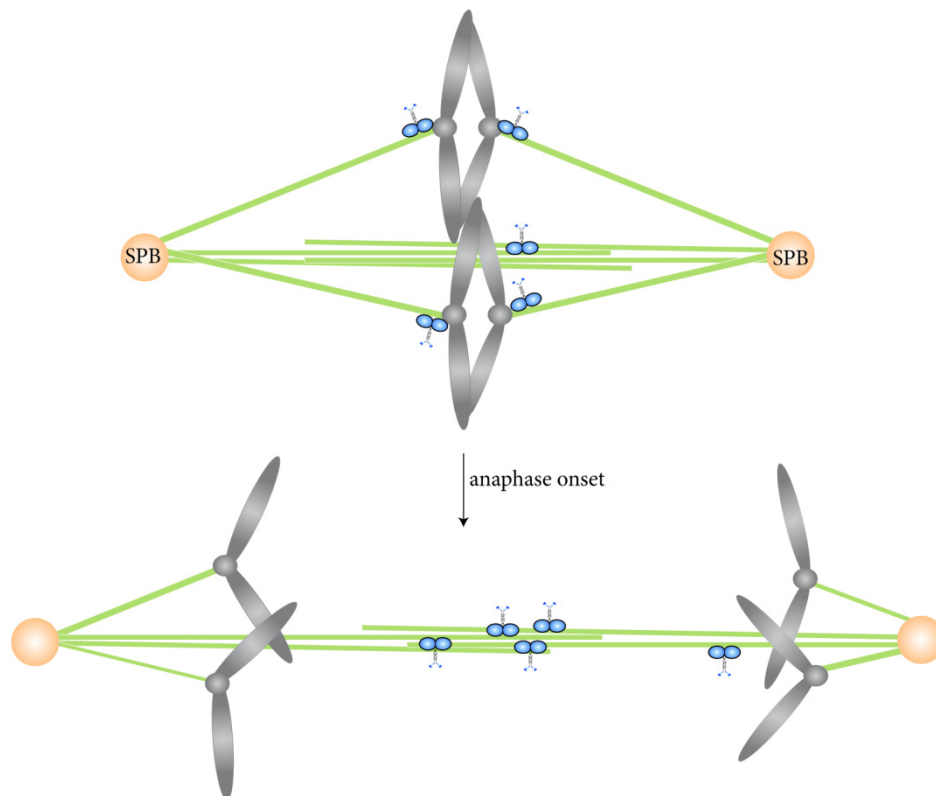


Figure 5. Dynamic relocation of Kip3 from kinetochore MTs to the spindle midzone upon anaphase onset. The motor (blue) clusters in metaphase in close proximity to kinetochores in a bilobed manner and is redistributed to the anaphase spindle after sister chromatid (grey) separation is initiated.

The budding yeast kinesin-14 member Kar3 was identified in a screen for karyogamy defects and is essential for nuclear fusion (Meluh and Rose, 1990). During vegetative growth it antagonizes Cin8 and Kip1 (kinesin-5) generated forces within the spindle midzone by exerting a counterbalancing, inward directed force on spindle MT arrays (Saunders and Hoyt, 1992; Gardner et al., 2008a). Additionally Kar3 provides the

integrity of the mitotic spindle by crosslinking parallel microtubules near spindle poles and assists in the process of transporting unattached kinetochores poleward before congression (Saunders et al., 1997; Tanaka et al., 2005b). The cell regulates the divergent functions of Kar3 by employing a remarkable mechanism to govern Kar3's subcellular localization: Kar3 forms a heterodimer with one of two accessory proteins that dictate motor localization and function. Kar3 in complex with Vik1 crosslinks and stabilizes parallel MTs at the spindle pole bodies during mitosis (Manning et al., 1999), whereas the Kar3-Cik1 heterodimer functions both in mitosis and meiosis by sliding anti-parallel MTs, stabilizing and destabilizing MT plus-ends (Maddox et al., 2003; Sproul et al., 2005; Gardner et al., 2008a). A crystallographic approach revealed that the carboxyterminal domain of Vik1 and presumably also of Cik1 is structurally similar to the catalytic motor core of kinesins, but lacks an ATP binding site (Allingham et al., 2007). This similarity led to the notion that Cik1 and Vik1 evolved from a common kinesin-14 ancestor and preserved their ability to bind microtubules by the retaining motor-fold but lost their nucleotide-binding requirement (Allingham et al., 2007).

There are two different Cik1 isoforms that have separate functions. During vegetative growth Cik1 is cyclically expressed and targeted for ubiquitin-mediated proteolysis by the APC^{cdh1} in each cell cycle. Treatment with the mating pheromone α -factor induces expression of a shorter Cik1 isoform that is devoid of the nuclear localization sequence and is unable to be ubiquitinated by APC^{cdh1} (Benanti et al., 2009). This study dissected the isoform-specific functions and demonstrated that the different isoforms cannot compensate for the loss of the other. Even though it is well established that Kar3 localization is dictated by the heterodimer configuration, how Cik1 mediates MT plus-end association of the motor complex whereas Vik1 facilitates minus-end accumulation is not understood. Moreover Kar3 was identified in a screen as a target of the major cell cycle kinase Cdc28, but the mode and consequences of this regulation are still unknown

and could possibly contribute to the different targeting destinations of Kar3-Vik1 and Kar3-Cik1 within the mitotic spindle (Ubersax et al., 2003).

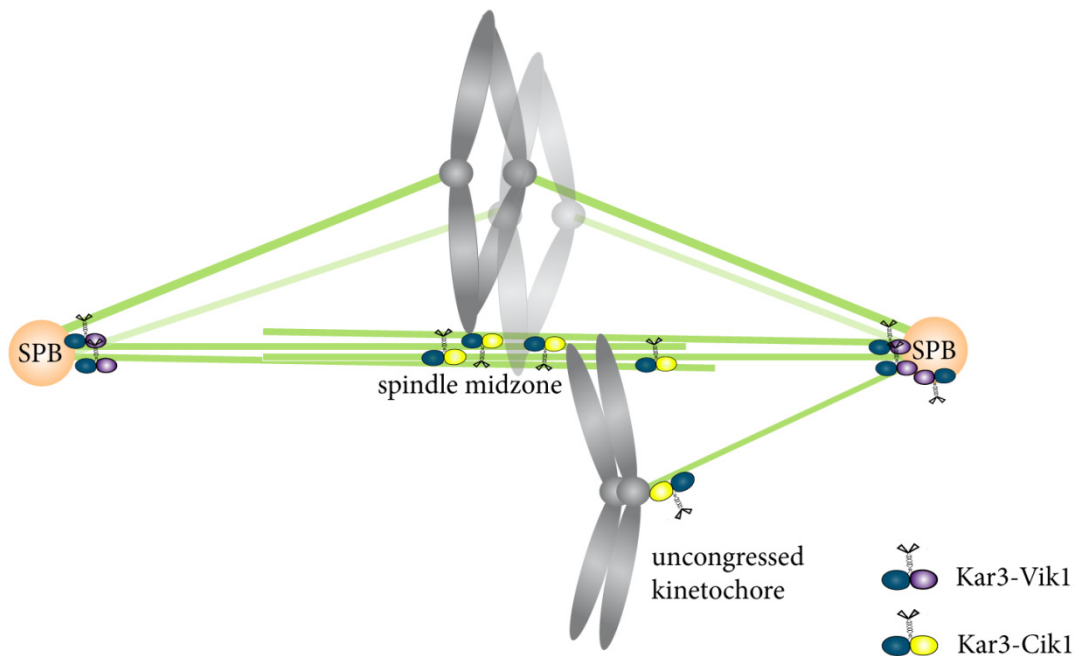


Figure 6. Localization dependencies of Kar3 during mitosis. The heterodimer composition dictates Kar3's subcellular localization: Kar3-Vik1 is recruited to SPBs and MT minus-ends, whereas heterodimerization with Cik1 brings Kar3 to the MT plus-ends.

2 Aim of the work

The conserved kinesin-8 and kinesin-14 motors are significantly involved in MT based processes throughout the cell cycle. Especially the correct assembly, maintenance and disassembly of the mitotic spindle require these motor molecules for precise coordination. Over the last two decades genetic experiments have elaborated the main contributions of the motors during mitosis. Simultaneously, the biophysical aspects of kinesin family members have been dissected carefully. How these molecular machines are embedded into the cellular context to carry out their specific functions, however, remains a challenging question. I aim to address this problem by investigating the molecular motor function of budding yeast kinesin-8 and kinesin-14 homologues during mitosis. Of particular interest will be the investigation of the spatiotemporal regulation that coordinates motor function within the mitotic spindle.

Kinesin-8 members are reported to control MT length homeostasis by combining their plus-end directed motility with a MT plus-end destabilizing activity. However, different MT subsets within the cell require a fine-tuned regulation of their length that might also change during the cell cycle. In order to unravel how this motor achieves the precise control of MT length I will examine the contribution of non-catalytic domains of budding yeast Kip3 to motor function *in vivo* and *in vitro*. To tackle this I will biochemically characterize different tail-truncated motors in comparison to full-length Kip3. I will further use live-cell microscopy to observe phenotypes that result from shortening Kip3s tail domain *in vivo*. In addition I will analyze posttranslational modifications of Kip3 to illuminate potential mechanisms of regulation.

Minus-end directed kinesin-14 motors have critical roles in spindle elongation and integrity. The budding yeast kinesin-14 Kar3 has been shown to accumulate on interpolar MT plus-ends in the spindle midzone upon heterodimerization with an adapter protein named Cik1. The observation that these proteins are interdependent for localization raises the question how a minus-end directed motor becomes enriched at the MT plus-end. To answer this question I will perform biochemical purifications of Kar3 and its dimerization partners to identify potential interacting proteins. I will perform reconstitution experiments to recapitulate plus-end loading of Kar3-Cik1 *in vitro*. In addition, live-cell microscopy will be used to analyze the motor behavior *in vivo*. A proteomic screen identified Kar3 as a target of the major cell cycle kinase Cdc28. I aim to analyze the phosphorylation state of Kar3 in detail to unravel how this motor protein is regulated within the cell.

3 Results

3.1 Results 1: Molecular mechanisms of kinesin-8 regulation in budding yeast

3.1.1 Expression and dynamic localization of Kip3p during cell cycle progression

Examination of Kip3p protein level in synchronized and subsequently released cells revealed a differential expression during cell cycle progression (Figure 7A). Concomitantly with raising Pds1p level in late G1/ early S phase Kip3p accumulates until it is most abundant in early anaphase when Pds1p degradation by the APC/C^{Cdc20} is already initiated (Figure 7A). The upregulation of Kip3p expression from S phase to anaphase implicates a potential requirement for this kinesin-8 during mitosis. To gain insight into Kip3's mitotic contribution, its subcellular localization was determined by live-cell imaging. Throughout the cell cycle Kip3p, fused to 3xGFP, decorates microtubules and accumulates at MT plus-ends in distinct spots. In metaphase the majority of Kip3p-3xGFP colocalized with the kinetochore protein Nuf2p-mCherry in a bilobed fashion. Upon anaphase onset Kip3p relocated to the anaphase spindle and concentrated at the spindle midzone with proceeding anaphase (Figure 7B). During mitosis Kip3p was also present on cytoplasmic MT plus-ends. The subcellular localization pinpoints the sites of action for Kip3 as a MT plus-end destabilizing enzyme of astral and nuclear MTs. The role of Kip3p can be easily deduced from its deletion phenotype. The absence of Kip3 causes extraordinary long astral MTs and an extended, often bent anaphase spindle (Cottingham and Hoyt, 1997).

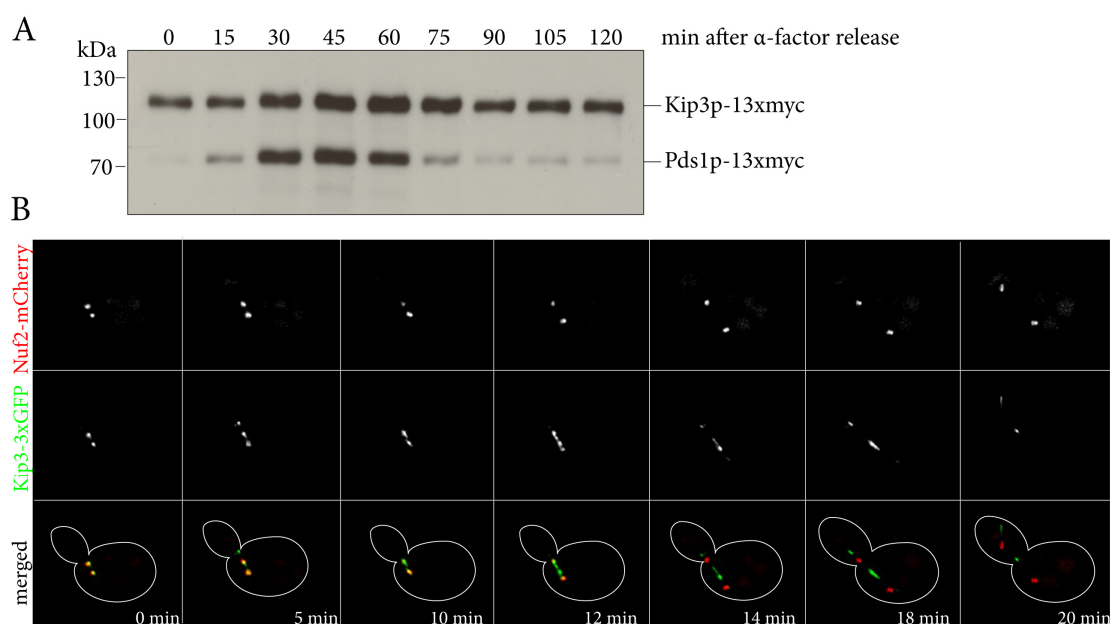


Figure 7. Expression and dynamic localization of Kip3p is coordinated by the cell cycle. A. Western blot analysis of 13x-myc tagged Kip3p and Pds1p during one cell cycle after release from α -factor induced G1 phase arrest. The expression state of Pds1p-13xmyc marks the cell cycle stage: Pds1p level rises from late G1 phase on until its destruction at anaphase onset. Note the increase in Kip3p in the time window between S phase and anaphase. B. Gallery, demonstrating the dynamic localization of Kip3p in meta- and anaphase. After anaphase onset Kip3p-3xGFP relocates to the spindle and accumulates at the spindle midzone with proceeding anaphase.

3.1.2 Analysis of affinity tag purified native Kip3p

The observed dynamic localization pattern of Kip3p posed the question whether interacting proteins or posttranslational modifications contribute in guiding this depolymerase to its site of action according to the cell cycle stage. To investigate this possibility a C-terminal tandem affinity tag was introduced into the endogenous *KIP3* locus and the motor was purified from log-phase yeast. Under stringent salt conditions of 300 mM KCl neither microtubule- nor kinetochore-associated proteins were identified by mass spectrometry analysis of the purification (Figure 8A). To increase the likelihood of detecting transient or low affinity interactions a single-step purification

using 6xFLAG tag at physiological salt conditions was employed (Figure 8B). Visualization of co-purifying proteins by SDS-PAGE and silver staining uncovered a predominant band co-purifying with Kip3p-6xFLAG. Mass spectrometry analysis identified all three Tubulin isoforms of budding yeast among the most abundantly co-purifying proteins. Consistent with the notion that ATP releases kinesins from the MT lattice, considerably more Tubulin was present in the purification in the absence of ATP (Figure 8B). Besides Tubulin significant amounts of heat shock protein 70 family members, Ssa2 and Ssb2, were detected in the native motor purification. Recently these proteins have been implicated in regulating the distribution of budding yeasts kinesin-5 motors thereby influencing spindle length (Makhnevych et al., 2012). Future experiments will reveal if this class of proteins affects the localization pattern of Kip3p. With low peptide counts two MAPs, She1p and Fin1p, were mapped among Kip3p's co-purifying proteins. However, localization of Kip3p was unchanged in cells deleterious for She1 (Woodruff et al., 2010).

The mass spectrometry analysis of native Kip3p identified several phosphopeptides that are summarized and further discussed in the following section.

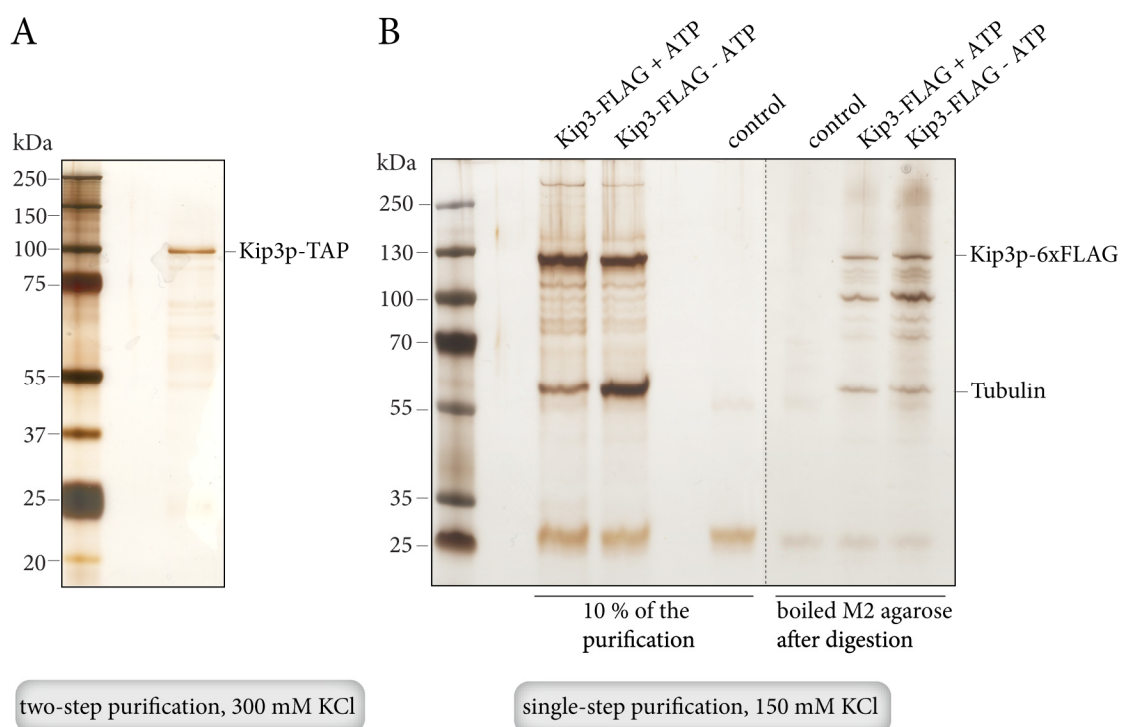


Figure 8. Affinity purifications of tagged Kip3p under indicated salt conditions. A. Silver stained SDS-PAGE of tandem affinity purified Kip3p. B. Single-step purification of the control and Kip3p-6xFLAG in the presence or absence of ATP on a silver stained SDS-PAGE.

3.1.3 Kip3p is phosphorylated by Cdc28p-Clb2p

A multitude of studies dissected the impact of phosphorylation on mitotic motors and compiled modifiable parameter ranging from localization pattern, MT binding, protein stability to control of autoinhibition (Cahu et al., 2008; Chee and Haase, 2010; Kim et al., 2010; Avunie-Masala et al., 2011). In order to determine if Kip3p is spatially or temporally phosphoregulated, affinity-purified native motor (Figure 8A and 8B) was analyzed for phosphorylated peptides using mass spectrometry. Three independent purifications revealed that most of the detected phosphosites cluster within Kip3p's tail domain (Figure 9D) and four of them match a minimal Cdc28 consensus site. To further verify the identified phosphosites *in vitro*, the full-length motor (Kip3p¹⁻⁸⁰⁵) and a tail-truncation (Kip3p¹⁻⁷⁰⁵) lacking the phosphosites assigned within Kip3's nonmotor

domain were expressed in baculovirus-infected Sf9 cells. Affinity purification from insect cell lysates with a hexahistidine (6xHis) tag fused to the N-termini of the kinesin constructs and subsequent cation exchange chromatography yielded a Kip3p fraction eluting at 350 mM salt (Figure 9A). *In vitro* kinase assays performed with recombinant Kip3p variants confirmed that Kip3p is a target of Cdc28p-Clb2p and furthermore corroborated the presence of most Cdc28 phosphorylation sites within the carboxyterminal 100 amino acids, since Kip3p¹⁻⁷⁰⁵ showed a strongly diminished γ -³²P incorporation compared to the full-length motor Kip3p¹⁻⁸⁰⁵ (Figure 9B). Mutation of three [S]-P sites that cluster within the nonmotor tail to alanine (Kip3p^{S730/734/736A}) reduced phosphorylation by Cdc28p significantly although not to the same level as the tail-truncated Kip3p¹⁻⁷⁰⁵ (Figure 9B). Upon mutation of two serines, S791/792A that are presumably targeted by a different kinase, no decrease in phosphorylation by Cdc28p/Clb2p was detected (Figure 9B). The identified phosphorylation sites derived from *in vivo* and *in vitro* experiments point towards the hypothesis that the nonmotor tail region of Kip3p is predominantly subjected to phosphoregulation (Figure 9C and 9D). However this regulation seems to involve several kinases due to the impossibility to assign all *in vivo* identified phosphosites to the particular kinases used in the *in vitro* kinase assays (Figure 9D).

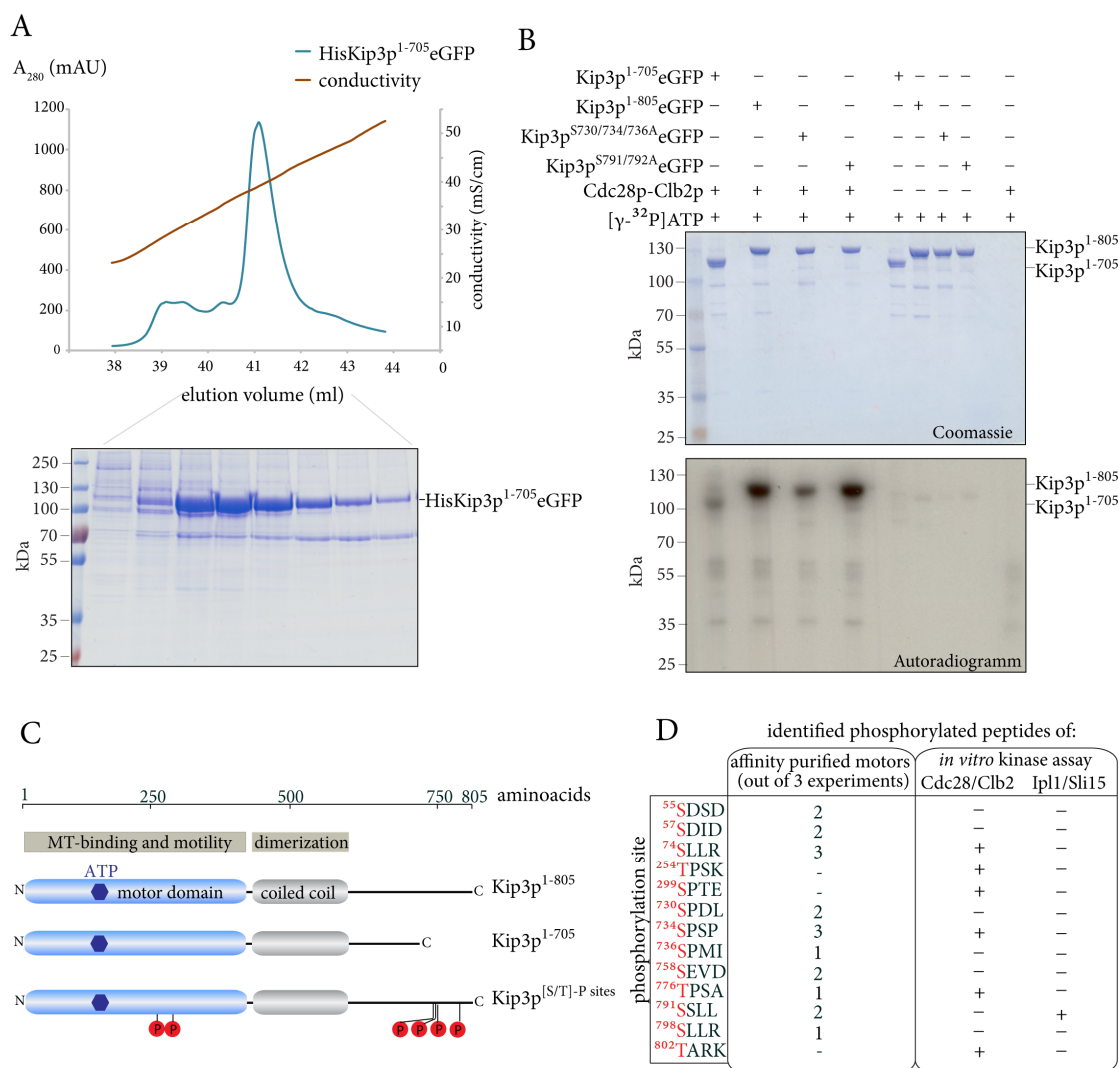


Figure 9. Kip3p is a target of Cdc28p/Clb2p *in vitro*. A. Representative cation exchange chromatogram of recombinantly expressed and purified Kip3p constructs. Kip3p elutes in a single-peak at 350 mM NaCl. B. *In vitro* kinase assay performed with recombinant motor and tandem affinity purified Cdc28p-Clb2p from yeast. Note that the phosphorylation of tail-truncated Kip3p¹⁻⁷⁰⁵ is significantly reduced. C. Model of the domain architecture of Kip3p and the tail-truncated motor. All identified phosphorylation sites that match a minimal Cdc28 consensus sequence [S/T]-P are highlighted in the lower model. D. Summary of identified phosphorylation sites from three purifications of native Kip3p from yeast extracts and *in vitro* kinase assays of recombinantly expressed Kip3p.

3.1.4 *In vivo* localization studies of Kip3p tail-truncations and phosphomutants

The preceding biochemical data uncovered the nonmotor domain of Kip3p as the predominant target of phosphoregulation; however, the consequences of phosphorylation and dephosphorylation on mitotic events remain to be identified. The following three sections will investigate the role of Kip3's tail domain and its posttranslational modification status *in vivo*. First, the localization of integrated Kip3 constructs fused to eGFP was monitored in a *kip3Δ* strain harboring Tubulin fused to mCherry (mCherry-Tub1). Live-cell imaging revealed that the tail-truncation of Kip3p¹⁻⁷⁰⁵ lacking the C-terminal phosphorylation sites behaved indistinguishably from full-length Kip3p, as it accumulated at the plus-ends of astral MTs and at the spindle midzone in late anaphase (Figure 10). This implies that plus-end directed motor activity in the tail domain truncation remains intact. The homodimer formation is a prerequisite for the remarkable processivity of Kip3p. In agreement with the plus-end enrichment of the tail domain truncation we show that Kip3p¹⁻⁷⁰⁵ homodimerizes *in vitro* (Figure 14C). In contrast, monomeric tail-less Kip3p¹⁻⁵⁰⁵ (Figure 14C) and Kip3p^{motor dead} (containing a defective ATP-binding pocket upon mutation of the Walker A motif) did not show the typical enrichment at the MT plus-ends but decorated the spindle uniformly (Figure 10). No spindle or MT decoration was observed for the dimeric tail version lacking the motor domain, Kip3p⁴⁴⁹⁻⁸⁰⁵, although expression was confirmed in Western blot analysis. This result is surprising since recent studies demonstrated spindle decoration by Kif18A's tail domain using microscopy. In addition biochemical experiments indicated the presence of an ATP-independent MT binding domain within the human and budding yeast kinesin-8's tail domain (Mayr et al., 2011; Stumpff et al., 2011; Su et al., 2011; Weaver et al., 2011). The MT binding affinity of Kip3 is reported to be between 10-100 fold lower than that of human Kif18A. The Kip3p⁴⁴⁹⁻⁸⁰⁵ tail construct also did not co-pellet with MTs in a co-sedimentation assay

under low salt conditions (Figure 13B). While these findings suggest that there is no strong microtubule-binding activity of the tail domain, it cannot be excluded that the carboxyterminal eGFP fusion might hinder the association of Kip3's nonmotor region and MTs.

Elimination of the phosphorylation cluster comprised of three juxtaposed minimal Cdc28 consensus sites in the tail (Kip3p^{3A}) did not alter the localization of the motor during the cell cycle. Mutation of all six potential Cdc28 phosphorylation sites to alanine, including two located in the motor domain (Kip3p^{6A}), prevented the motor from the characteristic MT plus-end accumulation (Figure 10). Since this mutant displayed MT decoration in all stages of the cell cycle it is conceivable that the catalytic motor activity is affected by the introduced mutations. Moreover, the distribution of the fluorescence signal of Kip3p^{6A} at late anaphase was strikingly different compared to all other mutants analyzed. Kip3p^{6A} was predominantly associated with astral MTs (Figure 10). This discriminates the localization pattern of Kip3p^{6A} from catalytically inactive Kip3p^{motor dead} and suggests a contribution of Cdc28 phosphorylation in the subcellular targeting of Kip3p. Future work will have to show which phosphorylation site combination accounts for the mislocalization phenotype of Kip3p^{6A} and if a phosphomimetic variant exhibits reciprocal behavior.

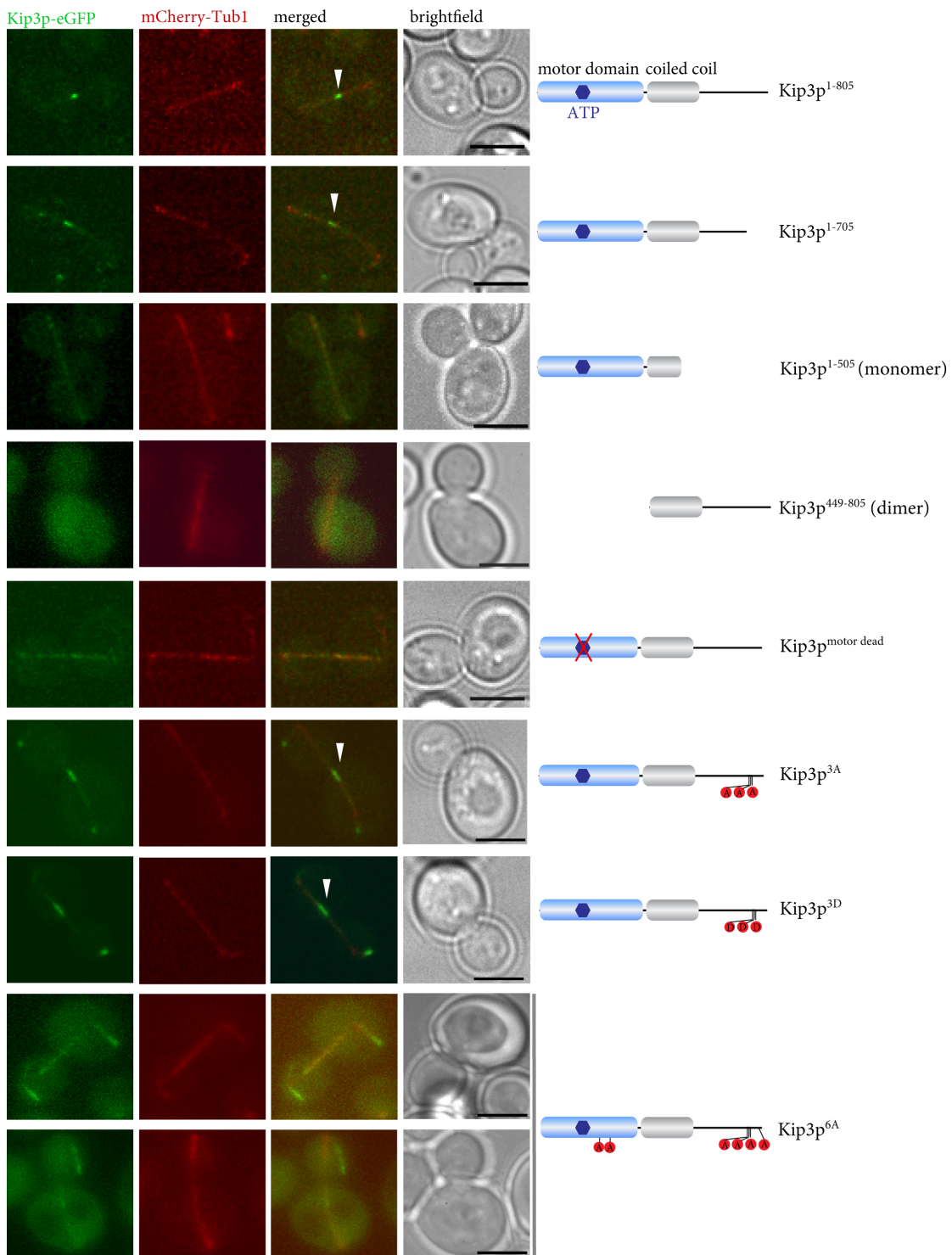


Figure 10. Localization gallery of Kip3p-eGFP truncations and phosphomutants in late anaphase. Live-cell imaging of chromosomally integrated Kip3 variants in a *kip3Δ*, mCherry-Tub1 background strain. Arrowheads indicate enrichment of the motor at the spindle midzone. Scale bar, 3 μ m.

3.1.5 Expression of the tail-truncation Kip3p¹⁻⁷⁰⁵ confers benomyl sensitivity

The hyperelongated MT phenotype of a *kip3* deletion mutant demonstrates the potency of this kinesin-8 motor as a MT destabilizing enzyme. An established assay to examine if Kip3 tail-truncations and phosphomutants influence the motor's regulatory function is to test benomyl sensitivity. Deletion of *KIP3* renders yeast resistant to the MT destabilizing drug benomyl, most likely because the absence of Kip3p's depolymerase activity counterbalances the drug induced effects on MTs. In agreement with the live-cell imaging and biochemical results the monomeric Kip3p¹⁻⁵⁰⁵, the tail domain Kip3p⁴⁴⁹⁻⁸⁰⁵, the catalytic inactive Kip3p^{motor dead}, the motor domain truncated Kip3⁸⁴⁻⁸⁰⁵ and the phosphomutant Kip3p^{6A} all phenocopy cells completely lacking Kip3p on benomyl plates (Figure 11). Consistent with previous findings, introducing a second copy of *KIP3* and thereby increasing the gene dosage 2-fold in wild-type *KIP3* cells causes a marked increase in benomyl sensitivity (Su et al., 2011). Strikingly the Kip3p¹⁻⁷⁰⁵ tail-truncation exhibits elevated benomyl sensitivity reminiscent of those entailed by doubling Kip3p levels. In order to delineate which region of Kip3's tail is responsible for the benomyl hypersensitivity tail-truncations eliminating blocks of 25 amino acids respectively were stably integrated into the *kip3Δ* strain and spotted onto benomyl plates with a reduced drug concentration. Unexpectedly, the truncations conferred benomyl sensitivity gradually with progressive shortening of the carboxyterminal tail (Figure 11., middle panel). The phenotype of the tail-truncated Kip3p¹⁻⁷⁰⁵ will be further dissected and discussed in the following sections.

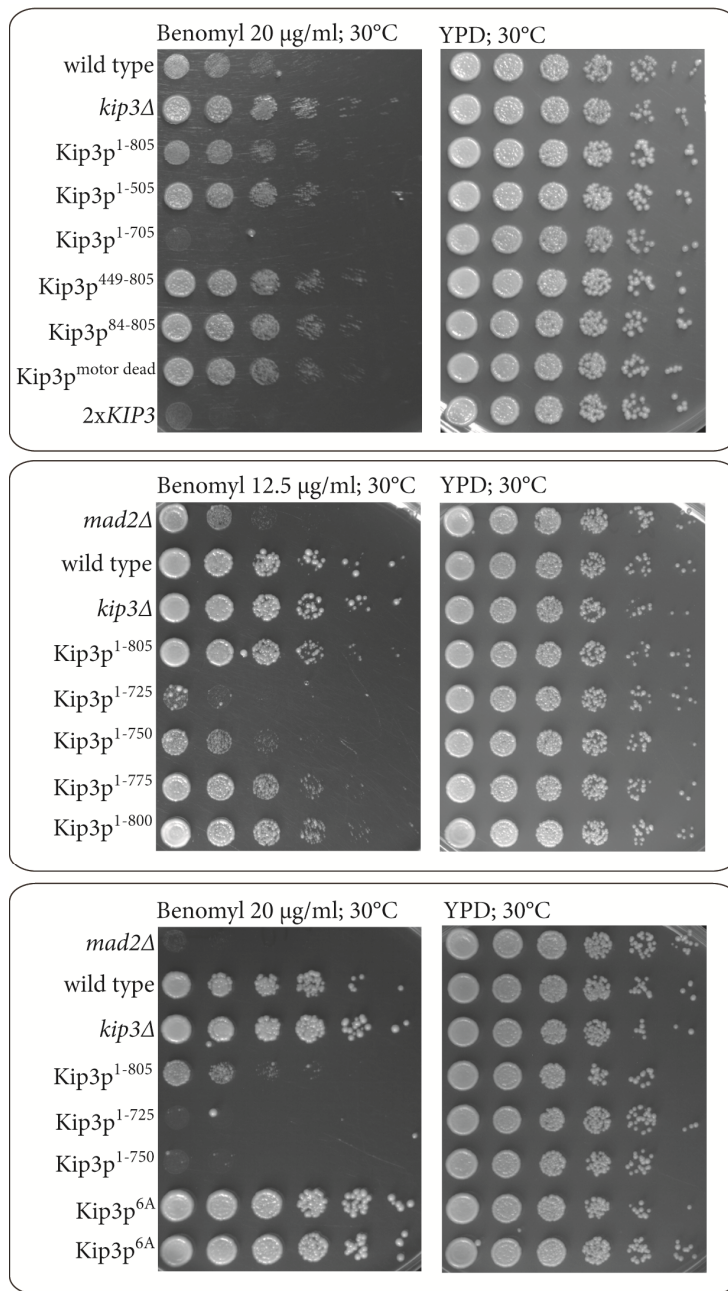


Figure 11. Differential effects of Kip3 tail-truncations and phosphomutants assayed on benomyl containing plates. The indicated Kip3 constructs were integrated into *kip3Δ* and spotted at 5-fold dilutions. Note the benomyl sensitivity of the doubled gene dosage of *KIP3* and the tail-truncation Kip3p¹⁻

705

3.1.6 The tail-truncated Kip3p¹⁻⁷⁰⁵ has opposite effects on spindle and astral MTs

The tail-truncation Kip3p¹⁻⁷⁰⁵ localized indistinguishably from full-length motor but exhibited benomyl sensitivity. A possible explanation for this would be a hyperactive motor molecule that would result in shortened MTs *in vivo*. To test this hypothesis live-cell recording was performed to visualize MTs (GFP-Tub1) after integration of Kip3 variants in a *kip3Δ* background. In addition, these imaging strains harbored a *cdc15-2* allele. Since MTs are dynamic in length, the *cdc15-2* induced late anaphase arrest adjusts the strains to the same cell cycle stage and thus allows easier comparison. Marking the spindle pole bodies (Spc42p-RedStar) further assists in identifying spindle ends. As expected, cells without a functional *KIP3* allele displayed an elongated spindle and extraordinary long astral MTs that often crossed the bud neck. Integration of full-length motor reversed the *kip3Δ* phenotype to normal MT length (Figure 12A-C). In cells with tail-truncated Kip3p¹⁻⁷⁰⁵ the measured anaphase spindle length was significantly shortened (Figure 12 A, B). This finding together with the increased benomyl sensitivity of Kip3p¹⁻⁷⁰⁵ supports the idea that this tail-truncation results in a motor molecule with increased activity at the anaphase spindle. Surprisingly, the majority of astral MTs were hyperelongated and often reached into the bud compartment in the presence of Kip3p¹⁻⁷⁰⁵ (Figure 12 A, C) which indicates the absence of a Kip3p depolymerase activity and phenocopies a *kip3Δ*. An obvious explanation would be that the truncated motor Kip3p¹⁻⁷⁰⁵ is incapable of localizing to astral MTs. Although the signal intensity of Kip3 in live-cell movies was not suitable for precise quantifications, Kip3p¹⁻⁷⁰⁵ was still detectable on astral MTs. Collectively these data indicate reciprocal effects of Kip3p¹⁻⁷⁰⁵ on different MT subsets within the cell. The Cdk1 phosphorylation mutant Kip3p^{6A} resembled a *kip3Δ* phenotype consisting of an elongated anaphase spindle and overgrown astral MTs (Figure 12 A-C) supporting the conclusion from the benomyl spot assay that Kip3p^{6A} is an inactive depolymerase.

Results

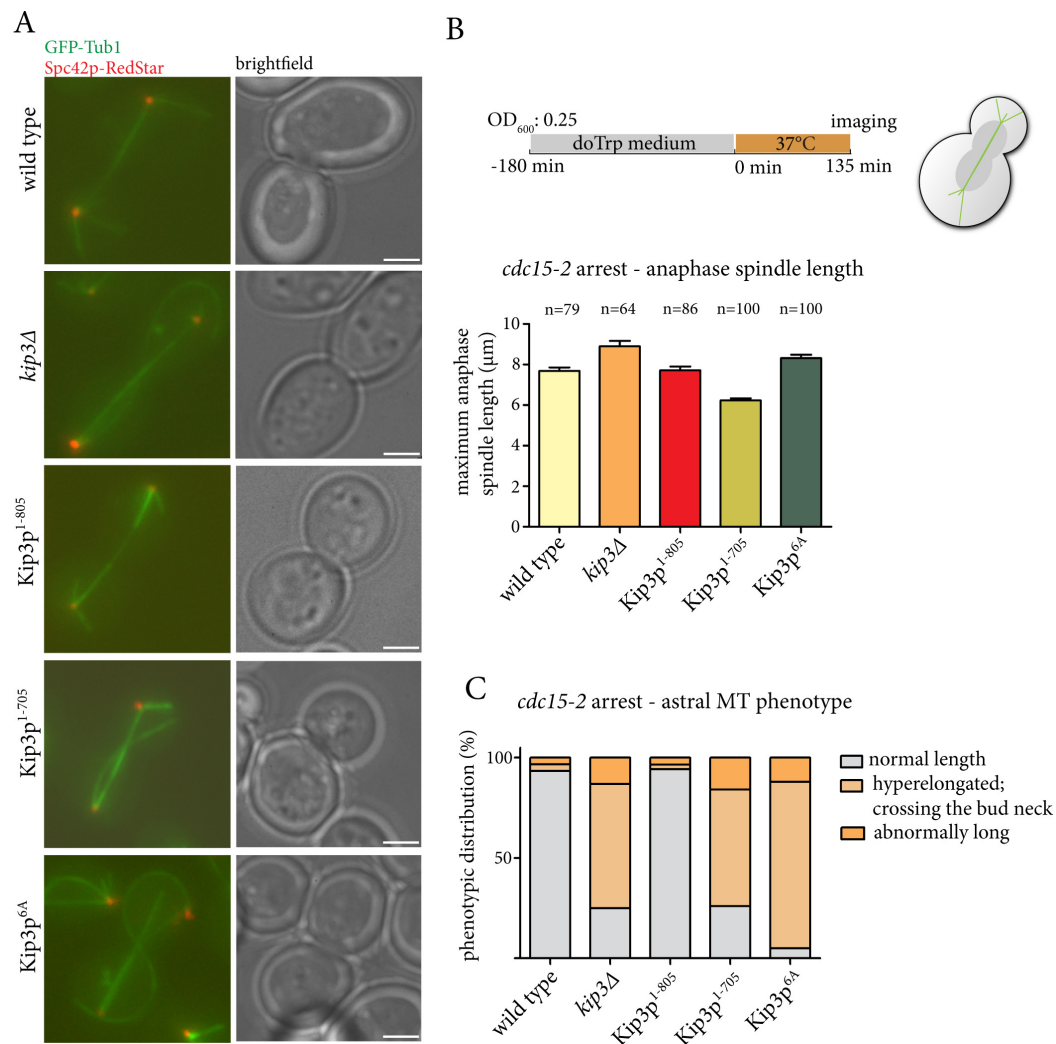


Figure 12. Localization gallery of Kip3p-eGFP truncations and phosphomutants in late anaphase. A. Live-cell imaging of chromosomally integrated Kip3 variants in a *kip3Δ*, GFP-Tub1, Spc42p-RedStar, *cdc15-2* background strain after shifting the cells for 135 min to the restrictive temperature. Scale bar, 2 μm. **B.** Measurement of anaphase spindle length in *cdc15-2* arrested cells reveals that the tail-truncated Kip3p¹⁻⁷⁰⁵ strikingly reduces spindle length. **C.** Dissection of the astral MT phenotype in three distinct subcategories analyzed in *cdc15-2* arrested cells.

3.1.7 Biochemical characterization of Kip3p and its tail-truncation mutant

The apparent gain of motor activity for the tail-truncated Kip3p¹⁻⁷⁰⁵ as documented in the benomyl spot assay and indicated by the short anaphase spindle raised the question whether this behavior is due to intrinsic biochemical properties of the motor molecule or is stimulated by accessory regulating proteins. To compare intrinsic motor activity of the tail-truncated Kip3p¹⁻⁷⁰⁵ to those of full-length Kip3p, a set of biochemical assays was performed. First, MT co-sedimentation assays were carried out to assess the MT binding activity and depolymerase activity of the motor. As expected, the major fraction of full-length Kip3p co-pelleted with GMPCPP-stabilized MTs in the absence of ATP and in the presence of AMPPMP, since the motor depends on ATP for MT detachment (Figure 13A). Upon addition of ATP the majority of Kip3p was found together with an increased amount of Tubulin in the supernatant of the co-sedimentation assay (Figure 13A). This outcome clearly demonstrates the functionality of full-length Kip3p as a MT destabilizing enzyme. Performing the same experiment with a mutant lacking the motor domains, Kip3p⁴⁴⁹⁻⁸⁰⁵, did not result in MT depolymerization and no MT binding was observed even under lowered salt conditions (Figure 13B). Applying the same assay to Kip3p¹⁻⁷⁰⁵ showed that with increasing amounts of motor more Tubulin was found in the supernatant fraction of the co-sedimentation assay. In line with the *in vivo* results it is apparent that the tail-truncated Kip3p¹⁻⁷⁰⁵ possesses a MT destabilizing activity. The quantification of the depolymerase activity between wild type and tail-truncated mutant was impossible due to considerable variations between the activity of different motor preparations.

Results

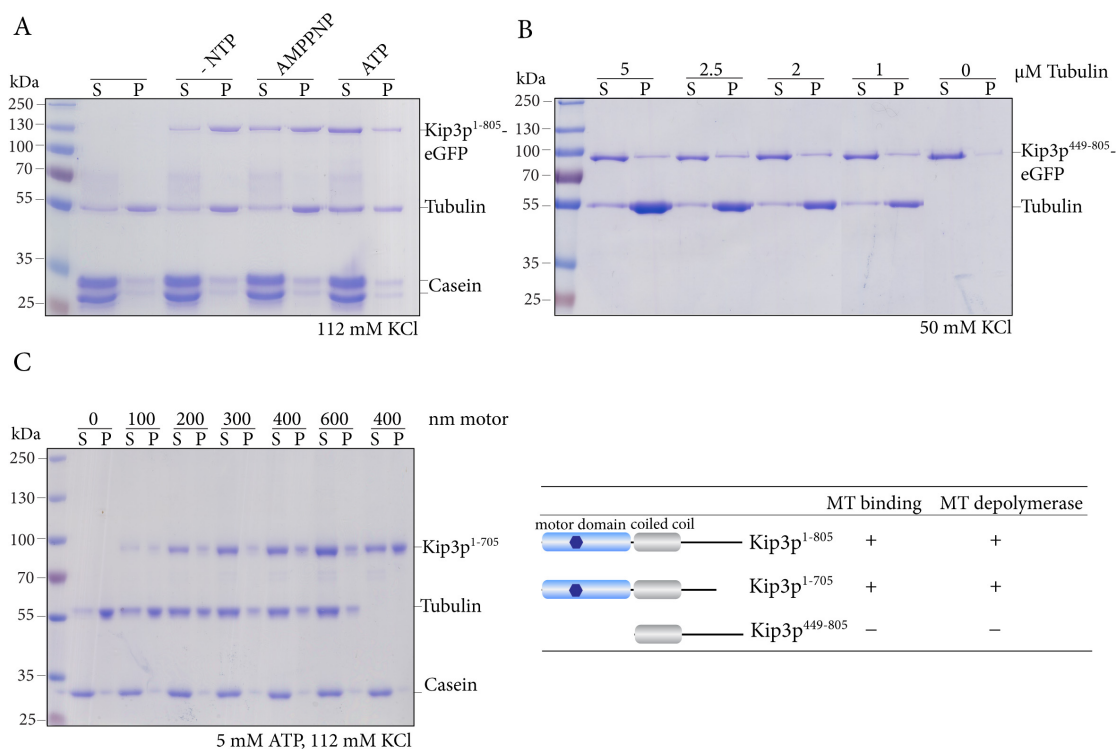


Figure 13. MT co-sedimentation assays demonstrate that Kip3p¹⁻⁷⁰⁵ and Kip3p¹⁻⁸⁰⁵ are MT destabilizing enzymes *in vitro*. A. MT co-sedimentation assay using GMPCPP-stabilized MTs of full-length Kip3p in the absence or presence of different nucleotides. Note that addition of 5 mM ATP stimulates MT depolymerase activity. B. No MT binding activity was observed in the MT co-sedimentation assay for the tail construct Kip3p⁴⁴⁹⁻⁸⁰⁵ even under low salt conditions. C. The tail-truncated Kip3p¹⁻⁷⁰⁵ is able to facilitate MT destabilization in the performed MT pelleting assay.

Several publications reported a secondary Tubulin binding site within Kip3's tail domain that could serve as a feedback-loop regulatory element constraining the motors depolymerase activity (Gupta et al., 2006; Su et al., 2011). To test the hypothesis that the hyperactive tail-truncation Kip3p¹⁻⁷⁰⁵ lacks this inhibitory feedback element, size exclusion chromatographic analysis was performed. Both full-length and tail-truncated motor were able to bind Tubulin thereby shifting the Tubulin elution fraction to a smaller elution volume (Figure 14A). This observation eliminates the possibility to explain the gain of motor activity upon truncation of the extreme 100 amino acids by the lack of a regulatory, nonmotor Tubulin binding site. In contrast, the kinesin-14

motor complex Kar3p-Cik1p was unable to bind Tubulin under the same conditions assuring that the Tubulin binding of the Kip3p constructs is not an artifact of the motor domain (Figure 14B).

Another potential explanation for the increase in activity of Kip3p¹⁻⁷⁰⁵ *in vivo* could be an alteration of protein stability by which more Kip3p¹⁻⁷⁰⁵ would accumulate through cell cycle progressions. Subsection 3.1.1 showed the cell cycle dependent expression pattern of wild type Kip3p. The time course experiment was repeated in a modified way: before the α -factor arrest strains expressing either full-length Kip3p, Kip3p¹⁻⁷⁰⁵ or the monomeric Kip3p¹⁻⁵⁰⁵ were combined, arrested and released. Time intervals were taken every 15 min and decreased to 5 min during the mitotic window. Western blot analysis visualized that similar to full-length Kip3p both truncations exhibited a cell cycle dependent expression pattern (Figure 14D). The different *in vivo* phenotypes of Kip3p and its truncations are therefore unlikely to be caused by changes in protein stability.

Results

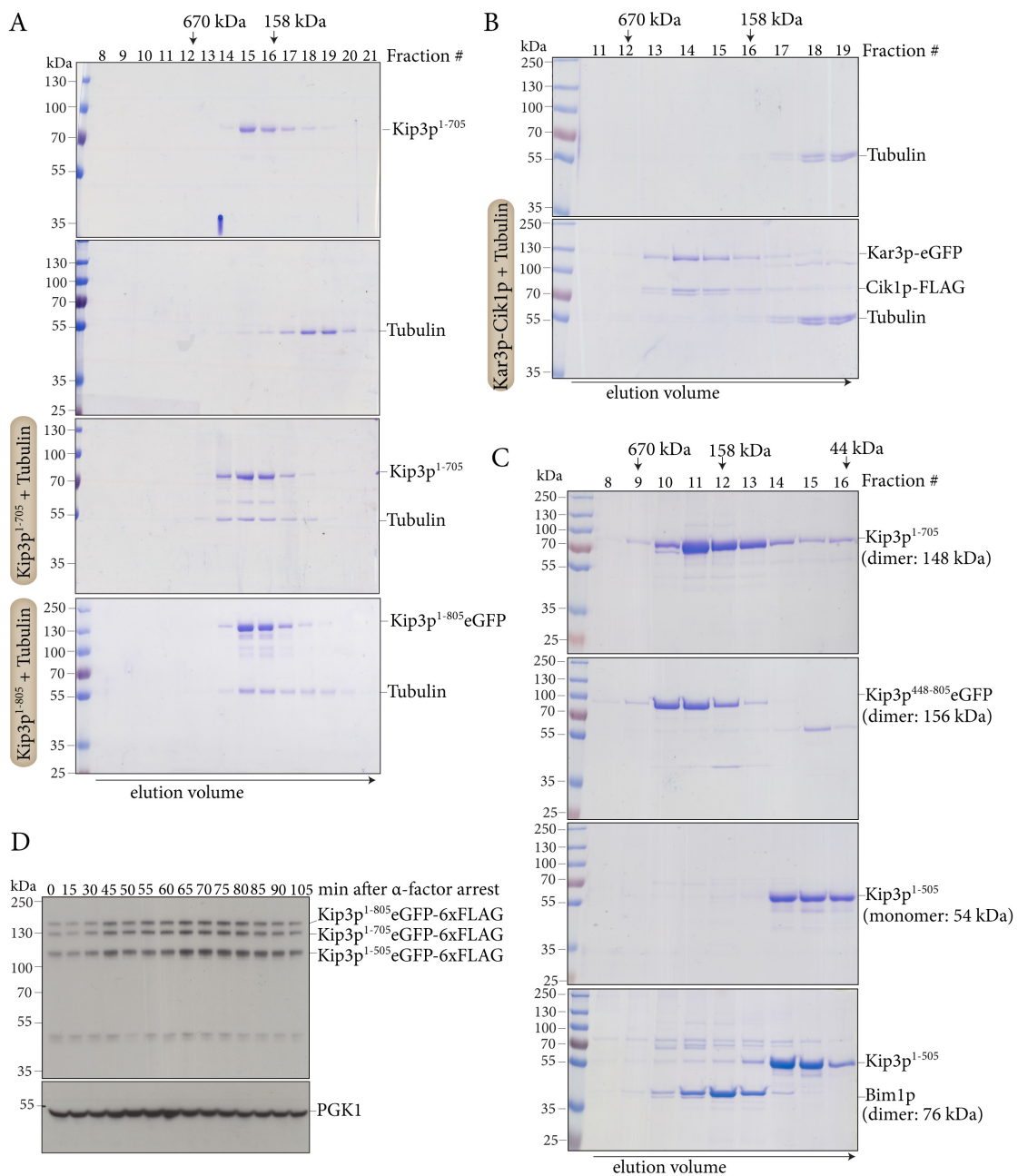


Figure 14. Both Kip3p¹⁻⁸⁰⁵ and Kip3p¹⁻⁷⁰⁵ are able to bind Tubulin dimers and show the same cell cycle dependent expression. A. Successive elution fractions on SDS-PAGE stained with Coomassie from size exclusion chromatographies performed either individually for motor and Tubulin or combined. Note that the Tubulin elution fractions shift to an earlier volume upon addition of full-length or tail-truncated motor. B. Size exclusion chromatography and subsequent SDS-PAGE analysis showing that Kar3p-Cik1p did not interact with Tubulin dimers. C. Size exclusion chromatographies do determine the dimerization status of Kip3p variants. D. Time course experiment following Kip3p expression level of full-length motor

and tail-truncations after release from α -factor induced arrest on a Western blot. PGK1 serves as a loading control.

The preceding biochemical comparison of full-length motor and tail-truncated variants cannot explain the phenotypic differences observed *in vivo*. Neither localization, protein stability, depolymerase activity nor the ability to bind Tubulin were altered upon truncation of the tail domain. In order to further ask if the *in vivo* manifested differences are intrinsic to the biochemical activity of the motor, TIRF (*total internal reflection fluorescence*) microscopy was used to determine the velocity of recombinant motor on taxol-stabilized MTs. It has been reported that tail-truncated human kinesin-8 displays an increase in velocity at the expense of decreased processivity (Stumpff et al., 2011). If this would be the case for Kip3p¹⁻⁷⁰⁵ too, it would be conceivable that the truncated version is more active because of the increase in velocity. Since kinesin-8 motors are the most processive kinesins, a potential decrease in processivity might have only a minor effect *in vivo*.

Kymographs of recorded movies of Kip3p-eGFP illustrate the gradient-like accumulation of motor molecules at the plus-end of the MT (Figure 15B, left kymograph). Upon decreasing the motor concentration to subnanomolar range single traces of individual motor molecules became apparent and motors were enriched at the MT plus-end due to the reported MT-plus-end dwell time of kinesin-8's (Figure 15B, right kymograph, (Varga et al., 2009)). Calculation of the observed velocities for Kip3p¹⁻⁷⁰⁵ and full-length motor did not show any significant difference. The analysis of motor velocities is in agreement with measured velocities from *in vivo* movies (4.43 $\mu\text{m}/\text{min}$; (Gupta et al., 2006)) and in range with those derived from *in vitro* studies (3.0 $\mu\text{m}/\text{min}$ (Varga et al., 2006)). The fact that the Kip3 truncation has different effects on different microtubules in the cell makes it unlikely that it is due to an intrinsic difference in

Results

motor activity. In support of this observation, the biochemical characterization has not revealed obvious differences in the activity between full-length and truncated motor.

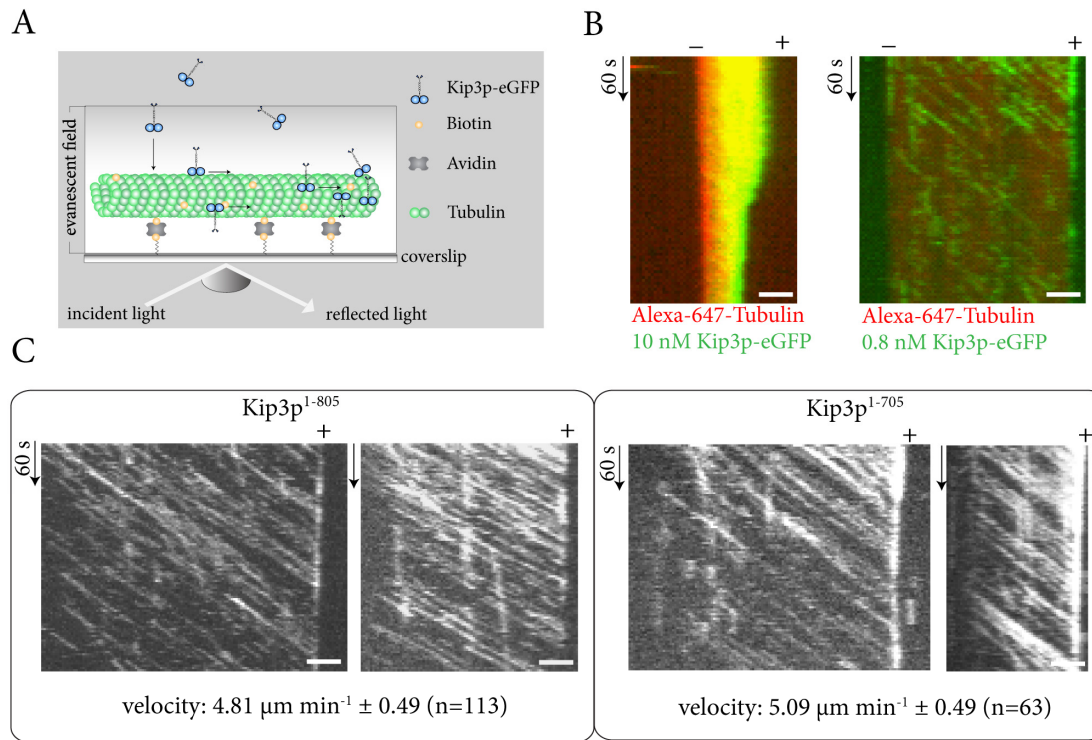


Figure 15. Kip3p1-805 and Kip3p1-705 move along stabilized MTs with the same velocity. A. Schematic representation of the TIRF microscopy imaging setup. B. Kymographs of two-color recordings taken at nanomolar and subnanomolar concentrations of Kip3p-eGFP. C. Representative kymographs derived from single-color recordings using unlabeled taxol-stabilized MTs. The velocities were calculated by tracing 100 individual motor molecules. Scale bar, 2 μm .

3.2 Results 2: Molecular analysis of kinesin-14 at the microtubule plus-end

3.2.1 The Kar3 accessory protein Cik1p co-purifies several +TIPs

Localization studies on the heterodimeric motor complex composed of Kar3p and Cik1p in mating pheromone-treated cells revealed an unexpected observation: although Kar3p-Cik1p is a minus-end directed kinesin, the motor complex couples MT plus-ends to the cortical shmoo tip (Maddox et al., 2003). During vegetative growth Kar3p-Cik1p decorates the anaphase spindle in a punctate manner which is believed to represent the accumulation of the motor at spindle midzone MT plus-ends (Gardner et al., 2008a). Further evidence for Kar3p-Cik1p functioning mainly at the plus-end comes from biochemical data that demonstrated a plus-end specific depolymerase activity for the motor complex *in vitro* (Sproul et al., 2005). Besides its role in spindle midzone maintenance, Kar3p-Cik1p was shown to contribute to the poleward transport of unattached kinetochores before their congression (Tanaka et al., 2005a). These findings have raised the question how the diverse mitotic functions of Kar3p in complex with Cik1p are achieved and regulated. Is the non-catalytic adapter protein Cik1p sufficient to govern Kar3 to a particular place of action or are additional proteins required for guiding the motor complex?

In order to identify potential interaction partner single-step affinity tag purifications of native Cik1p-FLAG from yeast extracts were analyzed by proteolytic digest and mass spectrometry. To distinguish between functions of Cik1p-Kar3p during karyogamy and mitotic division, FLAG tag purifications were performed from synchronized yeast cultures either to cover vegetative cell cycle stages or from α -factor arrested cells to imitate the mating response. The α -factor arrest mimics the mating situation during which a short isoform of Cik1p is expressed from an alternative start codon. To

investigate Kar3p-Cik1p during vegetative growth yeast cultures were logarithmically grown (log) or synchronized with either hydroxyurea to induce S phase arrest or nocodazole resulting in M phase arrested cells characterized by the absence of a mitotic spindle. In agreement with previous analysis an upregulated expression of the short isoform of Cik1p was observed after exposure to α -factor (Meluh and Rose, 1990; Benanti et al., 2009) (Figure 16A). Interestingly, Kar3p-eGFP migrated also faster when co-purified from α -factor arrested cells, which indicates either the presence of a truncated Kar3p during mating or posttranslational modifications during mitosis. As expected for a robust heterodimer formation between Cik1p and Kar3p mass spectrometry analysis revealed that Kar3p is indeed the major co-purifying protein having the second highest peptide counts in the different cell cycle stages (Figure 16B). As additional Cik1p co-purifying proteins three +TIPs were identified: Bik1p, Bim1p and Stu2p. None of those were found in the absence of microtubules in the nocodazole treated sample. This observation points to the hypothesis that the heterodimeric Kar3p-Cik1p might not only localize to microtubule plus-ends it might also physically interact with other +TIPs.

The observed role of Kar3p-Cik1p in the transport of unattached kinetochores would predict a direct interaction between the motor and the kinetochore during S phase when centromeres transiently detach from microtubules (Tanaka et al., 2005a). The only core kinetochore protein identified in Cik1p single-step affinity purifications was Ndc80p, a subunit of the Ndc80 complex, and the interaction was restricted to hydroxyurea-arrested cells. Two-hybrid screens have found potential interactions between Kar3p and Nuf2p, another subunit of the Ndc80 complex, and between Kar3p and Nnf1p, a subunit of the Mtw1 complex (Newman et al., 2000; Wong et al., 2007). Recently, the interaction between Kar3p-Cik1p and the Mtw1 complex was also observed in co-immunoprecipitation experiments (Jin et al., 2012). Hence a direct association between

Kar3p-Cik1p and core kinetochore proteins is very likely, but the precise interaction interface still remains unclear.

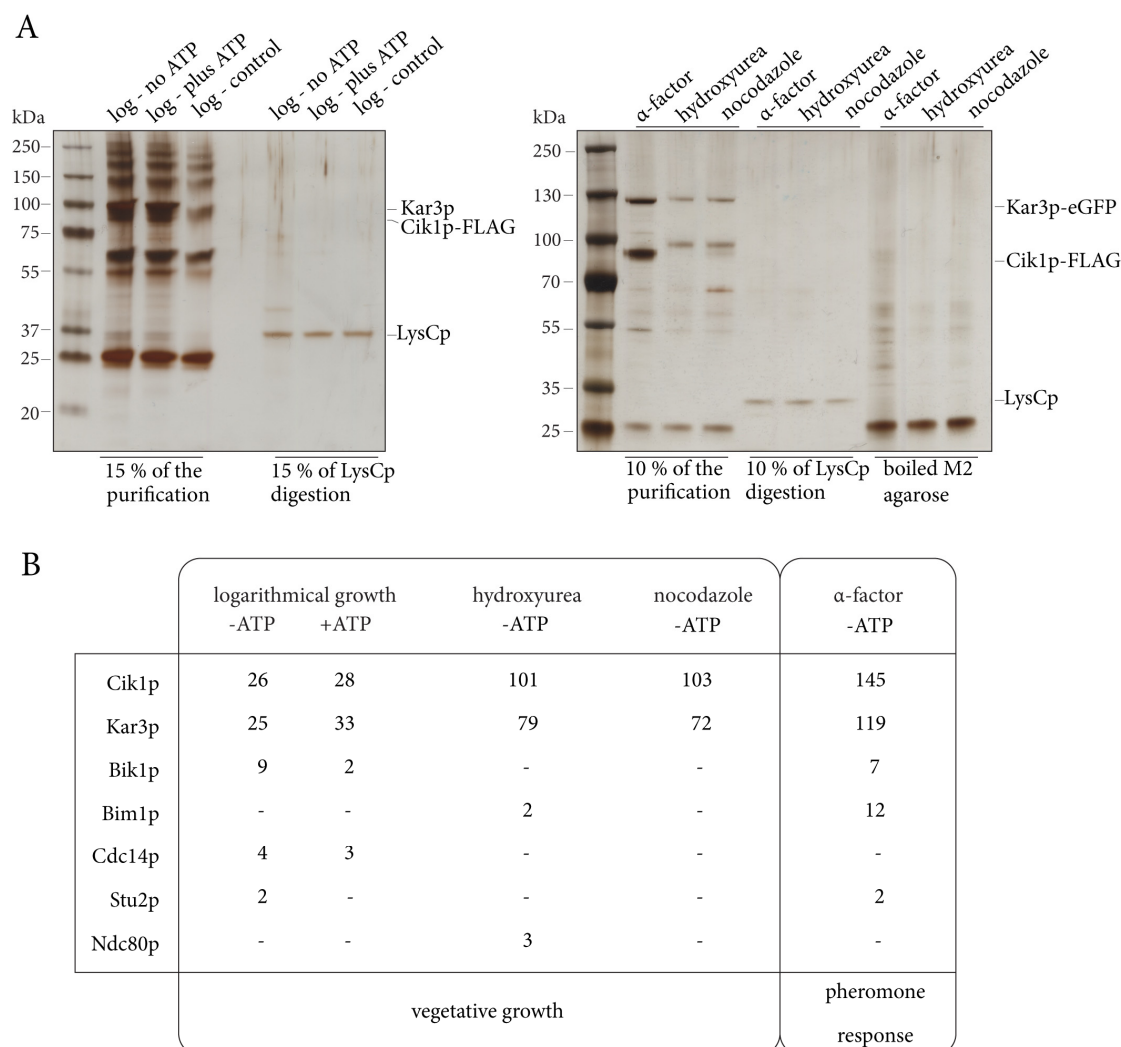


Figure 16. Single-step purifications of native Cik1p-FLAG from different cell cycle arrests. A. Silver-stained SDS-PAGE analysis of the Cik1p-FLAG purifications from yeast extracts and their proteolytic digestion by the endoproteinase LysC. The left gel shows the result for logarithmically grown cultures and the gel on the right side the cell cycle arrests. Note the faster migration of Cik1p-FLAG and Kar3p-eGFP from α-factor arrested cells. B. Selection of proteins identified by mass spectrometry, co-purifying with Cik1p-FLAG and their unique peptide counts under the indicated conditions.

As another Cik1p co-purifying protein the Cdc14p phosphatase was detected whose function is to regulate late mitotic events by dephosphorylating Cdc28 targets. In agreement, a studied showed that Kar3p is a target of Cdc28 (Ubersax et al., 2003). Phosphoregulation of the motor complex might be one tool to coordinate the mitotic functions of Kar3p-Cik1p and needs to be further investigated.

3.2.2 Localization of Kar3p during mitosis

Live-cell imaging of Kar3p fused to three tandem copies of GFP was conducted to analyze the subcellular localization during mitosis. The main fraction of Kar3p localized to spindle poles during mitosis, which is governed by the heterodimerization between Kar3p and Vik1p (Manning et al., 1999). A subset of Kar3p-3xGFP decorated the anaphase spindle (Figure 17A) and represents Kar3p-Cik1p complexes localizing to inter-polar MT plus-ends (Gardner et al., 2008a). Due to the weak signal of Kar3p-3xGFP on the spindle the exposure time was prolonged and deconvolution was omitted from movie processing. This setup allowed the visualization of Kar3p-3xGFP at the tip of nuclear MTs during meta- and anaphase (Figure 17B). Time-lapse movies revealed that the motor signal tracked growing and shrinking nuclear MTs. Note that Kar3p-3xGFP never decorated all nuclear MTs but rather localized infrequently to MT tips. Either Kar3p-Cik1p is recruited only to a particular subset of MTs, for example to fast growing MTs, or this microscopy approach is not sensitive enough to detect lower Kar3p concentrations on MT plus-ends.

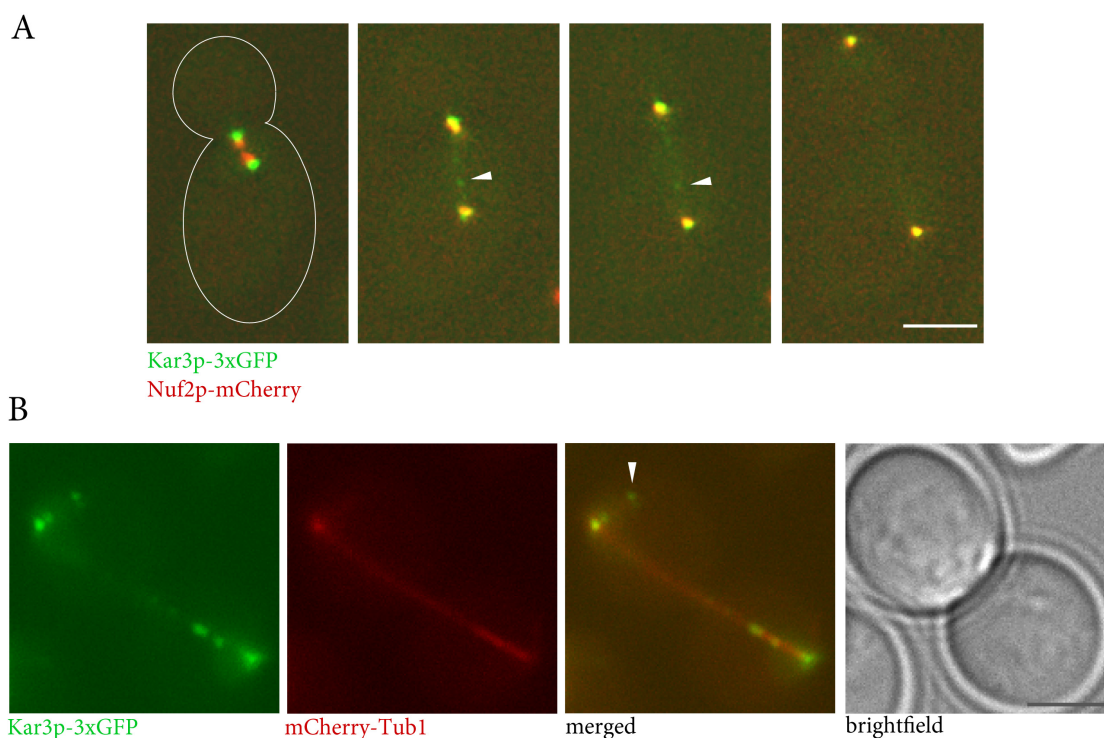


Figure 17. Localization of Kar3p-3xGFP in mitosis. A. Kar3p-3xGFP is recruited to spindle poles and does not colocalize with the kinetochore protein Nuf2p-mCherry in metaphase. During poleward sister chromatid segregation in anaphase the motor signal overlaps with the labeled kinetochore protein marker Nuf2p-mCherry. Scale bar, 3 μ m. White arrowheads indicate Kar3p-3xGFP on the anaphase spindle. B. The panel shows the sporadic decoration of nuclear MT tips by Kar3p-3xGFP (white arrowhead). Scale bar, 3 μ m.

3.2.3 The spindle localization of Kar3p-Cik1p depends on Bim1p in anaphase

What is the molecular basis of the observed MT plus-end recruitment of Kar3p-Cik1p? One potential interaction partner identified in the Cik1p-FLAG affinity purification (see 3.2.1) was Bim1p, the key regulator of plus-end networks. To determine if Bim1p contributes in recruiting the minus-end directed Kar3p-Cik1p motor complex to the microtubule plus-end, live-cell imaging of Kar3-3xGFP was performed in a *bim1* Δ strain. Whereas the localization of Kar3p-3xGFP at spindle poles was unchanged, no motor signal could be detected on anaphase spindles in the *bim1* Δ strain (Figure 18). This phenocopies Kar3p's subcellular distribution upon deletion of Cik1 (Figure 18) and

clearly indicates the requirement of both factors, Cik1p and Bim1p, for midzone localization of Kar3p. Consistent with the idea that the combination of Cik1p and Bim1p promotes plus-end accumulation *in vivo*, the sporadic decoration of nuclear MTs by Kar3-3xGFP could be detected in *vik1* Δ cells, but not in Bim1 or Cik1 deletion strains.

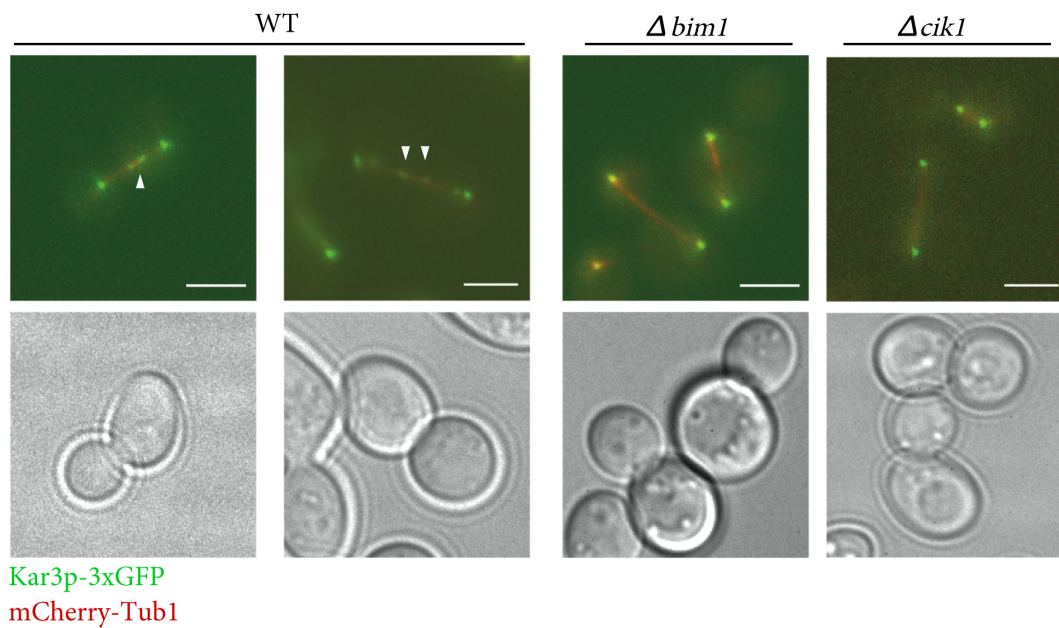


Figure 18. Localization of Kar3p to the spindle midzone in anaphase depends on both, Cik1p and Bim1p. The upper panel shows that Kar3p-3xGFP mainly localizes to spindle poles with a subset of motor molecules decorating the anaphase spindle in discrete spots (white arrowheads). The spindle localization of Kar3p-3xGFP is abolished in *bim1* Δ and *cik1* Δ cells. The lower panel depicts the corresponding brightfield images. Scale bar, 3 μ m.

3.2.4 Expression and Purification of full-length Kar3p-Cik1p

To investigate the molecular basis for a potential interaction between Kar3p-Cik1p and Bim1p I sought to express and purify the heterodimeric motor. So far biochemical data of Kar3p-Cik1p were derived from heterodimeric constructs containing large tail domain truncations within both proteins (Endow et al., 1994b; Mackey, 2004; Chu et al.,

2005; Sproul et al., 2005). Since kinesin tail domains are often mediating protein interactions the expression of the full-length heterodimer is important. To circumvent the difficulty that full-length motors often do not express in bacteria we took advantage of the galactose induced overexpression system in yeast. Coexpression of Cik1p fused to a C-terminal FLAG tag together with Kar3p enabled the purification of Kar3p in combination with Cik1p without enrichment for Kar3p-Vik1p heterodimers. Affinity purification followed by cation exchange chromatography yielded a sufficient amount of homogeneous Kar3p-Cik1p for biochemical studies (Figure 19).

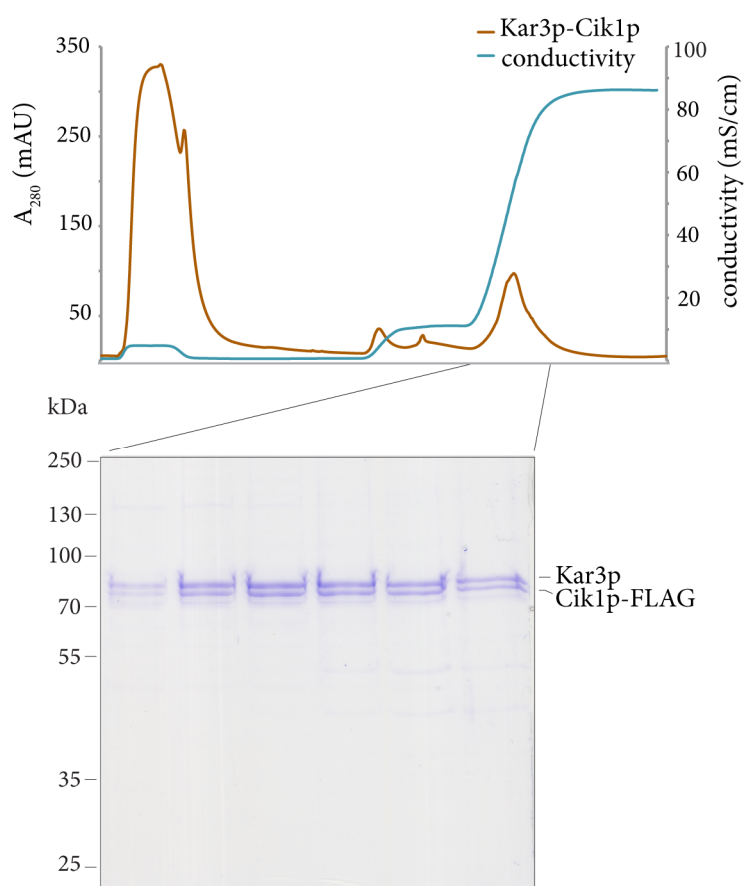


Figure 19. Cation exchange chromatography of Kar3p-Cik1p. The heterodimer elutes in a linear salt gradient at 350 mM NaCl. As judged from the corresponding Coomassie gel the heterodimer is composed of equimolar amounts of Kar3p and Cik1p.

3.2.5 Kar3p-Cik1p directly interacts with Bim1p

Live-cell imaging has revealed that Kar3p relies on Cik1p and Bim1p for MT plus-end recruitment. To biochemically investigate the interaction between the heterodimeric motor complex and Bim1p size exclusion chromatography was performed. The protocol to recombinantly express and purify Bim1p was already established in the lab (Zimniak et al., 2009). Elution of Kar3p-Cik1p as a single peak in the fractionation range of the gelfiltration required raising the salt concentration of the running buffer to 230 mM NaCl. Incubation of Kar3p-Cik1p with Bim1p followed by size exclusion chromatography and subsequent analysis of the elution profile by SDS-PAGE caused a clear shift towards a smaller elution volume compared to the individual gelfiltration runs (Figure 20). Coelution of the Kar3p-Cik1p heterodimer with the dimeric Bim1p demonstrates their direct interaction *in vitro* and explains the *in vivo* localization dependencies described in section 3.2.3.

In parallel a heterodimer composed of Cik1p and Kar3p-eGFP was purified applying the same protocol as described in 3.2.4. This motor complex showed the same behavior in gelfiltration analysis and MT-binding assays as Kar3p-Cik1p, indicating that GFP fused to Kar3's C-terminus does not interfere with heterodimerization and MT binding activity. In addition Kar3p-eGFP-Cik1p bound Bim1 to the same extent as Kar3p-Cik1p.

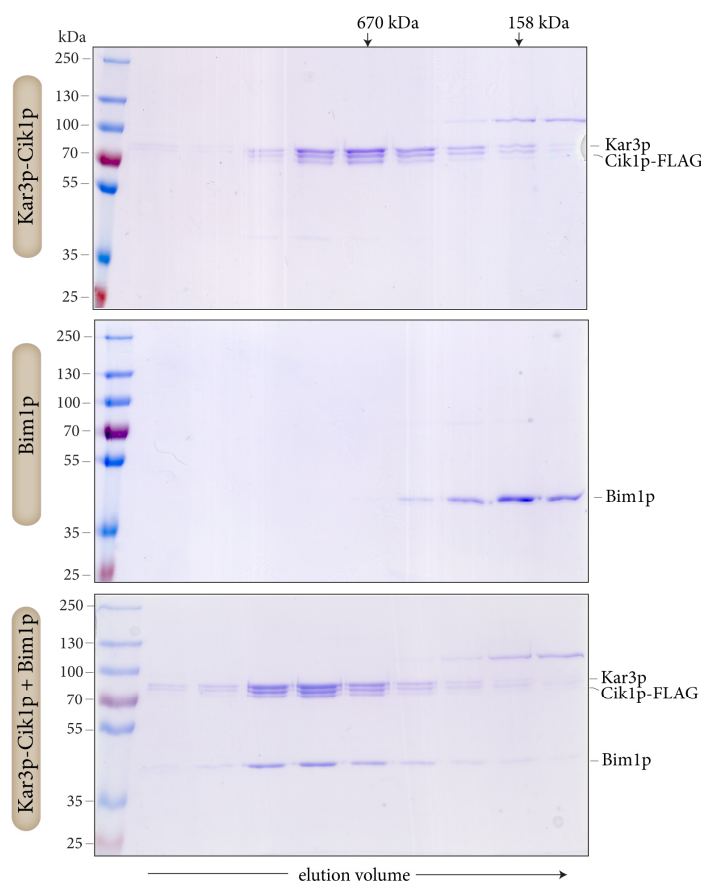


Figure 20. The Kar3p-Cik1p heterodimer interacts with Bim1p. Coomassie-stained SDS-PAGE analysis of gel filtration runs of the individual complexes and after combination.

3.2.6 Dissecting the interaction interface of Kar3p-Cik1p and Bim1p

The autonomous plus-end tracking Bim1p requires its N-terminal calponin homology domain for MT binding. The central coiled-coil region mediates homodimerization and the carboxyterminal EB1 homology (EBH) domain interacts with diverse cargo proteins (Akhmanova and Steinmetz, 2008; Zimniak et al., 2009). To map the interaction interface between Kar3p-Cik1p and Bim1p *in vitro* binding assays were performed with immobilized Bim1 truncation constructs encompassing either the N-terminal or C-terminal half of the protein. After incubation with the Kar3p-Cik1p complex, beads were washed and analyzed by SDS-PAGE. As expected, only full-length Bim1p and the

carboxyterminal fragment comprising the EBH domain efficiently coeluted with Kar3p-Cik1p (Figure 21A) indicating that binding of Kar3p-Cik1p is mediated by Bim1's C-terminus.

Usually complex formation between Bim1 and +TIPs is facilitated either upon recognition of the carboxyterminal EEY motif by CAP-Gly domain containing proteins or by association of Bim1 with proteins containing a conserved Ser-x-Ile-Pro (SxIP) motif. While neither Kar3p nor Cik1p contain a Cap-Gly domain, inspection of the extreme N-terminus of Cik1p revealed one canonical SxIP motif (Figure 21B). Notably, this motif is not found in the paralog Vik1p, it shows a high conservation among fungal Cik1 homologues and it is present in the longer isoform of Cik1p that participates in mitosis (Benanti et al., 2009). Mutation of the two SxIP motifs present in the Aurora B homolog Ipl1 has been demonstrated to abrogate binding to Bim1p (Zimniak et al., 2012). To test the role of the SxIP motif in Cik1p it was mutated to SxNN, expressed and purified in the presence of Kar3p and tested for association with Bim1p in pull-down assays (Figure 21C). The immobilized motor heterodimer devoid of a functional SxIP motif was still able to bind Bim1p in a concentration dependent manner. Thus, the SxIP motif of Cik1 is not strictly necessary for the association between Kar3p-Cik1p and Bim1p, yet the interaction appears weaker. Live-cell microscopy visualizing Cik1^{SxNN}-3xGFP in yeast confirmed the ability of this mutant to localize to the anaphase spindle. It appeared, however, that the signal was diminished compared to wild type.

To further define which region of Cik1 is essential for the interaction, the short mating isoform of Cik1 (Cik1p³⁵⁻⁵⁹⁴) and an additional N-terminally truncated construct of Cik1 (Cik1p²⁵⁰⁻⁵⁹⁴) was coexpressed with Kar3p and purified from yeast. *In vitro* binding assays revealed an extremely weak association between Cik1p²⁵⁰⁻⁵⁹⁴ and GST-Bim1p, whereas the short mating isoform, Cik1p³⁵⁻⁵⁹⁴, displayed Bim1p binding similar to full-length Cik1p (Figure 21E). This suggests that the described complex formation of

Kar3p-Cik1p and Bim1p might also play a role during mating and is not an exclusive feature of the mitotic isoform of Cik1p. The performed *in vitro* binding assays point to an interaction interface between Bim1's EBH domain and Cik1's N-terminus, but surprisingly the conserved SxIP motif does not appear to be strictly required for the interaction.

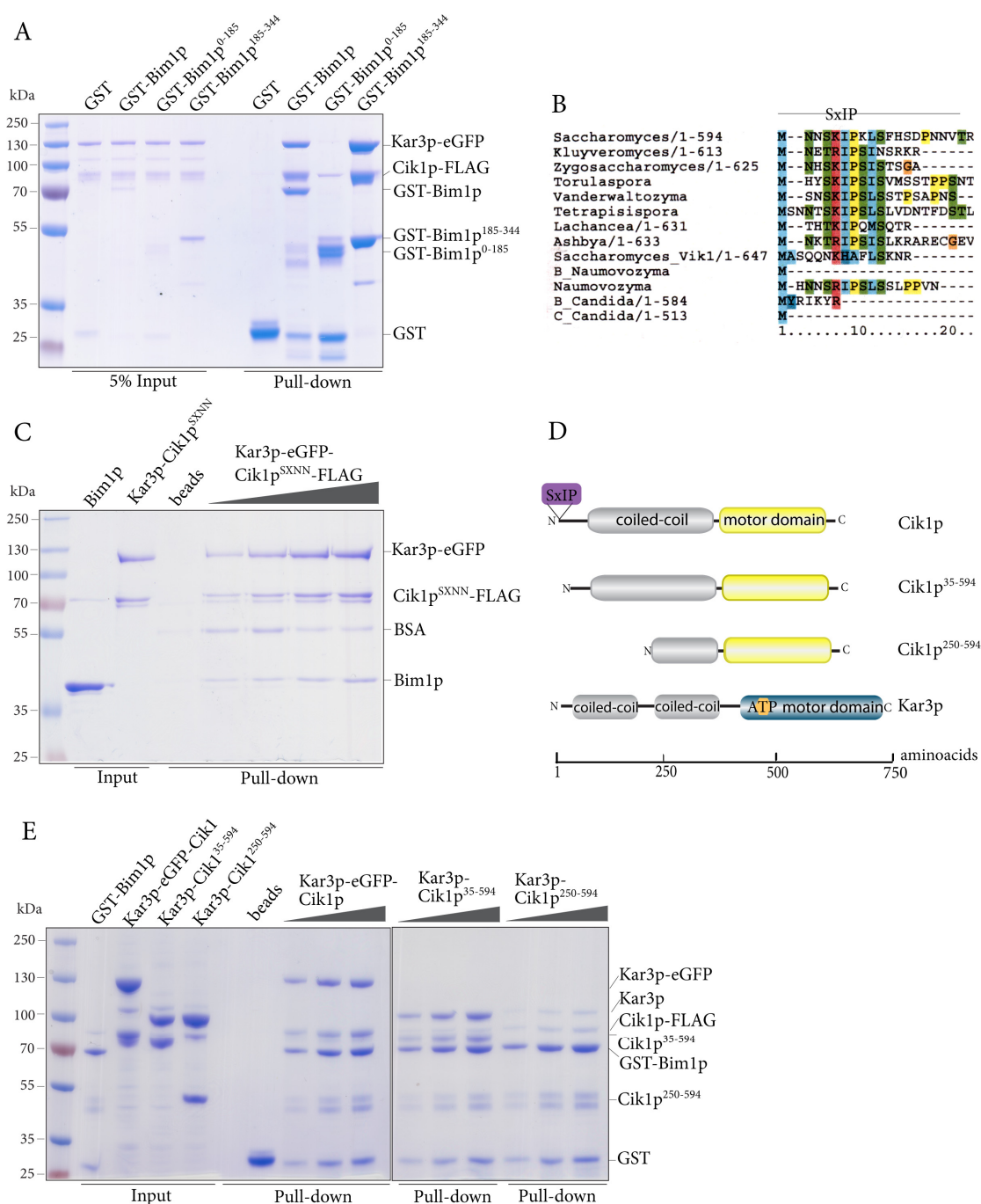


Figure 21. The C-terminus of Bim1p confers binding to the nonmotor domain of the Kar3p-Cik1p heterodimer. A. Pull-down experiments with immobilized Bim1 constructs or control GST-coupled beads. Only full-length Bim1p and the C-terminal fragment Bim1p¹⁸⁵⁻³⁴⁴ are able to bind Kar3p-Cik1p. B. Sequence alignment demonstrating the high level of SxIP motif conservation among fungal Cik1 homologues. C. Pull-down experiment with increasing concentrations of immobilized Kar3p-Cik1p^{SxNN} and constant amounts of Bim1p. After washing, bound complexes were eluted with 3xFLAG peptide revealing coelution of Bim1p with Kar3p-Cik1p^{SxNN} in a concentration dependent manner. D. Schematic illustration of the Cik1 constructs tested for binding to Bim1p. Note that all Cik1 variants are still able to dimerize with Kar3p. E. *In vitro* binding assay performed with immobilized GST-Bim1p shows impaired binding of Kar3p-Cik1p²⁵⁰⁻⁵⁹⁴ compared to Kar3p-Cik1p and Kar3p-Cik1p³⁵⁻⁵⁹⁴.

3.2.7 Bim1p assists Kar3p-Cik1p in MT-binding

The nonprocessive motor complex Kar3p-Cik1p binds MTs in a nucleotide-sensitive manner, whereas the adapter protein exhibits MT-binding activity on its own and determines the plus-end targeting of the heterodimer (Sproul et al., 2005). In order to investigate if Bim1p affects the MT-binding properties *in vitro* co-sedimentation assays with GMPCPP-stabilized MTs were carried out at relatively high ATP concentrations and under physiological salt conditions (140 mM NaCl). This setup facilitates cycling of the motor complexes between alternating states of MT attachment and detachment and results in the majority of Kar3p-Cik1p not co-pelleting with MTs (Figure 22A; upper gel). The same assay was performed in the presence of equimolar amounts of Bim1p. Although all heterodimer variants showed increased MT-binding activity upon incubation with Bim1p, the effect was weakest for Kar3p-Cik1p²⁵⁰⁻⁵⁹⁴, the construct that displayed only very faint Bim1p association as judged from the *in vitro* binding assays (Figure 21E). A significant portion of Kar3p co-pelleted with MTs when Kar3p-Cik1p and Kar3p-Cik1p³⁵⁻⁵⁹⁴ were premixed with Bim1p (Figure 22A, lower gel, Figure 22B). A similar result was observed when taxol-stabilized MT were incubated with Kar3p-eGFP-Cik1p and Bim1p and visualized by TIRF-microscopy (Figure 22C). Taken together

these experiments uncover a role for Bim1p in enhancing the MT-binding activity of Kar3p-Cik1p.

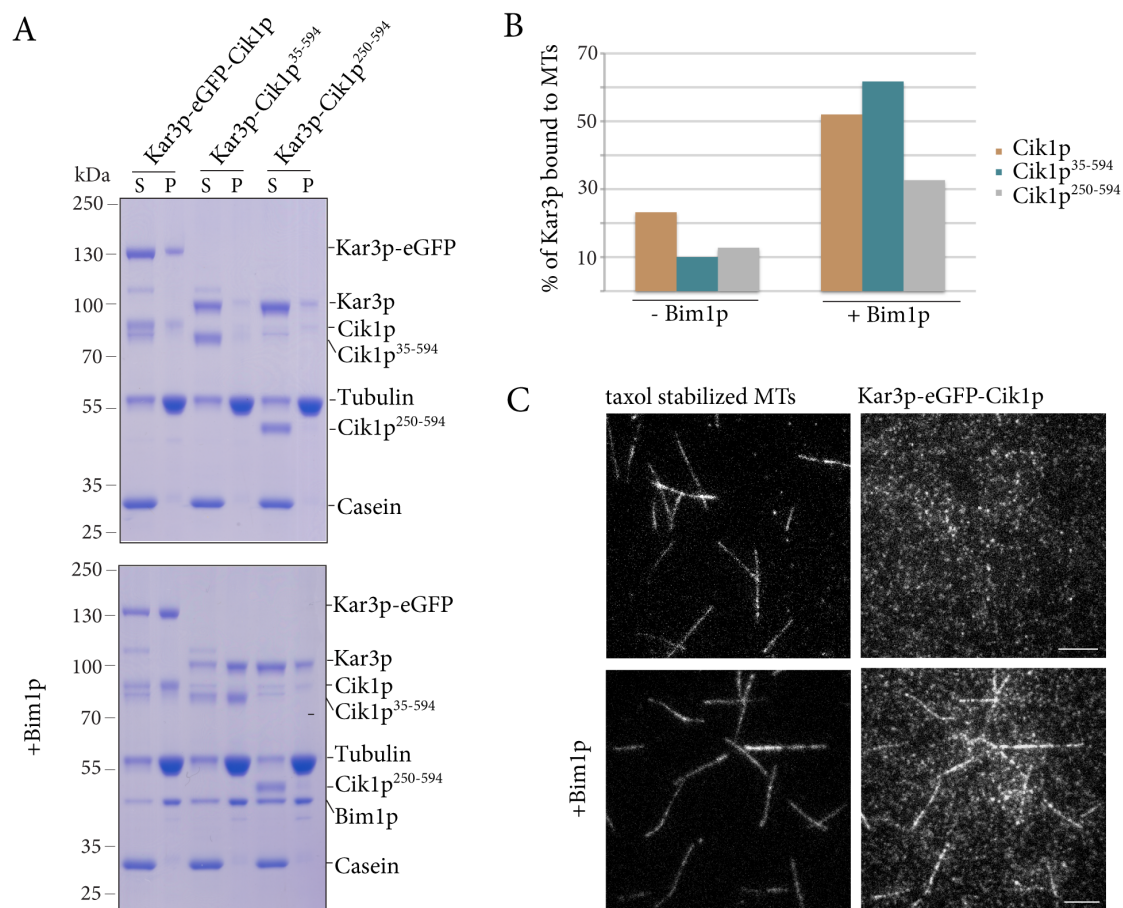


Figure 22. Bim1p stimulates the association of Kar3p-Cik1p to MTs. A. Co-sedimentation assays performed with 3.5 μ M GMPCPP-stabilized MTs, 500 nM of the motor complexes in the absence (upper gel) or presence of equimolar Bim1p (lower gel). Note the increase of motor co-pelleting with MTs after incubation with Bim1p. B. Quantification of the in A depicted co-sedimentation assay. C. Gallery visualizing the modulation of Kar3p-Cik1p's MT binding ability to taxol-stabilized MTs by Bim1p. Note that at high ATP concentrations and in the absence of Bim1p, Kar3p-eGFP does not efficiently decorate MTs. When the motor was premixed with Bim1p a significant enhanced MT-binding activity can be observed. Scale bar, 7 μ m.

3.2.8 Regulation of Kar3p during the cell cycle

A previous study found out that Cik1 protein levels oscillate during cell cycle progression, being low during G1 phase and peaking in mitosis, before the APC mediates Cik1p proteolysis (Benanti et al., 2009). To test if this regulation mode also applies to Kar3p, yeast cells were arrested in G1 phase by α -factor treatment. Samples were taken every 15 min after release and analyzed by Western blot analysis (Figure 23A). Compared to the loading control, Kar3p levels are low in the G1 arrest, peak during S phase and start declining before most of the cells are large budded (Figure 23A and B). This time course experiment identifies Kar3's cell cycle dependent expression pattern and raises the question if Kar3p is targeted by the APC for degradation in anaphase as it is the case for Cik1p (Benanti et al., 2009).

The purification of native Kar3p-Cik1p with subsequent mass spectroscopic analysis (section 3.2.1) detected phosphorylated peptides in respect to the cell cycle stage of sample. Both proteins were rarely phosphorylated in α -factor arrested cells and displayed maximal phosphorylation level during the HU arrest (Figure 23D). To visualize a potential phosphorylation-shift of Kar3p, samples from the time course experiment described before were loaded onto a SDS-PAGE gel that was supplemented with 30 μ M Phos-tag reagent followed by Western blot analysis (Kinoshita et al., 2006). In line with the mass spectrometry results, a slowly migrating form of phosphorylated Kar3p-eGFP was detected 30 min after release from α -factor arrest and disappeared in late anaphase around 105 min after the release. Half of the identified Kar3 phosphorylation sites in HU arrested cells match the minimal or full Cdc28 consensus sequence. In agreement with this, Kar3p was previously identified in a screen as a potential target of the Cdc28 kinase (Ubersax et al., 2003). Purified motor complex and Cdc28-Clb2 were used in an *in vitro* kinase assay and confirmed our *in vivo* data (Figure 23H). This assay clearly demonstrated that only the Kar3 subunit of the heterodimer is

subject to Cdc28 phosphorylation. However, effects of Kar3 phosphorylation on spindle integrity, localization and interaction with accessory proteins will be analyzed in the future.

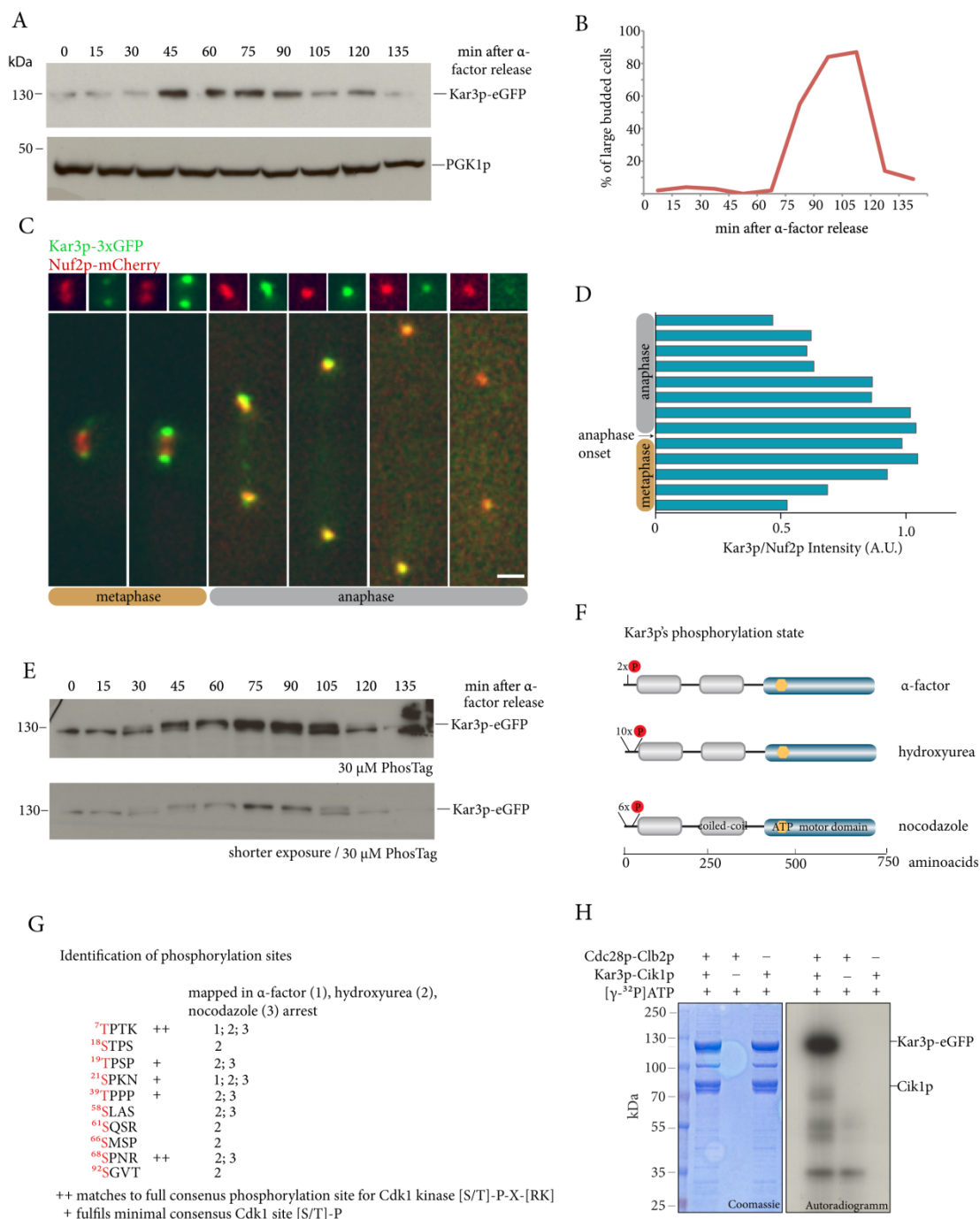


Figure 23. Kar3p is highly phosphorylated during mitosis *in vivo* and is targeted by Cdc28p-Clb2p *in vitro*. A. The upper gels shows the Western blot analysis of a time course experiment detecting Kar3p-eGFP level in 15 min intervals after release from α -factor arrest. Note the upregulation of Kar3 protein level during mitosis. PGK1 serves as a loading control. B. Budding index corresponding to the time course experiment depicted in A. C. Merged live-cell images following a transition from metaphase to late anaphase demonstrate the fluctuations of Kar3p-3xGFP intensities in comparison to Nuf2p-mCherry. Scale bar, 1 μ m. D. Ratio of the fluorescence intensities of the live-cell recording in C. E. Western blot of the time course analysis from A run on a SDS-PAGE supplemented with 30 μ m Phos-tag reagent. Note the appearance of a second, slower migrating Kar3p band at time point 30 that disappears when cells exit mitosis. F. Schematic illustration of the mass spectrometrically identified phosphorylation sites on Kar3 at the indicated cell cycle arrest. G. Overview showing which phosphorylation sites matches the Cdc28 consensus site. H. *In vitro* Cdc28p-Clb2p kinase assay performed with purified components clearly identifies Kar3p to be phosphorylated by the major cell cycle kinase.

4 Discussion

Mitotic motor molecules ensure accurate chromosome segregation. Although the biophysical aspects of kinesins have been carefully dissected, the regulation of individual family members in the cell remains largely unknown. This study analyzes the regulatory mechanisms that dictate budding yeast kinesin-8 and kinesin-14 motor activity in a spatiotemporal manner during mitosis. The budding yeast homologues of these kinesin families share some biochemical characteristics, for example MT plus-end localization and MT destabilization activity, but have different underlying molecular mechanisms (Sproul et al., 2005; Gupta et al., 2006; Varga et al., 2006). Here, biochemical characterization complemented by *in vivo* data and live-cell imaging revealed a motor regulation of kinesin-8 by its C-terminal tail domain, whereas an extrinsic adapter protein was identified to control kinesin-14's motor function in mitosis.

4.1 Insights into the role of the kinesin-8 Kip3 during mitosis

4.1.1 The subcellular localization of Kip3 unravels the need for regulation of its depolymerase activity

The visualization of hyperstable and elongated MTs in a *kip3Δ* background compellingly demonstrates the importance of this motor in controlling MT length homeostasis. *In vitro* studies uncovered the extremely high processivity of kinesin-8s that enables them to transport their own destabilizing activity towards the MT plus-end. Because of this remarkable processivity, longer MTs accumulate considerable more motor molecules at their plus-ends that in turn accelerate depolymerization. These findings are summarized in the length-dependent MT depolymerization model (antenna model) for human and budding yeasts kinesin-8s (Gupta et al., 2006; Varga et

al., 2006; Mayr et al., 2007; Varga et al., 2009). However, this notion is currently challenged by studies that carefully dissected the MT dynamics *in vivo* upon depletion of the respective kinesin-8. Unexpectedly, deleting kinesin-8 motors increased both MT rescue and catastrophe frequencies in human cells, budding yeast and *Schizosaccharomyces pombe* (Gupta et al., 2006; Unsworth et al., 2008; Du et al., 2010; Su et al., 2011). Strikingly, the fusion of Kip3's tail domain to a kinesin-1 motor domain resulted in extraordinary long cytoplasmatic MTs *in vivo* and had a MT stabilizing effect in an *in vitro* reconstitution system (Su et al., 2011). This study on Kip3 has expanded the antenna model by including a concentration dependent effect on MT dynamics: enrichment of Kip3 along longer MTs induces catastrophe events, whereas low Kip3 concentrations, for example on shrinking MTs, decrease the shrinkage rate and promote rescue (Su et al., 2011; 2012). The ability to stabilize short and shrinking MTs, while at the same time destabilizing long MTs would endow Kip3 with an ideal configuration to control MT length homeostasis.

Albeit Kip3 is dispensable for yeast viability the finding that Kip3 protein levels are dramatically upregulated from late G1 phase on argues for a requirement of the kinesin-8 motor not only in spindle disassembly where a high depolymerase activity is needed, but also during spindle formation and elongation. This seems to be a conserved feature as a similar cell cycle dependent expression has been documented for the human kinesin-8 members Kif18A and Kif18B (Mayr et al., 2007; Lee et al., 2010). At the onset of mitosis MT dynamics increase abruptly to allow spindle formation, this coincides with a gain of available kinesin-8 that might be required to fine-tune MT based processes (Desai and Mitchison, 1997).

Analog to the human kinesin-8, Kif18A, Kip3 accumulates at the plus-ends of metaphase spindle MTs colocalizing with a kinetochore marker ((Mayr et al., 2007; Stumpff et al., 2008) Figure 7B). Anaphase onset promotes rapid relocalization of Kip3 from kinetochores to the spindle until it becomes gradually enriched at the midzone with proceeding anaphase. This behavior cannot be described by the antenna model alone and suggests additional regulatory modes. According to the extended antenna model Kip3 would exhibit a maximum MT depolymerization rate in metaphase and late anaphase, due to the observed MT plus-end accumulation of Kip3 at this time points. While a high depolymerization activity of Kip3 is plausible in late anaphase in order to disassemble the spindle, a constant MT destabilization during metaphase seems rather unlikely since depletion of Kip3 does not alter metaphase spindle length (Woodruff et al., 2010; Wargacki et al., 2010a). By contrast, human Kif18A dampens MT dynamics during chromosome congression (Stumpff et al., 2008; Du et al., 2010). Due to the fact that the extended antenna model cannot explain this controversy we hypothesize the presence of an additional regulation mode that controls Kip3's depolymerase activity synchronized to the cell cycle. Independent of its motility, the MT destabilizing activity of Kip3 during metaphase must be down-regulated compared to spindle disassembly where a robust Kip3 activity is needed to depolymerize interpolar MTs (Woodruff et al., 2010; 2012).

Another argument for more complex regulation is that the different microtubule populations within the cell show very different behavior at the same time point. During anaphase Kip3 activity on interpolar microtubules needs to be restricted to allow elongation, while at the same time astral MT growth is restricted to allow interaction with the cortex for spindle positioning. Neither this study nor other groups have so far identified any interacting protein capable of modulating Kip3's depolymerase activity, therefore it is conceivable that posttranslational modifications take part in regulating Kip3's activity.

4.1.2 Regulation of Kip3 by Cdc28

Phosphorylation is a potent tool to modulate several parameters of mitotic motor function. The human and *Xenopus* kinesin-7 motor, Cenp-E, for example, is subject to an elaborate mode of phosphoregulation. Control of Cenp-E's activity during chromosome congression occurs on one hand via phosphorylation by either MPS1 or CDK1, which causes the relieve of the motor from its autoinhibited state, and secondly by Aurora kinases which phosphorylate Cenp-E and thereby reduce the MT binding affinity of the motor (Espeut et al., 2008; Kim et al., 2010). However, understanding the phosphoregulation of budding yeasts mitotic kinesins has largely remained elusive. So far only the kinesin-5 motor Cin8 is an identified and verified target of Cdc28 *in vivo* and *in vitro*. In this case dephosphorylation of Cin8 promotes binding to the pre-anaphase spindle and phosphorylation causes release of the motor from the anaphase spindle that reduces the spindle elongation rate (Chee and Haase, 2010; Avunie-Masala et al., 2011).

Indications for Kip3 as a Cdc28 substrate are based on a proteomic screen (Ubersax et al., 2003). Moreover it was shown that Kip3 is phosphorylated *in vivo* but most likely not by Ipl1 (Woodruff et al., 2010). My study provides evidence for a phosphoregulation of Kip3 by Clb2/Cdc28 and supports the observation that Ipl1 is not involved in regulation of this motor. Combining our knowledge derived from *in vivo* and *in vitro* experiments discloses a more complex phosphoregulation that might involve additional kinases. Half of the *in vivo* identified phosphorylation sites match a Cdc28 consensus sequence and the majority of these cluster within the extreme carboxyterminal 100 amino acids of Kip3. This finding supports the observation that especially the divergent nonmotor domains of kinesins are primarily subjected to phosphoregulation (Verhey and Hammond, 2009). Elimination of all six potential Cdc28 sites within Kip3 altered the motor activity and phenocopied a *kip3Δ* strain regarding benomyl sensitivity, astral

MT and spindle length. Although this phosphorylation-preventing mutant was capable in MT binding, the localization pattern was shifted towards a stronger decoration of astral MTs at the expense of midzone accumulation. Further experiments will have to dissect if the motor activity of this mutant is compromised and, if so, to what extent. Up to this point, this phosphorylation mutant indicates that Cdc28 is indeed a potential candidate to regulate Kip3's depolymerase activity and / or localization.

4.1.3 Contribution of Kip3's tail domain in regulating MT length homeostasis

The tail domain of human and budding yeast kinesin-8s was recently examined in detail. Three studies on human Kif18A concordantly described the existence of an additional MT binding site within the tail domain that is critical for the enormous processivity of the motor and increases the residence time at the MT plus-end (Mayr et al., 2011; Stumpff et al., 2011; Weaver et al., 2011). Visualization of the respective tail-only fragments in HeLa cells showed MT lattice decoration. Remarkably, the shortest of the tested tail-fragments, Kif18A⁸⁰²⁻⁸⁹⁸ was sufficient to bind MTs (Weaver et al., 2011). Although the tail domains of human and budding yeast kinesin-8 display no detectable similarity, also Kip3's tail has been reported to harbor a nonmotor MT binding site that increases processivity (Su et al., 2011). However, the reported weak MT binding activity of Kip3's tail domain *in vitro* was never observed during my study, though the tested tail domain encompassed nearly the same amino acids. This difference could be explained either by differential C-terminal tags that might interfere with MT binding or by the source of motor protein, since Kip3 used in this study was purified from Sf9 insect cells compared to overexpressed motor from yeast in (Su et al., 2011). A possible interference of the C-terminal eGFP tag with MT binding activity could also explain why we could not visualize the tail-only Kip3⁴⁴⁹⁻⁸⁰⁵-eGFP *in vivo* on the MT lattice (Figure 10).

Spindle length is a simple and reliable readout for the activity of kinesin-8 motors. The previously reported phenotypes for tail-truncated kinesin-8 molecules from budding yeast, fission yeast and human cells demonstrated the inability of these tail-shortened constructs to restore spindle length in a kinesin-8 deletion background (Unsworth et al., 2008; Mayr et al., 2011; Su et al., 2011). During our analysis we identified a Kip3 tail-truncation (Kip3¹⁻⁷⁰⁵) that localized indistinguishably from the full-length motor to MT plus-ends and the spindle midzone, indicating similar motor properties regarding processivity. Excitingly, this truncation was still able to regulate MT length *in vitro* and led to a shorter anaphase spindle *in vivo* (Figure 12A and B, Figure 13A). One plausible idea would be that our tail-truncation retains the motor activities but lacks regulatory elements that would inhibit its activity. Consistently, this mutant renders yeast highly sensitive to benomyl, similar to a 2-fold increased *KIP3* gene dosage (Figure 11). However, the lack of an inhibitive regulatory element cannot serve as the sole description for Kip3¹⁻⁷⁰⁵, since the observed astral MTs in this strain are abnormally elongated reminiscent of those in *kip3Δ*. Taken together this implies that the tail-truncated Kip3¹⁻⁷⁰⁵ behaves as a hyperactive motor within the spindle MTs, whereas it acts on astral MTs like a catalytic-dead motor. To this end we can only speculate about the origin of these divergent effects of Kip3¹⁻⁷⁰⁵ on different subsets of MTs. Kip3 has been implicated to interact with cortical factors to cooperatively regulate astral MT length during spindle positioning (Gupta et al., 2006). We assume that a so far unidentified factor is required to assist Kip3 in regulating astral MT length and that the tail-truncated Kip3¹⁻⁷⁰⁵ might be incapable of binding this factor. Conversely, a different factor or modification that normally restricts activity of Kip3 on the spindle is unable to regulate Kip3¹⁻⁷⁰⁵.

Although we cannot explain the tail-truncation phenotype completely, our mutant clearly shows that the intrinsic motor properties of Kip3 alone are not sufficient to

describe the motor function *in vivo*. Regulatory modes by posttranslational modification and / or interacting proteins are required to control MT length in the particular subcellular context. Subsequent work will have to refine the molecular mechanism of Kip3's tail elements. The benomyl spot assay presented in this work pointed out that the truncation of the very carboxyterminus in 25 amino acid increments affected motor functions gradually, instead of identifying one regulatory domain. The tail domain of Kip3 is responsible for defining its motor activity during cellular processes. Besides regulating the motor activity, the nonmotor domain of Kip3 is most likely targeted by extrinsic regulatory factors.

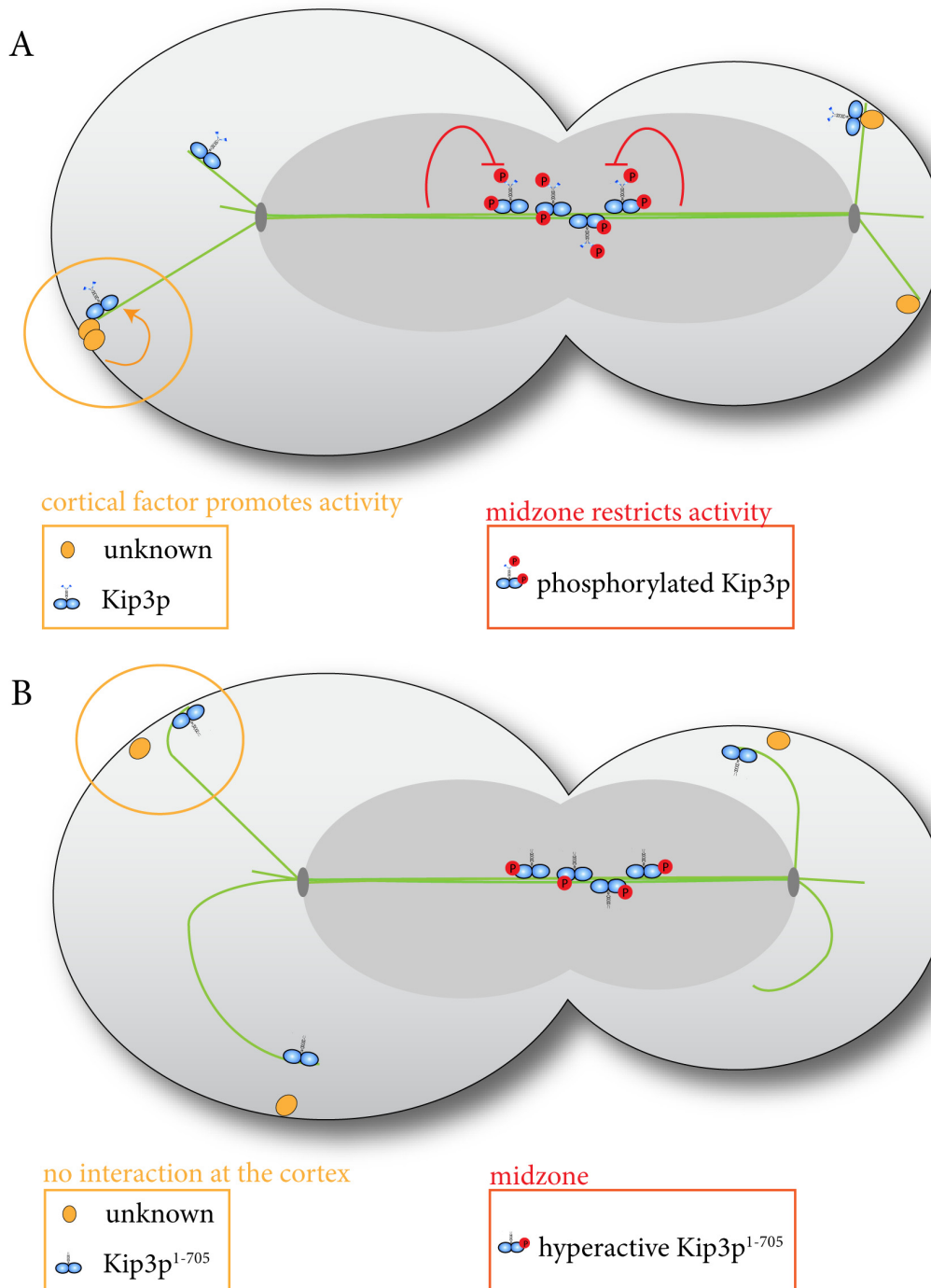


Figure 24. Conceptual model of the regulation of Kip3 during anaphase. A. In order to allow spindle elongation Kip3's motor activity on interpolar MTs is restricted presumably by proteins of the spindle midzone or by posttranslational modification. At the same time astral MT growth is restricted to allow interaction with the cortex. B. The tail-truncated Kip3¹⁻⁷⁰⁵ cannot be regulated at the spindle midzone resulting in a hyperactive motor and a shorter anaphase spindle. In contrary astral MTs are hyperelongated since Kip3¹⁻⁷⁰⁵ cannot be activated anymore by cortical stimuli.

4.2 Understanding kinesin-14 motor function at the MT plus-end

4.2.1 The EB1 homologue Bim1 targets Kar3-Cik1 to the MT plus-end

In addition to kinesin-8s, Kar3, a member of the kinesin-14 family, has been shown to combine motility with a MT destabilizing activity (Endow et al., 1994b). While it was at first believed that this minus-end directed motor shortens MT minus-ends, it has been demonstrated that Kar3 acts on MT plus-ends, to which it is targeted by the accessory protein Cik1 (Sproul et al., 2005). Several studies have revealed that Kar3's localization and function depend on the identity of its heterodimerization partner. Upon complex formation with Vik1, Kar3 is directed to spindle pole bodies, where it crosslinks parallel MTs (Manning et al., 1999). A depolymerase activity has not been observed for Kar3-Vik1, neither *in vitro* nor *in vivo* (Sproul et al., 2005; Allingham et al., 2007). When Kar3 forms a heterodimer with Cik1, it localizes to the plus-ends of interpolar MTs in anaphase (Gardner et al., 2008a). The noncatalytic proteins Cik1 and Vik1 are highly similar in structure and sequence (Manning et al., 1999; Allingham et al., 2007) and their subcellular localization depends on Kar3. Vice versa, the Kar3 signal appears mislocalized into bright nuclear patches in the absence of both adapter proteins (Manning et al., 1999). Thus the adaptor alone is not sufficient to specify the localization of Kar3, instead different composite interfaces are formed between Kar3 and the two adaptors and facilitate the particular subcellular localization. Of particular interest is therefore how the minus-end directed motor complex Kar3-Cik is loaded to MT-plus ends.

This study has discovered the association between the heterodimeric Kar3-Cik1 motor complex and the EB1 homologue Bim1. Live-cell imaging confirmed that Kar3-Cik1 relies on Bim1 for MT plus-end recruitment during mitosis. Bim1 seems to specifically interact with the Kar3-Cik1 heterodimer since the SPB-associated pool of Kar3-Vik1

was unchanged upon deletion of Bim1 (Figure 18). Kar3-Cik1 and Bim1 are critical for spindle positioning, anaphase spindle integrity and both complexes are indispensable for karyogamy (Meluh and Rose, 1990; Schwartz et al., 1997; Tirnauer et al., 1999; Maddox et al., 2003; Gardner et al., 2008a). Genetic experiments have suggested opposing effects of Kar3 and Bim1 on MTs since their simultaneous deletion suppressed the temperature sensitivity of a *kar3Δ*, but not the karyogamy defect (Tirnauer et al., 1999). By tethering Kar3-Cik1 to the MT plus-end Bim1 recruits a motor complex to its site of action that exhibits a converse effect on MT dynamics than Bim1 itself. Bim1 has been demonstrated to promote MT assembly *in vitro* by decreasing the frequency of catastrophes (Blake-Hodek et al., 2010). In support of this, *bim1Δ* strains display shorter and less dynamic cytoplasmic MTs (Tirnauer et al., 1999), while in the absence of Kar3 the length and number of cytoplasmic MTs increases (Saunders et al., 1997). Bim1 uses its autonomous plus-end tracking ability to govern association of hitchhiking proteins to the plus-end (Bieling et al., 2007). We show that among the multitude of Bim1 interacting proteins, that enable Bim1 to influence MT dynamics and control MT length, is the MT destabilizing enzyme Kar3-Cik1 (Figure 25). The result that the heterodimeric kinesin-14 complex depends on Bim1 for its subcellular localization is surprising since kinesins-14s contain an inherent MT binding ability within their motor domain and a nucleotide independent, nonmotor MT binding domain (Karabay and Walker, 1999). It will be important to investigate if and how Bim1-dependent loading of Kar3-Cik1 to the plus-end is spatiotemporally regulated. An unresolved question involves the unloading of Bim1 cargo proteins. Is Kar3-Cik1 immediately released from Bim1 upon contact with the plus-end to drive antiparallel MT sliding in the spindle midzone or does Bim1 tether Kar3-Cik1 continuously to the MT plus-end. Kar3 is a nonprocessive kinesin that detaches from microtubules after each ATPase cycle (Endow, 2003). Bim1 as an anchor could increase efficiency by facilitating repeated rounds of MT sliding of anti-parallel overlaps. In addition it will be interesting to

address if Bim1 dependent loading of Kar3-Cik1 also contributes to its described role in transporting kinetochores along the microtubule lateral surface (Tanaka et al., 2007). A plus-end loading would enhance the efficiency of collecting and transporting kinetochores towards the spindle pole.

Kinesin-14 motor function is highly conserved among eukaryotes (Peterman and Scholey, 2009). Is the interaction with EB proteins a common feature of members of the kinesin-14 family or yeast-specific? Very recently a publication has demonstrated plus-end loading of the fission yeast kinesin-14 Klp2 by the EB homologue Mal3 during meiotic nuclear positioning (Mana-Capelli et al., 2012). It is tempting to speculate that in higher eukaryotes kinesin-14 molecules might rely on EB proteins for their function during mitosis.

On the other hand our results raise the question if the heterodimer combination Kar3-Vik1 requires additional factors for its localization, too. Explanations for the minus-end accumulation of *Drosophila melanogaster* kinesin-14 Ncd are based on the presence of parallel MT bundles that might influence MT binding and unbinding rates (Fink et al., 2009). However, this subject remains speculative so far.

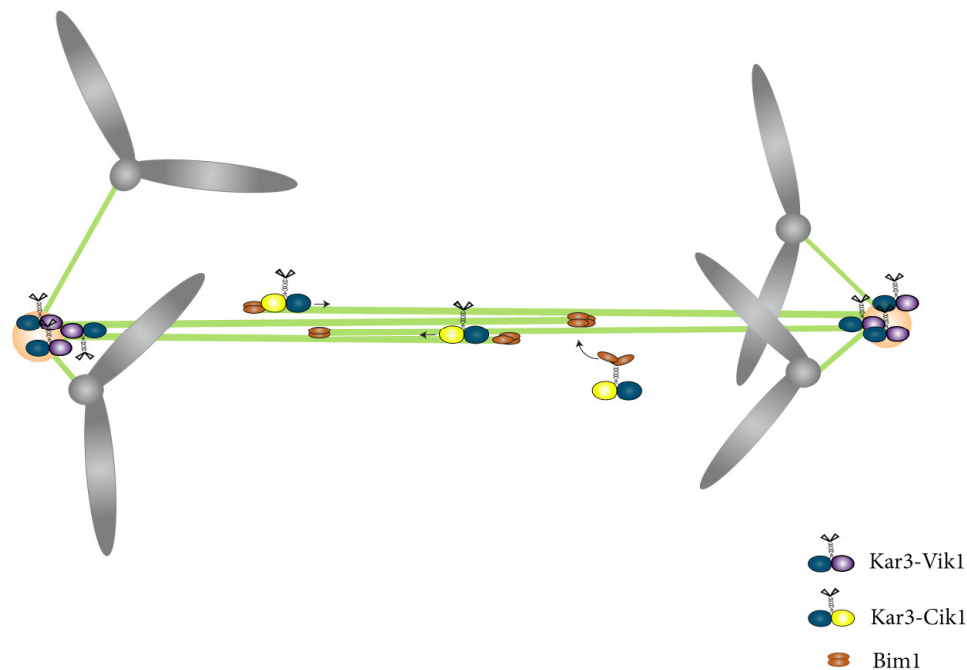


Figure 25. Schematic illustration of Bim1 dependent loading of Kar3-Cik1 onto MT plus-ends in anaphase. In our current working model Bim1 binds Kar3-Cik1 in the absence of MTs and promotes recruitment of the motor complex to MT plus-ends of interpolar MTs.

4.2.2 Defining the binding interface between Kar3-Cik1 and Bim1

The recruitment of cargo proteins to Bim1 is mediated by diverse mechanisms (Akhmanova and Steinmetz, 2008). One of those is based on the presence of a conserved Ser-x-Ile-Pro (SxIP) motif in Bim1 interacting proteins (Honnappa et al., 2009). While neither Kar3 nor Vik1 contain an obvious Bim1 binding motif, the extreme unstructured N-terminus of Cik1 encompasses a canonical SxIP motif. Interestingly this motif is only present in the mitosis-specific, longer Cik1 isoform (Benanti et al., 2009). Although we also identified Bim1 as co-purifying with the mating specific Cik1 isoform that lacks the SxIP motif, its presence in the mitotic Cik1 molecule might pinpoint an essential requirement of the association of Kar3-Cik1 and Bim1 especially during anaphase. It was reported that mutation of the SxIP motifs in the Aurora B homologue

Ipl1 completely abrogates Bim1 association (Zimniak et al., 2012). However, here we show that Cik1 without a functional SxIP motif is still capable in binding to Bim1. We assume that the Kar3-Cik1 interaction is also critical during mating, as both proteins are indispensable for karyogamy (Meluh and Rose, 1990; Tirnauer et al., 1999; Maddox et al., 2003). During mating cells reorganize their cytoskeleton, fuse their cell bodies and migrate haploid nuclei toward one another. The current model is that Kar3-Cik1 crosslinks overlapping microtubule bundles emerging from each nucleus and pulls them together by depolymerizing MT plus-ends and its MT sliding ability (Meluh and Rose, 1990; Maddox et al., 2003; Sproul et al., 2005). Thus loading of Kar3-Cik1 onto plus-ends during mating is absolutely essential and supposedly mediated by Bim1. In agreement my biochemical analysis showed that the short Cik1 isoform in complex with Kar3 is indeed a binding partner of Bim1 *in vitro*.

Cik1 and Vik1 share a highly similar sequence and structure, especially within their C-terminal catalytic inactive motor homology domain (Manning et al., 1999; Allingham et al., 2007). Assuming that Bim1 selectively binds Kar3-Cik1, not Kar3-Vik1, the most likely element responsible for the Bim1 interaction is therefore the N-terminus of Cik1. From *in vivo* analysis of Cik1 localization in a *kar3Δ* it is obvious, that Cik1 is unable to be recruited by Bim1 in the absence of Kar3 (Manning et al., 1999). Therefore only the dimerized Kar3-Cik1 is a cargo of Bim1. Support for this idea comes from our analysis of N-terminally truncated Cik1 as part of the heterodimer Kar3-Cik1²⁵⁰⁻⁵⁹⁴. This mutant was capable of forming a heterodimer, but highly inefficient in Bim1 association (Figure 21). This outcome indicates that the N-terminus of Cik1 primarily contributes to establish the Bim1-binding interface of the kinesin heterodimer. However, a small amount of Bim1 was still interacting with this Cik1 truncated heterodimer. Hence, the recognition of Kar3-Cik1 by Bim1 seems to involve not only one particular region within Cik1, presumably the whole coiled-coil region formed between the nonmotor N-termini of Cik1 and Kar3 facilitate Bim1 binding. The interface receives an important

contribution from Kar3 as well. This is especially interesting because Kar3 seems to be the site of phosphoregulation.

4.2.3 Kar3 is highly phosphorylated during mitosis

Previous studies have identified Kar3 as a target protein of the major cell cycle kinase Cdc28 with the tendency to be more efficiently phosphorylated by the S phase complex Clb5-Cdc28 than by Clb2-Cdc28 (Ubersax et al., 2003). Our study has indeed defined the highest number of phosphorylation sites on Kar3 in S phase arrested cells (Figure 23). Strikingly, half of the identified phosphosites match a Cdc28 consensus sequence and cluster in Kar3's aminoterminal nonmotor domain. So far the physiological relevance of this phosphoregulation remains unknown and will be subject of further studies. Firstly, analyzing the phosphorylation status of Kar3 in complex with Vik1 during mitosis would clarify if Cdc28 selectively targets Kar3-Cik1. In this case several parameters could be affected: the kinesin motor and depolymerase activity, protein stability, the MT binding affinity or the interaction with Bim1. Interestingly, Kar3-Cik1 seems to be removed successively from the spindle with proceeding anaphase in order to allow spindle elongation (Figure 23). The timing of removal coincides with the nucleolar release of Cdc14 phosphatase that reverses Cdc28 phosphorylation. Thus, it is conceivable that dephosphorylation of Kar3-Cik1 triggers either release from the spindle midzone or facilitates APC/C^{Cdh1} mediated proteolysis. A previous study has demonstrated that the APC/C^{Cdh1} targets Cik1 for ubiquitin-mediated degradation (Benanti et al., 2009). We have uncovered that also Kar3 is expressed cyclically during mitosis and it is tempting to propose a similar regulation of Kar3's protein level as it has been shown for Cik1. Ongoing experiments will help to define the role of Cdc28 phosphorylation in regulating the motor function of Kar3-Cik1.

5 Material & Methods

5.1 Strains & Plasmids

5.1.1 Strains

SWY14	<i>MAT a; leu2, ura3-52, trp1, prb1-1122, pep4-3, pre1-451, Kip3-STAG-TEV-ZZ::KanMX</i>
SWY150	<i>MAT a, ura3-1, leu2-3,112, trp1-1, his3,11,15, ade2-1, can1-100, pAB1234-2u Gal-Clb2-TAP::URA3</i>
DDY1503	<i>MAT a, his3Δ200, leu2-3,112, ura3-52, ade2-101, mad2::URA3</i>
DDY1810	<i>MAT a; ura3-52, trp1, prb1-1122, pep4-3, pre1-451, leu2-3,112, HIS3</i>
KDY1	<i>Mat α, Nuf2-mCherry::KanMx, leu2-3,112, his3Δ200, ura3-52, lys2-801, his3Δ200::Kar3-3xGFP::HIS3</i>
KDY2	<i>MAT a; leu2-3, ura3-52, trp1, prb1-1122, pep4-3, pre1-451, Cik1-FLAG::KanMX</i>
KDY3	<i>MAT a; leu2-3, ura3-52, trp1, prb1-1122, pep4-3, pre1-451, Cik1-FLAG::KanMX, his3Δ200::Kar3-3xGFP::HIS3</i>
KDY4	<i>MAT a; lys2-801, ADE2; cdc20::TRP1::GAL1/10-CDC20, mCherry-Tubulin::URA3, his3Δ200::Kar3-3xGFP::HIS3</i>
CMY4	<i>MAT a, kip3Δ::KanMX, ade2-1, leu2-3,112, ura3-52, his3Δ200</i>
CMY29	<i>MAT a, Kip3-13xmyc::HIS3, Pds1-13myc::LEU2, lys2-801, ura3-52,</i>
CMY 65	<i>MAT a, his3Δ200::Kip3-3xGFP::HIS3, Nuf2-mCherry::KanMX, leu2-3,112, ura3-52</i>
CMY115	<i>MAT alpha, kip3Δ::KanMX, pHIS3::mCherry-Tub1::URA3, leu2-3, his3Δ200::Kip3⁴⁴⁹⁻⁸⁰⁵-eGFP::HIS3,</i>
CMY117	<i>MAT alpha, kip3Δ::KanMX, pHIS3::mCherry-Tub1::URA3, leu2-3,112, his3Δ200::Kip3^{3D}-eGFP::HIS3.</i>
CMY118	<i>MAT alpha, kip3Δ::KanMX, pHIS3::mCherry-Tub1::URA3, leu2-3,112, his3Δ200::Kip3^{3A}-eGFP::HIS3</i>
CMY158	<i>MAT a; leu2, ura3-52, trp1, prb1-1122, pep4-3, pre1-451, 2μ-pGAL-Cik1-Flag pGal-Kar3-eGFP::TRP1</i>

Material & Methods

CMY159	<i>MAT a; leu2, ura3-52, trp1, prb1-1122, pep4-3, pre1-451, 2μ-pGAL-Cik1-Flag pGal-Kar3::TRP1</i>
CMY161	<i>MAT a; leu2, ura3-52, trp1, prb1-1122, pep4-3, pre1-451, leu2-3,112::Kip3-eGFP-6xFLAG::LEU2</i>
CMY162	<i>MAT a; ura3-52, trp1, prb1-1122, pep4-3, pre1-451, Δkip3::KanMX, pRS305::LEU2</i>
CMY163	<i>MAT a; ura3-52, trp1, prb1-1122, pep4-3, pre1-451, Δkip3::KanMX, leu2-3,112::Kip3-eGFP-6xFLAG::LEU2</i>
CMY164	<i>MAT a; ura3-52, trp1, prb1-1122, pep4-3, pre1-451, Δkip3::KanMX, leu2-3,112::Kip3¹⁻⁵⁰⁵-eGFP-6xFLAG::LEU2</i>
CMY165	<i>MAT a; ura3-52, trp1, prb1-1122, pep4-3, pre1-451, Δkip3::KanMX, leu2-3,112::Kip3¹⁻⁷⁰⁵-eGFP-6xFLAG::LEU2</i>
CMY166	<i>MAT a; ura3-52, trp1, prb1-1122, pep4-3, pre1-451, Δkip3::KanMX, leu2-3,112::Kip3⁴⁴⁹⁻⁸⁰⁵-eGFP-6xFLAG::LEU2</i>
CMY173	<i>MAT a; ura3-52, trp1, prb1-1122, pep4-3, pre1-451, Δkip3::KanMX, leu2-3,112::Kip3⁸⁵⁻⁸⁰⁵-eGFP-6xFLAG::LEU2</i>
CMY175	<i>MAT a; ura3-52, trp1, prb1-1122, pep4-3, pre1-451, Δkip3::KanMX, leu2-3,112::Kip3^{motor}dead-eGFP-6xFLAG::LEU2</i>
CMY178	<i>MAT a; leu2, ura3-52, trp1, prb1-1122, pep4-3, pre1-451, 2μ-pGAL-Cik1^{SXNN}-Flag pGal-Kar3::TRP1</i>
CMY179	<i>MAT a; leu2, ura3-52, trp1, prb1-1122, pep4-3, pre1-451, 2μ-pGAL-Cik1^{SXNN}-Flag pGal-Kar3-eGFP::TRP1</i>
CMY189	<i>MAT alpha, kip3Δ::KanMX, leu2-3,112::Kip3-eGFP-6xFLAG::LEU2, pHIS3::mCherry-Tub1::URA3,</i>
CMY190	<i>MAT alpha, kip3Δ::KanMX, leu2-3,112::Kip3¹⁻⁵⁰⁵-eGFP-6xFLAG::LEU2, pHIS3::mCherry-Tub1::URA3, HIS3,</i>
CMY191	<i>MAT alpha, kip3Δ::KanMX, leu2-3,112::Kip3¹⁻⁷⁰⁵-eGFP-6xFLAG::LEU2, pHIS3::mCherry-Tub1::URA3, HIS3,</i>
CMY192	<i>MAT alpha, kip3Δ::KanMX, leu2-3,112::Kip3^{motor}dead-eGFP-6xFLAG::LEU2, pHIS3::mCherry-Tub1::URA3, HIS3,</i>
CMY193	<i>MAT alpha, kip3Δ::KanMX, leu2-3, pHIS3::mCherry-Tub1::URA3,</i>

CMY196	<i>MAT alpha, pHIS3::mCherry-Tub1::URA3, leu2-3,112, his3Δ200::Kar3-3xGFP::HIS3,</i>
CMY197	<i>MAT alpha, pHIS3::mCherry-Tub1::URA3, leu2-3,112, his3Δ200:: Kar3-3xGFP::HIS3, bim1Δ::KanMX</i>
CMY202	<i>MAT a; lys2-801, cdc20::TRP1::GAL1/10-CDC20, mCherry-Tubulin::URA3, his3Δ200::Kar3-3xGFP::HIS3, Δcik1::KanMX</i>
CMY203	<i>MAT a; lys2-801, cdc20::TRP1::GAL1/10-CDC20, mCherry-Tubulin::URA3, his3Δ200::Kar3-3xGFP::HIS3, Δvik1::KanMX</i>
CMY221	<i>MAT alpha, lys2-801am, his3D200, ade2-1, cdc15-2::LEU2, Spc42RedStar::cloneNAT, GFP-Tub1::URA3, kip3Δ::KanMX, leu2-3,112::Kip3-eGFP-6xFLAG::LEU2</i>
CMY222	<i>MAT alpha, lys2-801am, his3D200, ade2-1, TRP1, cdc15-2::LEU2, Spc42RedStar::cloneNAT, GFP-Tub1::URA3, kip3Δ::KanMX</i>
CMY224	<i>MAT alpha, lys2-801am, his3D200, ade2-1, TRP1, cdc15-2::LEU2, Spc42RedStar::cloneNAT, GFP-Tub1::URA3</i>
CMY229	<i>MAT alpha, lys2-801am, his3D200, ade2-1, TRP1, cdc15-2::LEU2, Spc42RedStar::cloneNAT, GFP-Tub1::URA3, kip3Δ::KanMX, Kip3¹⁻⁷⁰⁵-eGFP-6xFLAG::LEU2</i>
CMY234	<i>MAT a, kip3Δ::KanMX, ade2-1, ura3-52, his3Δ200, leu2-3,112::Kip3¹⁻⁸⁰⁵::LEU2</i>
CMY235	<i>MAT a, kip3Δ::KanMX, ade2-1, ura3-52, his3Δ200, leu2-3,112::Kip3¹⁻⁷²⁵::LEU2</i>
CMY236	<i>MAT a, kip3Δ::KanMX, ade2-1, ura3-52, his3Δ200, leu2-3,112::Kip3¹⁻⁷⁵⁰::LEU2</i>
CMY237	<i>MAT a, kip3Δ::KanMX, ade2-1, ura3-52, his3Δ200, leu2-3,112::Kip3¹⁻⁷⁷⁵::LEU2</i>
CMY238	<i>MAT a, kip3Δ::KanMX, ade2-1, ura3-52, his3Δ200, leu2-3,112::Kip3¹⁻⁸⁰⁰::LEU2</i>
CMY242	<i>MAT a, kip3Δ::KanMX, ade2-1, ura3-52, his3Δ200, leu2-3,112::Kip3^{6A}-eGFPFLAG::LEU2</i>
CMY243	<i>MAT a, kip3Δ::KanMX, pHIS3::mCherry-Tub1::URA3, his3Δ200, lys2-801, leu2-3,112::Kip3^{6A}-eGFP-6xFLAG::LEU2</i>
CMY245	<i>MAT alpha, his3D200, ade2-1, cdc15-2::LEU2, Spc42RedStar::cloneNAT, GFP-Tub1::URA3, kip3Δ::KanMX, leu2-3,112:: Kip3^{6A}-eGFP-6xFLAG::LEU2,</i>

5.1.2 Plasmids

<i>pCM4</i>	<i>pFastBac1 Kip3</i>
<i>pCM20</i>	<i>pFastBac1 Kip3-eGFP</i>
<i>pCM33</i>	<i>pFastBac1 Kip3-eGFP S730A S734A S736A</i>
<i>pCM46</i>	<i>pFastBac1 Kip3¹⁻⁵⁰⁵-eGFP</i>
<i>pCM47</i>	<i>pFastBac1 Kip3¹⁻⁷⁰⁵-eGFP</i>
<i>pCM51</i>	<i>pFastBac1 Kip3-eGFP S791A S792A</i>
<i>pCM55</i>	<i>pFastBac1 Kip3-eGFP G196A K197A T198A</i>
<i>pCM64</i>	<i>pFastBac1 Kip3-eGFP-6xFLAG</i>
<i>pCM65</i>	<i>pFastBac1 Kip3⁴⁴⁹⁻⁸⁰⁵-eGFP-6xFLAG</i>
<i>pCM83</i>	<i>pESC-TRP Cik1-FLAG Kar3-eGFP</i>
<i>pCM107</i>	<i>pESC-TRP Cik1-FLAG Kar3</i>
<i>pCM122</i>	<i>pESC-TRP Cik1^{SXNN}-FLAG Kar3-eGFP</i>
<i>pCM123</i>	<i>pESC-TRP Cik1^{SXNN}-FLAG Kar3</i>
<i>pCM136</i>	<i>pESC-TRP Cik1³⁴⁻⁵⁹⁴-FLAG Kar3</i>
<i>pCM137</i>	<i>pESC-TRP Vik1-FLAG Kar3</i>
<i>pCM141</i>	<i>pESC-TRP Cik1²⁵⁰⁻⁵⁹⁴ Kar3</i>

5.2 Yeast Genetics

5.2.1 Yeast strain construction

Standard YEP medium containing 1% (w/v) yeast extract and 2% (w/v) peptone supplemented with 2% (v/v) glucose was used to grow cells in liquid culture. The basic recipe was followed to prepare YEPD-plates containing 2% (w/v) bacto agar. All yeast strains were generated employing standard procedures. C-terminal tags and deletions were constructed according to a PCR-based method described previously (Longtine et

al., 1998). Gene deletion primers contained 55-60 base pair homology to the respective endogenous locus and replaced the targeted gene with a selectable marker. Verification of correct integration occurred via PCR and/ or sequencing. The integration of fluorescently tagged genes or mutant genes into yeast strains was accomplished by using linearized pRS vectors containing the gene of interest and a selectable yeast marker gene (HIS3, TRP1, LEU2). The pRS constructs encompassed the respective 5'UTR and 3'UTR region (around 200-250 base pairs) surrounding the cloned gene. Mutation of phosphorylation sites and point mutations were introduced using the QuickChange Multi Site-Directed Mutagenesis kit (Stratagene). Deletion mutants were generated applying the Phusion Site-Directed Mutagenesis kit (Finnzymes). Yeast transformations were performed following the standard procedure described previously (Schiestl and Gietz, 1989).

5.2.2 Spot Assay

The desired strains were grown o/n in YPD medium. The next day cells were diluted to $OD_{600} = 0.5$ and further diluted in 1:5 steps in a 96 well plate. This dilution series was spotted on benomyl and YPD plates and incubated at 30°C for two to three days to compare growth phenotypes. The concentration of benomyl within plates varied from 10 to 20µg/ml. The respective amount of nourseothricin (Jena Bioscience) was added to standard cultivation plates before pouring.

5.3 Live-cell imaging

An overnight culture of the desired strain was diluted back next morning to $OD_{600} = 0.25$ in doTRP synthetic medium containing 2% glucose. After rotating the cells for several hours they were adhered for 15 min on concanavalin A-coated cover slips or culture dishes (Matek). To remove unattached cells a quick washing step was performed

before the cover slips were sealed with vacuum grease or culture dishes were filled with doTRP synthetic medium. Images were taken at ambient temperature using a Deltavision (Applied Precision) microscopy system. The Olympus IX-71 microscope in the Deltavision system was equipped with a 100x oil immersion objective lens (Olympus: NA1.40) and a CoolSnap HQ CCD camera (Photometrics). 6-8 z-stacks (0.35 μm) per time point were projected to two-dimensional images (SoftWoRx software). Time-lapse recordings took z-stacks in 20 to 30 s intervals. Deconvolution by SoftWoRx was used in some experiments to increase weak signals. Metamorph and ImageJ were used for further analysis. Spindle length of *cdc15-2* arrested strains was measured in Metamorph.

5.4 Tandem affinity purification of Kip3 from yeast extracts and mass spectrometry analysis

12 l of C-terminally tagged Kip3p-S-TEV-ZZ strain was grown to $\text{OD}_{600} = 1.2$, harvested by centrifugation and washed with PBS. After resuspension in a minimal amount of water the yeast suspension was drop-frozen in liquid nitrogen. Droplets were broken either by using a blender or a freezer mill. Usually 30 g of the resulting powder was dissolved in 30 ml of 2x Hyman buffer (100 mM Bis-Tris propan ph 7.0, 200 mM KCl, 10 mM EDTA, 10 mM EGTA, 20% (v/v) glycerol) plus freshly added protease inhibitors and phosphatase inhibitors (1 mM PMSF, 1x Protease Inhibitor Cocktail Set IV (Calbiochem), 0.1 M β -glycerophosphate, 1x phosphatase inhibitor cocktail (20 mM sodium pyrophosphate, 10 mM sodium azide, 20 mM sodium fluoride, 0.8 mM sodium ortovanadate)). The lysate was quickly sonicated for 30 s, Triton X-100 was added to a final concentration of 1% and the extract was centrifuged at 10 k rpm in a SS-34 rotor for 20 min, followed by an additional centrifugation step at 45 k rpm in a Ti70 rotor for 30 min at 4°C. To remove unspecific interactions with the column material the supernatant was pre-cleared over a CL-6B sepharose column pre-equilibrated with 1x

Hyman buffer. The salt concentration of the flow through was raised to 300 mM KCl (or in case of a low stringency purification to 200 mM KCl). The flow through was combined with 0.65 ml IgG sepharose that was activated before by the following washing procedure: 10 ml TST (50 mM Tris-HCl pH 7.5, 150 mM NaCl, 0.1% Tween-20), 1ml NH₄OAc pH 3.4, 5 ml TST, 1 ml NH₄OAc pH 3.4, 5 ml TST, 5 ml 1x Hyman (with 300 mM KCl). IgG beads and extract were combined for 3 h with gentle rotation at 4°C. Subsequently beads were collected in a disposable column (Bio-Rad) and washed with 15 ml 1x Hyman buffer (300 mM KCl, low stringency conditions: 200 mM KCl), 25 ml 1x Hyman buffer (300 mM KCl, low stringency conditions: 200 mM KCl, 1 mM DTT, 0.1% Tween-20) and resuspended in TEV cleavage buffer (1x Hyman, 300 mM KCl/ 200 mM KCl, 1mM DTT, 0.1% Tween-20). After addition of TEV protease (home-made) to a concentration of 0.1 mg/ml the bound Kip3 was cleaved off the beads overnight at 4°C. The supernatant was removed from the beads and added to pre-equilibrated 85 µl S-Protein agarose slurry and incubated for 3 h with rotation at 4°C. The resin was washed with 10 ml 1x Hyman buffer before eluting bound proteins from the beads by adding 3x 60 µl of 100 mM glycine pH 2.0. A fraction of the purified proteins were analyzed by SDS-PAGE followed by silver staining (standard protocol). Mass spectrometry including in-solution digest and sample analysis, was carried out by the Protein Chemistry department of the IMP.

5.5 Expression and purifications of kinesin complexes

5.5.1 Overexpression of Kar3-Cik1-FLAG complexes in yeast

Cloning the respective genes into the overexpressing pESC-TRP vector was done following the instruction manual (Agilent, pESC Yeast Epitope Tagging Vectors). 1 µl non-linearized pESC-Kar3-Cik1-FLAG (for example pCM83) was transformed into the protease deficient strain DDY1810 according to the standard yeast transformation

protocol. The transformation was plated on doTrp plates for several days. From this plate a preculture was grown in doTrp medium plus 2% (v/v) glucose to further inoculate a 200 ml culture in selective doTrp medium plus 2% glucose. After cells reached a sufficiently high cell density they were diluted to $OD_{600} = 0.06$ in 6l doTrp supplemented with 2% (v/v) raffinose. Cultures were grown for 14-18 h until $OD_{600} = 1.2$. At this time point expression was induced by adding 2% (v/v) galactose, 40g bacto-peptone and 20g yeast extract to the cultures. After induction cells were grown for 8-10 h, harvested by centrifugation, washed with PBS and drop-frozen in liquid nitrogen. Droplets were grinded in a freezer mill.

5.5.2 Purification of FLAG-tagged Kar3-Cik1 from yeast using M2 affinity agarose

10 g of freezer mill powder was dissolved in 15 ml of buffer A (25 mM Hepes pH 7.2, 1 mM $MgCl_2$, 0.1 mM EGTA, 0.1 mM EDTA, 0.1% Tween-20, 5% sucrose, 300 mM NaCl, 0.01 mM ATP, 1 mM PMSF, 1x protease inhibitor Cocktail Set IV (Calbiochem)). Lysis occurred on ice and took 30-60 min. The dissolved lysate was centrifuged for 20 min at 19 k rpm, 4°C in a SS-34 rotor. A subsequent centrifugation step was performed at 35 k rpm for 60 min, 4°C in a Ti-90 rotor. 450 μ l M2 affinity agarose (Sigma) was incubated with the supernatant for 1 h, gently rotating at 4°C. Afterwards the agarose was washed 5-6 times with buffer A (adjusted to 150 mM NaCl). Elution of the purified kinesin heterodimer from the M2 affinity agarose was achieved by applying 1 volume of 3xFLAG peptide (2 mg/ml). The elution procedure was repeated 3-4 times. In order to remove the 3xFLAG peptide a cation exchange chromatography (MonoS 5/50 GL, GE Healthcare) was performed in running buffer (10 mM Hepes pH 7.2, 150 mM NaCl, 1 mM $MgCl_2$, 1 mM DTT, 1 mM EGTA). After binding of the motor to the column a salt gradient eluted the pure motor fraction at 250 mM salt as a single peak. The respective peak elution fractions were supplemented with glycerol (final concentration: 10%) and

the protein concentration was determined using the DC Protein Assay kit (Bio-Rad). The kinesin fractions were snap-frozen in liquid nitrogen and stored at -80°C.

5.5.3 Expression and purification of Kip3 constructs using baculo-virus infected Sf9 insect cells

Full-length Kip3, tail-truncations and phosphomutants with and without a C-terminal eGFP tag were cloned into the vector pFastBac1 N-terminally fused to a 6xHis tag. Cloning, bacmid production, verification of bacmid inserts by PCR, transfection of Sf9 cells, production of virus stocks and the expression in baculo-virus infected Sf9 insect cells was done following the Bac-to-Bac Baculovirus Expression System guide from Invitrogen. For a standard purification 1l logarithmically growing Sf9 suspension cells with a cell density of 1×10^6 cells/ml were infected with 6-8 ml of P2 virus stock. Cultures were grown for 72 h at 27°C, harvested by centrifugation, washed with PBS and stored at -80°C. The pellet was dissolved in lysis buffer (50 mM $\text{Na}_2\text{HPO}_4^-$ NaH_2PO_4 pH 7.4, 400 mM NaCl, 35 mM imidazole, 10% glycerol, 0.1% Tween-20, 1.5 mM MgCl_2 , 1 mM PMSE, 0.5 mM ATP, 10 mM β -mercaptoethanol, 1x protease inhibitors (Roche)). The lysate was sonicated 3x 30 sec before centrifugation at 19k rpm for 20 min. The collected supernatant was incubated with pre-equilibrated NiNTA agarose (Quiagen) for 2 h at 4°C. Afterwards the agarose was washed four times in batch format with wash buffer (lysis buffer adjusted to 350 mM NaCl, 25 mM imidazole, 1 mM MgCl_2 , 0.1 mM ATP). Elution took place upon incubation of the NiNTA agarose with an equal amount of elution buffer (lysis buffer adjusted to 200 mM NaCl, 1 mM MgCl_2 , 325 mM imidazole). Imidazole removal and buffer exchange to cation exchange chromatography buffer A (25 mM Hepes pH 7.5, 200 mM NaCl, 1.5 mM MgCl_2 , 10% glycerol, 0.5 mM DTT, 0.01 mM ATP) was conducted on a PD-10 column (GE Healthcare). The sample was subjected to cation exchange chromatography using a MonoS 5/50 GL column (GE Healthcare). In a linear salt gradient to 1M NaCl with 10 bed volumes Kip3 constructs

eluted around 350 mM NaCl. The respective elution fractions were supplemented with glycerol (final concentration: 10%) and ATP (final 0.1 mM) and the protein concentration was determined using the DC Protein Assay kit (Bio-Rad). The kinesin fractions were snap-frozen in liquid nitrogen and stored at -80°C.

5.6 Kinase assays

Recombinant motor proteins were incubated with tandem affinity purified Cdc28-Clb2-TAP (purified from yeast cells) and γ -[³²P]ATP in Cdk1 buffer (25 mM Hepes pH 7.6, 100 mM KCl, 2 mM MgCl₂, 1 mM DTT, 1mM EGTA, 5% glycerol, 20 mM β -glycerophosphate). The reaction was carried out for 30 min at 30°C, separated by SDS-PAGE and exposed to an autoradiography film (Kodak). For mass spectrometry analysis of *in vitro* phosphorylation assays, the respective motor preparation was dephosphorylated prior to the kinase assay by lambda phosphatase treatment (NEB).

5.7 Microtubule co-sedimentation assay / Depolymerase assay

Porcine brain Tubulin used for MT co-sedimentation assays and TIRF microscopy was purified according to a standard protocol (Ashford et al., 1998). GMPCPP-stabilized MTs were prepared by mixing 22.25 μ M Tubulin, 1 mM DTT, 1.5 mM GMPCPP in PEM buffer (80 mM Pipes, pH 6.8, 1 mM EGTA, 1mM MgCl₂) on ice. A subsequent incubation step at 35°C for 45 min facilitated MT assembly. For MT co-sedimentation assays freshly prepared GMPCPP-MTs were diluted to the indicated concentrations (either fixed MT concentrations from 1-3.5 μ M or varying concentrations ranging from 0.5-5 μ M depending on the type of experiment) and incubated with pre-cleared mitotic motors (either at a constant concentration or for the course of depolymerase assays in increasing concentrations from 0.1 -1 μ M). The reaction was performed in PEM buffer supplemented with 112 mM KCl, 0.1 mg/ml casein and, if not indicated otherwise, in

the presence of 5 mM ATP. After incubation at RT for 15 min the microtubule-bound and -unbound fractions were separated by ultracentrifugation at 60 k rpm for 20 min at 25°C (TL100 rotor, Beckman). The supernatants were transferred to a fresh tube and the pellets were extensively dissolved in an equivalent volume of ice-cold PEM. Analysis of the co-sedimentation assay was conducted by Coomassie-stained SDS-PAGE and subsequent densitometric quantification with ImageJ.

5.8 Size exclusion chromatography of motor complexes

Size exclusion experiments to determine Kip3's dimerization status were performed on a Superose 6 3.2/30 (GE Healthcare) at 4°C. The running buffer was composed of 25 mM Hepes (pH ?), 250 mM NaCl, 5% glycerol, 1 mM MgCl₂, 1 mM DTT. The interaction studies of Kar3-Cik1 and Bim1 were conducted on a Superose 6 3.2/30 (GE Healthcare) at 4°C under the following conditions: 25 mM Hepes (pH?), 225 mM NaCl, 1 mM MgCl₂, 0.1 mM EGTA, 0.1 mM EDTA, 0.1 mM DTT, 0.01 mM ADP. Protein elution was monitored by absorbance (wavelength of 280 nm) and the elution fractions were analyzed by SDS-PAGE and subsequent Coomassie staining.

5.9 *In vitro* binding assays

Varying amounts (0.1-1 μM) of recombinant GST-Bim1, or GST-Bim1 truncations, were immobilized on 30 μl glutathione-Sepharose in 0.5 ml binding buffer (10 mM Hepes pH 7.2, 250 mM NaCl, 1 mM MgCl₂, 1 mM EGTA, 0.5 mM DTT, 0.05% NP-40). The binding partner was added in a constant concentration between 500 nM and 1 μM. After rotation for 1 h at 4°C, beads were washed three times with 500 μl binding buffer and analyzed by SDS-PAGE and Coomassie staining.

For the reciprocal pull down experiments varying amounts of Kar3-Cik1-FLAG constructs (0.1-0.5 μ M) were added to 30 μ l M2 affinity agarose (Sigma) that was pre-blocked in 0.5% BSA containing binding buffer. The binding partner was added in a concentration of approximately 500 nM and incubated for 1 h at 4°C. Afterwards the M2 agarose was washed for three times and bound proteins were eluted with 35 μ l 3xFLAG peptide (2mg/ml). Finally the elution was analyzed on SDS-PAGE and Coomassie staining.

5.10 TIRF microscopy setup

Perfusion chambers were prepared using biotinylated coverslips (MicroSurfaces Inc.), three double-sided tapes (Scotch 3MM) and glass slides. The resulting flow cell was blocked with 1% (w/v) pluronic F-127 (Sigma-Aldrich) for 1 h at ambient temperature. Afterwards the chamber was incubated with 0.3 mg/ml Avidin DN (Vector Laboratories) in PEM buffer for 30 min and washed afterwards with PEM buffer. Fluorescently labeled or unlabeled, taxol-stabilized, biotinylated MTs were applied to the chamber, incubated for 3-5 min before washing the chamber with PEM supplemented with 100 mM KCl, 0.5 mg/ml casein, 0.5% β -mercaptoethanol, 4.5 μ g/ml glucose, 200 μ g/ml glucose-oxidase, 35 μ g/ml catalase, 5 nM taxol. Afterwards the motor (or motor + Bim1) was introduced into the chamber in the presence of PEM buffer supplemented with 100 mM KCl, 0.5 mg/ml casein, 0.5% β -mercaptoethanol, 4.5 μ g/ml glucose, 200 μ g/ml glucose-oxidase, 35 μ g/ml catalase, 16.6 nM taxol, 6.6 mM ATP, 0.06% Tween-20 and 0.13 % (w/v) methylcellulose. Recordings were taken using a TIRF3 microscopy system (Carl Zeiss, Inc.) operated with Axiovision software (Carl Zeiss, Inc.) and equipped with a 100x Plan-Apochromat 1.46 NA objective. Time-lapse movies were acquired every 3 s using an electron-multiplying charge-coupled device camera (Cascade II, Photometrics). Analysis of the recordings was conducted in Metamorph by creating kymographs.

6 Abbreviations

+TIP(s)	microtubule plus-end tracking protein(s)
6xHis	six times histidine tag
AMPPNP	adenylyl-imidodiphosphate
ATP	adenosine tri-phosphate
bp	base pair
do	drop-out
DTT	Dithiothreitol
(e)GFP	(enhanced) green fluorescent protein
g	gram
GMPCPP	guanosine 5'-[α,β -methylene]triphosphate
GST	glutathione-S-transferase
h	hour
kDa	kilo Dalton
l	liter
mg	milligram
min	minute
ml	milliliter
MT(s)	microtubule(s)
NiNTA	nickel-nitrilotriacetic acid
NTP	nucleotide

Abbreviations

o/n	over night
PBS	Phosphate Buffered Saline
PMSF	Phenylmethylsulfonylfluorid
rpm	revolutions per minute
RT	room temperature
sec	second
SPB	spindle pole body
TEV	tobacco etch virus
TIRF	total internal reflection fluorescence
WB	western blot
wt	wild type
YEP	yeast extract peptone
YPD	yeast extract peptone dextrose

7 References

- Aist, J.R., Bayles, C.J., Tao, W., and Berns, M.W. (1991). Direct experimental evidence for the existence, structural basis and function of astral forces during anaphase B in vivo. *Journal of Cell Science* 100 (Pt 2), 279–288.
- Akhmanova, A., and Steinmetz, M.O. (2008). Tracking the ends: a dynamic protein network controls the fate of microtubule tips. *Nat Rev Mol Cell Biol* 9, 309–322.
- Allingham, J.S., Sproul, L.R., Rayment, I., and Gilbert, S.P. (2007). Vik1 Modulates Microtubule-Kar3 Interactions through a Motor Domain that Lacks an Active Site. *Cell* 128, 1161–1172.
- Avunie-Masala, R., Movshovich, N., Nissenkorn, Y., Gerson-Gurwitz, A., Fridman, V., Kõivomägi, M., Loog, M., Hoyt, M.A., Zaritsky, A., and Gheber, L. (2011). Phosphoregulation of kinesin-5 during anaphase spindle elongation. *Journal of Cell Science* 124, 873–878.
- Benanti, J.A., Matyskiela, M.E., Morgan, D.O., and Toczyski, D.P. (2009). Functionally Distinct Isoforms of Cik1 Are Differentially Regulated by APC/C-Mediated Proteolysis. *Molecular Cell* 33, 581–590.
- Bieling, P., Laan, L., Schek, H., Munteanu, E.L., Sandblad, L., Dogterom, M., Brunner, D., and Surrey, T. (2007). Reconstitution of a microtubule plus-end tracking system in vitro. *Nature* 450, 1100–1105.
- Biernat, J., Gustke, N., Drewes, G., Mandelkow, E.M., and Mandelkow, E. (1993). Phosphorylation of Ser262 strongly reduces binding of tau to microtubules: distinction between PHF-like immunoreactivity and microtubule binding. *Neuron* 11, 153–163.
- Blake-Hodek, K.A., Cassimeris, L., and Huffaker, T.C. (2010). Regulation of microtubule dynamics by Bim1 and Bik1, the budding yeast members of the EB1 and CLIP-170 families of plus-end tracking proteins. *Mol. Biol. Cell* 21, 2013–2023.
- Blangy, A., Lane, H.A., d'Hérin, P., Harper, M., Kress, M., and Nigg, E.A. (1995). Phosphorylation by p34cdc2 regulates spindle association of human Eg5, a kinesin-related motor essential for bipolar spindle formation in vivo. *Cell* 83, 1159–1169.
- Brady, S.T. (1985). A novel brain ATPase with properties expected for the fast axonal transport motor. *Nature* 317, 73–75.

References

- Brouhard, G.J., Stear, J.H., Noetzel, T.L., Al-Bassam, J., Kinoshita, K., Harrison, S.C., Howard, J., and Hyman, A.A. (2008). XMAP215 is a processive microtubule polymerase. *Cell* 132, 79–88.
- Brust-Mascher, I., Sommi, P., Cheerambathur, D.K., and Scholey, J.M. (2009). Kinesin-5-dependent poleward flux and spindle length control in *Drosophila* embryo mitosis. *Mol. Biol. Cell* 20, 1749–1762.
- Cahu, J., Olichon, A., Hentrich, C., Schek, H., Drinjakovic, J., Zhang, C., Doherty-Kirby, A., Lajoie, G., and Surrey, T. (2008). Phosphorylation by Cdk1 increases the binding of Eg5 to microtubules in vitro and in *Xenopus* egg extract spindles. *PLoS ONE* 3, e3936.
- Chee, M.K., and Haase, S.B. (2010). B-cyclin/CDKs regulate mitotic spindle assembly by phosphorylating kinesins-5 in budding yeast. *PLoS Genet* 6, e1000935.
- Chu, H.M.A., Yun, M., Anderson, D.E., Sage, H., Park, H.W., and Endow, S.A. (2005). Kar3 interaction with Cik1 alters motor structure and function. *The EMBO Journal* 24, 3214–3223.
- Cohen, T.J., Guo, J.L., Hurtado, D.E., Kwong, L.K., Mills, I.P., Trojanowski, J.Q., and Lee, V.M.Y. (2011). The acetylation of tau inhibits its function and promotes pathological tau aggregation. *Nat Commun* 2, 252.
- Cottingham, F.R., and Hoyt, M.A. (1997). Mitotic spindle positioning in *Saccharomyces cerevisiae* is accomplished by antagonistically acting microtubule motor proteins. *J Cell Biol* 138, 1041–1053.
- Cottingham, F.R., Gheber, L., Miller, D.L., and Hoyt, M.A. (1999). Novel roles for *saccharomyces cerevisiae* mitotic spindle motors. *J Cell Biol* 147, 335–350.
- Cytrynbaum, E.N., Scholey, J.M., and Mogilner, A. (2003). A force balance model of early spindle pole separation in *Drosophila* embryos. *Biophysj* 84, 757–769.
- Desai, A., and Mitchison, T.J. (1997). Microtubule polymerization dynamics. *Annual Review of Cell and ...*
- Desai, A., Verma, S., Mitchison, T.J., and Walczak, C.E. (1999). Kin I kinesins are microtubule-destabilizing enzymes. *Cell* 96, 69–78.
- Ding, R., McDonald, K.L., and McIntosh, J.R. (1993). Three-dimensional reconstruction and analysis of mitotic spindles from the yeast, *Schizosaccharomyces pombe*. *J Cell Biol* 120, 141–151.

- Drechsel, D.N., Hyman, A.A., Cobb, M.H., and Kirschner, M.W. (1992). Modulation of the dynamic instability of tubulin assembly by the microtubule-associated protein tau. *Mol. Biol. Cell* 3, 1141–1154.
- Du, Y., English, C.A., and Ohi, R. (2010). The Kinesin-8 Kif18A Dampens Microtubule Plus-End Dynamics. *Current Biology* 20, 374–380.
- Endow, S.A. (2003). Kinesin motors as molecular machines. *Bioessays* 25, 1212–1219.
- Endow, S.A., Chandra, R., Komma, D.J., Yamamoto, A.H., and Salmon, E.D. (1994a). Mutants of the *Drosophila* *ncd* microtubule motor protein cause centrosomal and spindle pole defects in mitosis. *Journal of Cell Science* 107 (Pt 4), 859–867.
- Endow, S.A., Kang, S.J., Satterwhite, L.L., Rose, M.D., Skeen, V.P., and Salmon, E.D. (1994b). Yeast Kar3 is a minus-end microtubule motor protein that destabilizes microtubules preferentially at the minus ends. *The EMBO Journal* 13, 2708–2713.
- Endres, N.F., Yoshioka, C., Milligan, R.A., and Vale, R.D. (2006). A lever-arm rotation drives motility of the minus-end-directed kinesin Ncd. *Nature* 439, 875–878.
- Espeut, J., Gaussen, A., Bieling, P., Morin, V., Prieto, S., Fesquet, D., Surrey, T., and Abrieu, A. (2008). Phosphorylation relieves autoinhibition of the kinetochore motor Cenp-E. *Molecular Cell* 29, 637–643.
- Ferenz, N.P., Paul, R., Fagerstrom, C., Mogilner, A., and Wadsworth, P. (2009). Dynein antagonizes eg5 by crosslinking and sliding antiparallel microtubules. *Curr. Biol.* 19, 1833–1838.
- Fink, G., Hajdo, L., Skowronek, K.J., Reuther, C., Kasprzak, A.A., and Diez, S. (2009). The mitotic kinesin-14 Ncd drives directional microtubule-microtubule sliding. *Nature Publishing Group* 11, 717–723.
- Galjart, N. (2010). Plus-end-tracking proteins and their interactions at microtubule ends. *Curr. Biol.* 20, R528–R537.
- Gandhi, R., Bonaccorsi, S., Wentworth, D., Doxsey, S., Gatti, M., and Pereira, A. (2004). The *Drosophila* kinesin-like protein KLP67A is essential for mitotic and male meiotic spindle assembly. *Mol. Biol. Cell* 15, 121–131.
- Gandhi, S.R., Gierliński, M., Mino, A., Tanaka, K., Kitamura, E., Clayton, L., and Tanaka, T.U. (2011). Kinetochore-dependent microtubule rescue ensures their efficient and sustained interactions in early mitosis. *Developmental Cell* 21, 920–933.

- Gard, D.L., and Kirschner, M.W. (1987a). A microtubule-associated protein from *Xenopus* eggs that specifically promotes assembly at the plus-end. *J Cell Biol* *105*, 2203–2215.
- Gard, D.L., and Kirschner, M.W. (1987b). Microtubule assembly in cytoplasmic extracts of *Xenopus* oocytes and eggs. *J Cell Biol* *105*, 2191–2201.
- Gard, D.L., Becker, B.E., and Josh Romney, S. (2004). MAPping the eukaryotic tree of life: structure, function, and evolution of the MAP215/Dis1 family of microtubule-associated proteins. *Int. Rev. Cytol.* *239*, 179–272.
- Gardner, M.K., Haase, J., Myhre, K., Molk, J.N., Anderson, M., Joglekar, A.P., O'Toole, E.T., Winey, M., Salmon, E.D., Odde, D.J., et al. (2008a). The microtubule-based motor Kar3 and plus end binding protein Bim1 provide structural support for the anaphase spindle. *The Journal of Cell Biology* *180*, 91–100.
- Gardner, M.K., Odde, D.J., and Bloom, K. (2008b). Kinesin-8 molecular motors: putting the brakes on chromosome oscillations. *Trends in Cell Biology* *18*, 307–310.
- Gilbert, S.P., Webb, M.R., Brune, M., and Johnson, K.A. (1995). Pathway of processive ATP hydrolysis by kinesin. *Nature* *373*, 671–676.
- Goshima, G., Nédélec, F., and Vale, R.D. (2005). Mechanisms for focusing mitotic spindle poles by minus end-directed motor proteins. *J Cell Biol* *171*, 229–240.
- Gouveia, S.M., and Akhmanova, A. (2010). Chapter One - Cell and Molecular Biology of Microtubule Plus End Tracking Proteins : End Binding Proteins and Their Partners (Elsevier Inc.).
- Gupta, M.L., Carvalho, P., Roof, D.M., and Pellman, D. (2006). Plus end-specific depolymerase activity of Kip3, a kinesin-8 protein, explains its role in positioning the yeast mitotic spindle. *Nature Publishing Group* *8*, 913–923.
- Hackney, D.D. (1994). Evidence for alternating head catalysis by kinesin during microtubule-stimulated ATP hydrolysis. *Proc Natl Acad Sci U S A* *91*, 6865–6869.
- Hackney, D.D., and Jiang, W.W. (2000). Assays for kinesin microtubule-stimulated ATPase activity. *Methods Mol Biol* *164*, 65–71.
- Hammond, J.W., Blasius, T.L., Soppina, V., Cai, D., and Verhey, K.J. (2010). Autoinhibition of the kinesin-2 motor KIF17 via dual intramolecular mechanisms. *The Journal of Cell Biology* *189*, 1013–1025.

- Hartwell, L.H.L., and Weinert, T.A.T. (1989). Checkpoints: controls that ensure the order of cell cycle events. *Science* 246, 629–634.
- Hatsumi, M., and Endow, S.A. (1992). Mutants of the microtubule motor protein, nonclaret disjunctional, affect spindle structure and chromosome movement in meiosis and mitosis. *Journal of Cell Science* 101 (Pt 3), 547–559.
- Hayashi, I., Wilde, A., Mal, T.K., and Ikura, M. (2005). Structural basis for the activation of microtubule assembly by the EB1 and p150Glued complex. *Molecular Cell* 19, 449–460.
- Hirokawa, N. (1998). Kinesin and dynein superfamily proteins and the mechanism of organelle transport. *Science* 279, 519–526.
- Hirokawa, N., Noda, Y., Tanaka, Y., and Niwa, S. (2009). Cytoskeletal motors: Kinesin superfamily motor proteins and intracellular transport. 1–15.
- Honnappa, S., Gouveia, S.M., Weisbrich, A., Damberger, F.F., Bhavesh, N.S., Jawhari, H., Grigoriev, I., van Rijssel, F.J.A., Buey, R.M., Lawera, A., et al. (2009). An EB1-Binding Motif Acts as a Microtubule Tip Localization Signal. *Cell* 138, 366–376.
- Howard, J., and Hyman, A.A. (2007). Microtubule polymerases and depolymerases. *Current Opinion in Cell Biology* 19, 31–35.
- J Pines, T.H. (1987). Molecular cloning and characterization of the mRNA for cyclin from sea urchin eggs. *The EMBO Journal* 6, 2987.
- Janke, C., and Bulinski, J.C. (2011). Post-translational regulation of the microtubule cytoskeleton: mechanisms and functions. *Nat Rev Mol Cell Biol* 12, 773–786.
- Jin, F., Liu, H., Li, P., Yu, H.-G., and Wang, Y. (2012). Loss of Function of the Cik1/Kar3 Motor Complex Results in Chromosomes with Syntelic Attachment That Are Sensed by the Tension Checkpoint. *PLoS Genet* 8, e1002492.
- Kapitein, L.C., Peterman, E.J.G., Kwok, B.H., Kim, J.H., Kapoor, T.M., and Schmidt, C.F. (2005). The bipolar mitotic kinesin Eg5 moves on both microtubules that it crosslinks. *Nature* 435, 114–118.
- Karabay, A., and Walker, R.A. (1999). Identification of microtubule binding sites in the Ncd tail domain. *Biochemistry* 38, 1838–1849.
- Kim, Y., Holland, A.J., Lan, W., and Cleveland, D.W. (2010). Aurora Kinases and Protein Phosphatase 1 Mediate Chromosome Congression through Regulation of CENP-E. *Cell* 142, 444–455.

- Kinoshita, E., Kinoshita-Kikuta, E., Takiyama, K., and Koike, T. (2006). Phosphate-binding tag, a new tool to visualize phosphorylated proteins. *Mol. Cell Proteomics* 5, 749–757.
- Kinoshita, K., Arnal, I., Desai, A., Drechsel, D.N., and Hyman, A.A. (2001). Reconstitution of physiological microtubule dynamics using purified components. *Science* 294, 1340–1343.
- Kinoshita, K., Habermann, B., and Hyman, A.A. (2002). XMAP215: a key component of the dynamic microtubule cytoskeleton. *Trends in Cell Biology* 12, 267–273.
- Lampert, F., and Westermann, S. (2011). A blueprint for kinetochores - new insights into the molecular mechanics of cell division. *Nat Rev Mol Cell Biol* 12, 407–412.
- Lawrence, C.J., Dawe, R.K., Christie, K.R., Cleveland, D.W., Dawson, S.C., Endow, S.A., Goldstein, L.S.B., Goodson, H.V., Hirokawa, N., Howard, J., et al. (2004). A standardized kinesin nomenclature. *J Cell Biol* 167, 19–22.
- Leduc, C., Padberg-Gehle, K., Varga, V., Helbing, D., Diez, S., and Howard, J. (2012). Molecular crowding creates traffic jams of kinesin motors on microtubules. *Proc. Natl. Acad. Sci. U.S.a.* 109, 6100–6105.
- Lee, Y.M., Kim, E., Park, M., Moon, E., Ahn, S.-M., Kim, W., Hwang, K.B., Kim, Y.K., Choi, W., and Kim, W. (2010). Cell cycle-regulated expression and subcellular localization of a kinesin-8 member human KIF18B. *Gene* 466, 16–25.
- Longtine, M.S., McKenzie, A., Demarini, D.J., Shah, N.G., Wach, A., Brachat, A., Philippsen, P., and Pringle, J.R. (1998). Additional modules for versatile and economical PCR-based gene deletion and modification in *Saccharomyces cerevisiae*. *Yeast* 14, 953–961.
- Mackey, A.T. (2004). Mechanistic Analysis of the *Saccharomyces cerevisiae* Kinesin Kar3. *Journal of Biological Chemistry* 279, 51354–51361.
- Maddox, P.S., Stemple, J.K., Satterwhite, L., Salmon, E.D., and Bloom, K. (2003). The minus end-directed motor Kar3 is required for coupling dynamic microtubule plus ends to the cortical shmoo tip in budding yeast. *Current Biology* 13, 1423–1428.
- Makhnevych, T., Wong, P., Pogoutse, O., Vizeacoumar, F.J., Greenblatt, J.F., Emili, A., and Houry, W.A. (2012). Hsp110 is required for spindle length control. *The Journal of Cell Biology* 198, 623–636.

- Mana-Capelli, S., McLean, J.R., Chen, C.-T., Gould, K.L., and McCollum, D. (2012). The kinesin-14 Klp2 is negatively regulated by the SIN for proper spindle elongation and telophase nuclear positioning. *Mol. Biol. Cell*.
- Manning, A.L., Bakhoun, S.F., Maffini, S., Correia-Melo, C., Maiato, H., and Compton, D.A. (2010). CLASP1, astrin and Kif2b form a molecular switch that regulates kinetochore-microtubule dynamics to promote mitotic progression and fidelity. *The EMBO Journal* 29, 3531–3543.
- Manning, B.D., Barrett, J.G., Wallace, J.A., Granok, H., and Snyder, M. (1999). Differential regulation of the Kar3p kinesin-related protein by two associated proteins, Cik1p and Vik1p. *J Cell Biol* 144, 1219–1233.
- Mastrorade, D.N., McDonald, K.L., Ding, R., and McIntosh, J.R. (1993). Interpolar spindle microtubules in PTK cells. *J Cell Biol* 123, 1475–1489.
- Maurer, S.P., Fourniol, F.J., Bohner, G., Moores, C.A., and Surrey, T. (2012). EBs recognize a nucleotide-dependent structural cap at growing microtubule ends. *Cell* 149, 371–382.
- Mayer, T.U., Kapoor, T.M., Haggarty, S.J., King, R.W., Schreiber, S.L., and Mitchison, T.J. (1999). Small molecule inhibitor of mitotic spindle bipolarity identified in a phenotype-based screen. *Science* 286, 971–974.
- Mayr, M.I., Hümmer, S., Bormann, J., Grüner, T., Adio, S., Woehlke, G., and Mayer, T.U. (2007). The Human Kinesin Kif18A Is a Motile Microtubule Depolymerase Essential for Chromosome Congression. *Current Biology* 17, 488–498.
- Mayr, M.I., Storch, M., Howard, J., and Mayer, T.U. (2011). A non-motor microtubule binding site is essential for the high processivity and mitotic function of kinesin-8 Kif18A. *PLoS ONE* 6, e27471.
- McDonald, K.L., Edwards, M.K., and McIntosh, J.R. (1979). Cross-sectional structure of the central mitotic spindle of *Diatoma vulgare*. Evidence for specific interactions between antiparallel microtubules. *J Cell Biol* 83, 443–461.
- McDonald, K.L., O'Toole, E.T., Mastrorade, D.N., and McIntosh, J.R. (1992). Kinetochore microtubules in PTK cells. *J Cell Biol* 118, 369–383.
- Meadows, J.C., Shepperd, L.A., Vanoosthuyse, V., Lancaster, T.C., Sochaj, A.M., Buttrick, G.J., Hardwick, K.G., and Millar, J.B.A. (2011). Spindle checkpoint silencing requires association of PP1 to both Spc7 and kinesin-8 motors. *Developmental Cell* 20, 739–750.

- Meluh, P.B., and Rose, M.D. (1990). KAR3, a kinesin-related gene required for yeast nuclear fusion. *Cell* 60, 1029–1041.
- Mitchison, T., and Kirschner, M. (1984). Dynamic instability of microtubule growth. *Nature* 312, 237–242.
- Newman, J.R., Wolf, E., and Kim, P.S. (2000). A computationally directed screen identifying interacting coiled coils from *Saccharomyces cerevisiae*. *Proc Natl Acad Sci U S A* 97, 13203–13208.
- Nicklas, R.B., and Kubai, D.F. (1985). Microtubules, chromosome movement, and reorientation after chromosomes are detached from the spindle by micromanipulation. *Chromosoma* 92, 313–324.
- Ogawa, T., Nitta, R., Okada, Y., and Hirokawa, N. (2004). A common mechanism for microtubule destabilizers-M type kinesins stabilize curling of the protofilament using the class-specific neck and loops. *Cell* 116, 591–602.
- Peterman, E.J.G., and Scholey, J.M. (2009). Mitotic microtubule crosslinkers: insights from mechanistic studies. *Curr. Biol.* 19, R1089–R1094.
- Peters, C., Brejc, K., Belmont, L., Bodey, A.J., Lee, Y., Yu, M., Guo, J., Sakowicz, R., Hartman, J., and Moores, C.A. (2010). Insight into the molecular mechanism of the multitasking kinesin-8 motor. *The EMBO Journal* 29, 3437–3447.
- Rank, K.C., Chen, C.J., Cope, J., Porche, K., Hoenger, A., Gilbert, S.P., and Rayment, I. (2012). Kar3Vik1, a member of the kinesin-14 superfamily, shows a novel kinesin microtubule binding pattern. *The Journal of Cell Biology* 197, 957–970.
- Rice, L.M., Montabana, E.A., and Agard, D.A. (2008). The lattice as allosteric effector: structural studies of alpha-beta- and gamma-tubulin clarify the role of GTP in microtubule assembly. *Proc. Natl. Acad. Sci. U.S.A.* 105, 5378–5383.
- Rischitor, P.E., Konzack, S., and Fischer, R. (2004). The Kip3-like kinesin KipB moves along microtubules and determines spindle position during synchronized mitoses in *Aspergillus nidulans* hyphae. *Eukaryotic Cell* 3, 632–645.
- Saunders, W., Hornack, D., Lengyel, V., and Deng, C. (1997). The *Saccharomyces cerevisiae* kinesin-related motor Kar3p acts at preanaphase spindle poles to limit the number and length of cytoplasmic microtubules. *J Cell Biol* 137, 417–431.
- Saunders, W.S., and Hoyt, M.A. (1992). Kinesin-related proteins required for structural integrity of the mitotic spindle. *Cell* 70, 451–458.

- Schnitzer, M.J., and Block, S.M. (1997). Kinesin hydrolyses one ATP per 8-nm step. *Nature* 388, 386–390.
- Scholey, J.M., Porter, M.E., Grissom, P.M., and McIntosh, J.R. (1985). Identification of kinesin in sea urchin eggs, and evidence for its localization in the mitotic spindle. *Nature* 318, 483–486.
- Schwartz, K., Richards, K., and Botstein, D. (1997). BIM1 encodes a microtubule-binding protein in yeast. *Mol. Biol. Cell* 8, 2677–2691.
- Sharp, D.J., Yu, K.R., Sisson, J.C., Sullivan, W., and Scholey, J.M. (1999). Antagonistic microtubule-sliding motors position mitotic centrosomes in *Drosophila* early embryos. *Nat Cell Biol* 1, 51–54.
- Sproul, L.R., Anderson, D.J., Mackey, A.T., Saunders, W.S., and Gilbert, S.P. (2005). Cik1 Targets the Minus-End Kinesin Depolymerase Kar3 to Microtubule Plus Ends. *Current Biology* 15, 1420–1427.
- Stearns, T., and Kirschner, M. (1994). In vitro reconstitution of centrosome assembly and function: the central role of gamma-tubulin. *Cell* 76, 623–637.
- Stumpff, J., Dassow, von, G., Wagenbach, M., Asbury, C., and Wordeman, L. (2008). The Kinesin-8 Motor Kif18A Suppresses Kinetochore Movements to Control Mitotic Chromosome Alignment. *Developmental Cell* 14, 252–262.
- Stumpff, J., Du, Y., English, C.A., Maliga, Z., Wagenbach, M., Asbury, C.L., Wordeman, L., and Ohi, R. (2011). A Tethering Mechanism Controls the Processivity and Kinetochore-Microtubule Plus-End Enrichment of the Kinesin-8 Kif18A. *Molecular Cell* 43, 764–775.
- Su, X., Ohi, R., and Pellman, D. (2012). Move in for the kill: motile microtubule regulators. *Trends in Cell Biology* 1–9.
- Su, X., Qiu, W., Gupta, M.L., Jr, Pereira-Leal, J.B., Reck-Peterson, S.L., and Pellman, D. (2011). Mechanisms Underlying the Dual-Mode Regulation of Microtubule Dynamics by Kip3/Kinesin-8. *Molecular Cell* 43, 751–763.
- Svoboda, K., Schmidt, C.F., Schnapp, B.J., and Block, S.M. (1993). Direct observation of kinesin stepping by optical trapping interferometry. *Nature* 365, 721–727.
- Tanaka, K., Kitamura, E., Kitamura, Y., and Tanaka, T.U. (2007). Molecular mechanisms of microtubule-dependent kinetochore transport toward spindle poles. *The Journal of Cell Biology* 178, 269–281.

References

Tanaka, K., Mukae, N., Dewar, H., van Breugel, M., James, E.K., Prescott, A.R., Antony, C., and Tanaka, T.U. (2005a). Molecular mechanisms of kinetochore capture by spindle microtubules. *Nature* *434*, 987–994.

Tanaka, T.U., Stark, M.J.R., and Tanaka, K. (2005b). Kinetochore capture and bi-orientation on the mitotic spindle. *Nat Rev Mol Cell Biol* *6*, 929–942.

Tanenbaum, M.E., Macurek, L., van der Vaart, B., Galli, M., Akhmanova, A., and Medema, R.H. (2011). A complex of Kif18b and MCAK promotes microtubule depolymerization and is negatively regulated by Aurora kinases. *Curr. Biol.* *21*, 1356–1365.

Tao, L., Mogilner, A., Civelekoglu-Scholey, G., Wollman, R., Evans, J., Stahlberg, H., and Scholey, J.M. (2006). A homotetrameric kinesin-5, KLP61F, bundles microtubules and antagonizes Ncd in motility assays. *Current Biology* *16*, 2293–2302.

Tirnauer, J.S., O'Toole, E., Berrueta, L., Bierer, B.E., and Pellman, D. (1999). Yeast Bim1p promotes the G1-specific dynamics of microtubules. *J Cell Biol* *145*, 993–1007.

Troxell, C.L., Sweezy, M.A., West, R.R., Reed, K.D., Carson, B.D., Pidoux, A.L., Cande, W.Z., and McIntosh, J.R. (2001). *pkl1(+)* and *klp2(+)*: Two kinesins of the Kar3 subfamily in fission yeast perform different functions in both mitosis and meiosis. *Mol. Biol. Cell* *12*, 3476–3488.

Ubersax, J.A., Woodbury, E.L., Quang, P.N., Paraz, M., Blethrow, J.D., Shah, K., Shokat, K.M., and Morgan, D.O. (2003). Targets of the cyclin-dependent kinase Cdk1. *Nature* *425*, 859–864.

Unsworth, A., Masuda, H., Dhut, S., and Toda, T. (2008). Fission yeast kinesin-8 Klp5 and Klp6 are interdependent for mitotic nuclear retention and required for proper microtubule dynamics. *Mol. Biol. Cell* *19*, 5104–5115.

Vale, R.D. (2003). The molecular motor toolbox for intracellular transport. *Cell* *112*, 467–480.

Vale, R.D., Reese, T.S., and Sheetz, M.P. (1985). Identification of a novel force-generating protein, kinesin, involved in microtubule-based motility. *Cell* *42*, 39–50.

Varga, V., Leduc, C., Bormuth, V., Diez, S., and Howard, J. (2009). Kinesin-8 Motors Act Cooperatively to Mediate Length-Dependent Microtubule Depolymerization. *Cell* *138*, 1174–1183.

- Varga, V.V., Helenius, J.J., Tanaka, K.K., Hyman, A.A.A., Tanaka, T.U.T., and Howard, J.J. (2006). Yeast kinesin-8 depolymerizes microtubules in a length-dependent manner. *Nat Cell Biol* 8, 957–962.
- Verhey, K.J., and Hammond, J.W. (2009). Cytoskeletal motors: Traffic control: regulation of kinesin motors. 1–13.
- Verhey, K.J., Kaul, N., and Soppina, V. (2011). Kinesin assembly and movement in cells. *Annu Rev Biophys* 40, 267–288.
- Walker, R.A.R., O'Brien, E.T.E., Pryer, N.K.N., Soboeiro, M.F.M., Voter, W.A.W., Erickson, H.P.H., and Salmon, E.D.E. (1988). Dynamic instability of individual microtubules analyzed by video light microscopy: rate constants and transition frequencies. *J Cell Biol* 107, 1437–1448.
- Wang, H.-W., and Nogales, E. (2005). Nucleotide-dependent bending flexibility of tubulin regulates microtubule assembly. *Nature* 435, 911–915.
- Wargacki, M., Tay, J., Muller, E., Asbury, C., and Davis, T. (2010a). Kip3, the yeast kinesin-8, is required for clustering of kinetochores at metaphase. *Cc* 9, 76–75.
- Wargacki, M.M., Tay, J.C., Muller, E.G., Asbury, C.L., and Davis, T.N. (2010b). Kip3, the yeast kinesin-8, is required for clustering of kinetochores at metaphase. *Cc* 9, 2581–2588.
- Weaver, L.N., Ems-McClung, S.C., Stout, J.R., LeBlanc, C., Shaw, S.L., Gardner, M.K., and Walczak, C.E. (2011). Kif18A Uses a Microtubule Binding Site in the Tail for Plus-End Localization and Spindle Length Regulation. *Current Biology* 1–7.
- West, R.R., Malmstrom, T., Troxell, C.L., and McIntosh, J.R. (2001). Two related kinesins, klp5+ and klp6+, foster microtubule disassembly and are required for meiosis in fission yeast. *Mol. Biol. Cell* 12, 3919–3932.
- Wong, J., Nakajima, Y., Westermann, S., Shang, C., Kang, J.-S., Goodner, C., Houshmand, P., Fields, S., Chan, C.S.M., Drubin, D., et al. (2007). A protein interaction map of the mitotic spindle. *Mol. Biol. Cell* 18, 3800–3809.
- Woodruff, J.B., Drubin, D.G., and Barnes, G. (2010). Mitotic spindle disassembly occurs via distinct subprocesses driven by the anaphase-promoting complex, Aurora B kinase, and kinesin-8. *The Journal of Cell Biology* 191, 795–808.

References

- Woodruff, J.B., Drubin, D.G., and Barnes, G. (2012). Spindle assembly requires complete disassembly of spindle remnants from the previous cell cycle. *Mol. Biol. Cell* 23, 258–267.
- Wordeman, L., and Mitchison, T.J. (1994). Dynamics of microtubule assembly in vivo. *Modern Cell Biology* 13, 287–301.
- Yildiz, A., Tomishige, M., Vale, R.D., and Selvin, P.R. (2004). Kinesin walks hand-over-hand. *Science* 303, 676–678.
- Zimniak, T., Fitz, V., Zhou, H., Lampert, F., Opravil, S., Mechtler, K., Stolt-Bergner, P., and Westermann, S. (2012). Spatiotemporal regulation of Ipl1/Aurora activity by direct Cdk1 phosphorylation. *Curr. Biol.* 22, 787–793.
- Zimniak, T., Stengl, K., Mechtler, K., and Westermann, S. (2009). Phosphoregulation of the budding yeast EB1 homologue Bim1p by Aurora/Ipl1p. *The Journal of Cell Biology* 186, 379–391.

8 Curriculum Vitae

Christine Mieck

Home address	Nationality	German
Wassergasse 24/7	Date of Birth	May 3 rd 1984
1030 Wien	email.	mieck@imp.ac.at
Austria		

UNIVERSITY

Since 11/2008	PhD student at the Research Institute of Molecular Pathology (IMP), Vienna Thesis: “Kinesin motor function at the microtubule plus-end”
10/2006-09/2008	“Biochemistry and Molecular Cellbiology” (Master of Science) at the University Witten/Herdecke, Germany Thesis: “Generation of induced pluripotent stem cells via nonviral episomal vector”
10/2003 - 09/2006	“Molecular Medicine” at the University of Ulm, Germany Bachelor of Science, Thesis: “The impact of mono- and polyclonal neutralizing antibodies on the spread of the cytomegalovirus in a human organculture”

SELECTED PRACTICAL EXPERIENCE

11/2007 – 01/2008 Research project at the Department of Immunology, University
Witten/Herdecke

Isolation of murine stem and progenitor cells, cultivation of stem cells with varying cytokine supplements, migration assays, FACS analyses, western blot analysis of signal molecules downstream the cytokine receptors

07/2007 – 10/2007 Internship at the Radiation Oncology, Beth Israel Deaconess
Medical Center, Harvard Medical School, Boston

Impact of heat shock factor 1 (HSF1) on the ploidy of prostate carcinoma cells employing siRNA-mediated silencing of HSF1

03/2007 – 04/2007 Research project at the Department of Physical Chemistry,
University of Witten/Herdecke

Protein isolation and kinetic stopped-flow analyses of nucleotide exchange at the bacterial single recognition particle FFH

PUBLICATIONS

Kassmer SH, Niggemann B, Punzel M, Mieck C, Zänker KS, Dittmar T.

Cytokine combinations differentially influence the SDF-1 α -dependent migratory activity of cultivated murine hematopoietic stem and progenitor cells. *Biol Chem.* 2008 July, 389(7):863-72

9 Acknowledgement

Analytically speaking this work is composed of pipetting, thinking, reading, ups and downs, pipetting again ... interspersed with some coffee breaks. However, I could never have accomplished this study without the help and support of lots of people.

In the first place I would like to thank my supervisor Dr. Stefan Westermann for his constant guidance and helpful advices that often broadened my perspective. His enthusiasm and encouragement have been a driving force throughout this PhD.

Thanks to all past and current member of the Westermann lab – Tom, Evi, Fabi, Gabi, Peter, Babet, Michi, Vero, Franci, Paulina, Gülsah and Balazs – for creating a pleasant and creative lab atmosphere. You were so helpful in discussions, but also in providing moral support. It was a pleasure to work with you!

I would also like to acknowledge the support from the “outside world”: Katja, Fabi, Gerhard, Max. You are amazing friends that turned Vienna into home sweet home (jerkwater town). Thanks also to the cycling connection for amazing holidays and funny Wienerwald tours.

I am grateful that I had a cosy drey. Thank you Borries.

Special thanks to my parents Gabi & Klaus and my brother Sebastian for patience, support and love.